SURFACE CAPTURE USING NEAR-REAL-TIME PHOTOGRAMMETRY FOR A COMPUTER NUMERICALLY CONTROLLED MILLING SYSTEM

Reto Wildschek, B.Sc (Eng), Cape Town

April 1989

Submitted to the University of Cape Town in partial fulfilment for the degree of Master of Science in Engineering.

I, Reto Wildschek, submit this thesis in partial fulfilment of the requirements for the degree of Master of Science in Engineering. I affirm that this is my original work and that it has not been submitted in this or a similar form for a degree at any University.

ABSTRACT

During the past three years, a research project has been carried out in the Department of Mechanical Engineering at UCT, directed at developing a system to accurately reproduce three-dimensional (3D), sculptured surfaces on a three axis computer numerically controlled (CNC) milling machine. Sculptured surfaces are surfaces that cannot easily be represented mathematically. The project was divided into two parts: the development of an automatic non-contact 3D measuring system, and the development of a milling system capable of machining 3D sculptured surfaces (Back, 1988). The immediate need for such a system exists for the manufacture of medical prostheses.

The writer undertook to investigate the measurement system, with the objective to develop a non-contact measuring system that can be used to 'map' a sculptured surface so that it can be represented by a set of XYZ coordinates in the form required by the milling system developed by Back (1988).

This thesis describes the development of a PC-based near-real-time photogrammetry system (PHOENICS) for surface capture. The topic is intoduced by describing photogrammetric principles as used for non-contact measurements of objects.

A number of different algorithms for image target detection, centering and matching is investigated. The approach to image matching adopted was the projection of a regular grid onto the surface with subsequent matching of conjugate grid intersections. A general algorithm which automatically detects crosses on a line and finds their accurate centres was developed. This algorithm was then extended from finding the crosses on a line, to finding all the intersection points of a grid. The algorithms were programmed in TRUE BASIC and specifically adapted for use with PHOENICS as an object point matching tool.

The non-contact surface measuring technique which was developed was used in conjunction with the milling system developed by Back (1988) to replicate a test object. This test proved that the combined system is suitable for the manufacture of sculptured surfaces.

The accuracy requirements for the manufacture of medical prostheses can be achieved with the combined measuring and milling system. At an object-to-camera distance of 0.5 m, points on a surface can be measured with an accuracy of approximately 0.3 mm at an interval of 5 mm. This corresponds to a relative accuracy of 1:1600. Back (1988) reported an average undercutting error of 0.46 mm for the milling system. This combines to an uncertainty of 0.55 mm.

Finally, the limitations of PHOENICS at its prototype stage as a surface measuring tool are discussed, in particular the factors influencing the system's accuracy. PHOENICS is an ongoing project and the thesis is concluded by some recommendations for further research work.

ACKNOWLEDGEMENTS

The author would like to gratefully acknowledge the contribution of the following:

My supervisor, Mr. Andrew Sass, for his help and guidance,

My supervisor, Assoc. Prof. Heinz Rüther, for his continual encouragement and interest, and who was always willing to give of his time,

Mr. Nicky Parkyn and Assoc. Prof. Heinz Rüther, for the use of their computer programs,

The CSIR, for their financial assistance,

The staff of the Surveying Department.

CONTENTS

Page

ABSTRACT i
ACKNOWLEDGEMENTS iii
LIST OF ILUSTRATIONS viii

1.0 INTRODUCTION 1

2.0 PHOTOGRAMMETRY 7
2.1 Introduction and Definition 7
2.2 Applications 12
2.3 Basic Geometry of the Single Photograph 14
2.3.1 Projections 14
2.3.2 Image and Object Space 16
2.3.3 Interior Orientation 17
2.3.4 Exterior Orientation 17
2.3.5 The Collinearity Condition 18
2.4 Obtaining the Third Dimension from Two Overlapping Photographs 20
2.5 Projective Transformation - Restitution of the Object 22

3.0 DEVELOPMENT OF A PC-BASED NRTP SYSTEM 25

4.0 IMAGE AQUISITION WITH CCD CAMERAS 32
4.1 The Vidicon Camera Tube 33
4.2 Solid State Sensors 35
4.3 CCD Cameras 36
4.3.1 Interline vs Frame Transfer 38
4.3.2 CCD Performance Features 41
4.4 CCD vs Vidicon Tube Cameras 42

Page

5.0 A REVIEW OF IMAGE MATCHING AND NRTP SYSTEMS 44
5.1 Isis Scanner 45
5.2 Mapvision 46
5.3 A RTP System for Object Measurement at the National Research Council of Canada 47
5.4 A Close-Range Mapping System at the University of Illinois 48
5.5 Robot Vision at the National Research Council of Canada 50
5.6 Rasterstereography 51
5.7 A System for Capturing Facial Surface Information at the University of Minesota 53
5.8 Digital Image Correlation 54
5.9 Conclusions 55

6.0 DEVELOPING AN AUTOMATIC IMAGE TARGET DETECTION AND MATCHING ALGORITHM 56
6.1 Problem Formulation 56
6.1.1 Problem Statement 56
6.1.2 Requirements 56
6.1.3 Constraints 57
6.1.4 Criteria 57
6.2 Concept Formation 64
6.2.1 Finding Corresponding Points 65
6.2.2 Target Recognition and Centering 68
6.2.3 Line Following 74
6.3 Summary and Conclusions 76

7.0 DISCUSSION OF SOLUTION 77
7.1 A General Line Following and Cross Detection Algorithm 77
7.1.1 Line Detection 79

Page

7.1.2 Line Following and Cross Detection 79
7.1.3 Accurate Cross Positioning 84
7.2 Cross Detection, Centering and Matching for PHOENICS 86

8.0 TESTING THE CROSS DETECTION AND CENTERING ALGORITHM 90
8.1 Precision of Finding a Cross in an Image 90
8.1.1 Obtaining the First Approximation to the Cross Centre 90
8.2 Precision of Determining the Cross Centre 91
8.3 Accuracy of Measuring a Surface 95
8.3.1 Choice of Test Surface and Control Field 95
8.3.2 Surface Measurement with PHOENICS 97
8.3.3 Results of Measuring the Test Surface 99

9.0 DISCUSSION OF THE ERRORS AND LIMITATIONS OF PHOENICS 101
9.1 Accuracy Limitations in Measuring a Surface with PHOENICS 101
9.2 Limitations of Surface Measurement with PHOENICS 103

10.0 CONCLUSIONS AND RECOMMENDATIONS 106
10.1 Conclusions 106
10.2 Recommendations 107
10.3 Closing remarks 108

11.0 REFERENCES 110

12.0 BIBLIOGRAPHY 114

APPENDICES Page

A. Derivation of the Orientation Matrix A-1

B. Derivation of the Collinearity Condition B-1

C. Epipolar Geometry C-1

D. A Method of Interfacing the PIP Image Processing Board with a Computer Language other than those it supports D-1

E. Evaluation of Using the Weighted Mean Technique for Determining the Position of a Line-Section with Sub-Pixel Accuracy E-1

F. List of Programs for Use with PHOENICS F-1
F.1 TRUE BASIC Programs F-1
F.2 PIP Image Processor Macros F-2

G. A Set of Typical Images which were used for Surface Measurement with PHOENICS G-1

H. Coordinates of the Control Frame H-1

I. Sample Output of Photogrammetric Software for the Test Sphere I-1

LIST OF ILLUSTRATIONS

FIGURES Page

1.1 Mathematically generated surface which was machined with the milling system 3

2.1 Overview of remote sensing 8
2.2a Relative orientation 10
2.2b Absolute orientation 11
2.3 Orthographic projections 15
2.4 Perspective projections 15
2.5 Image and object space 16
2.6 Interior orientation 17
2.7 Exterior orientation by omega, phi and kappa 18
2.8 Collinearity condition 19
2.9 Geometry of two overlapping photographs 20

3.1 Schematic of PHOENICS hardware configuration 27
3.2 PHOENICS hardware 28
3.3 Control point target design for PHOENICS 31

4.1 Vidicon camera tube 33
4.2 CCD MOS strucure 37
4.3 Interline charge transfer 38
4.4 Frame charge transfer 39

5.1 Principle of operation of the Isis Scanner 45
5.2 Image correlation along epipolar lines 49
5.3 Optical beam deflection assembly 50
5.4 Cross- and line rasterstereography 52

6.1 Example of a grey image 59
6.2 Pixel intensities of a grey image 60

FIGURES Page

6.3 Thresholding 61
6.4 Example of a binary image 62
6.5 Pixel intensities of a binary image 63
6.6 The pixeling effect 64
6.7 Grids for object targeting 67
6.8 Circular targets 70
6.9 Cross centering with higher order moments 71
6.10 Modelling a cross as the intersection of two lines 72
6.11 Modelling a cross as the intersection of two line segments 73
6.12 Line following using a search-circle 75

7.1 Flow diagram of a general line following and cross detection algorithm 78
7.2 Search-circle used for line following and cross detection 80
7.3 Line and circle configurations characteristic of the number of search-circle intersections found .. 81
7.4 Finding the first approximation to the points on the lines which form a cross 84
7.5 Determining the position of the centre of the line to sub-pixel accuracy 85
7.6 Cross detection, centering, and matching with PHOENICS 87

8.1 Pixel intensity profiles across two typical lines 94
8.2 Control frame and test surface 96
8.3 Surface measurement with PHOENICS 98

A.1 Three-dimensional right-handed coordinate system A-1

FIGURES Page

B.1 Diagram of the collinearity condition B-1
B.2 Image coordinate system rotated so that it is parallel to the object space B-2

C.1 Epipolar plane and epipolar lines C-1

E.1 Pixel intensity profiles of two typical line sections E-2

G.1 Grey image (left) for determining the control points G-2
G.2 Thresholded image (left) for determining the contol points G-3
G.3 Grey image (left) for determining the object points G-4
G.4 Thresholded image (left) for determining the object points G-5
G.5 Grey image (right) for determining the control points G-6
G.6 Grey image (right) for determining the object points G-7
G.7 Image for determining the object points with a graduated grid overlayed G-8

H.1 Numbering of control frame H-2

TABLES Page

8.1 Maximum deviations in x and y of the calculated cross position from the mean cross centre 92
8.2 Results of measuring the test sphere with PHOENICS 100

E.1 Pixel intensity values of two typical line sections E-1
E.2 Results of applying the weighted mean technique for finding the position of a line section E-3

H.1 Coordinates of control frame H-1

CHAPTER ONE

1.0 INTRODUCTION

During the past three years, a research project has been carried out in the Department of Mechanical Engineering at UCT, directed at developing a system to accurately reproduce three-dimensional (3D), sculptured surfaces on a three axis computer numerically controlled (CNC) milling machine. Sculptured surfaces are surfaces that cannot easily be represented mathematically. Duncan and Mair (1983) describe these surfaces as "those surface shapes which cannot continuously be generated and have the arbitrary or complex character of forms traditionally modelled by sculptors".

The need for the system arose because the Biomedical Engineering department wanted to produce prostheses such as shoe inserts and sockets for amputee stumps efficiently and quickly. They wanted a non-contacting measuring system to accurately measure, for example, the stump of an amputee or a deformed foot with as little patient discomfort as possible. These measurements are then to be used to machine either a positive or a negative image of the surface.

The first design was undertaken by Berelowitz in 1986 as an undergraduate thesis. Berelowitz (1986) used a digital camera called a 'TopoScanner' (Vaughn, Brooking, Price and Ireland, 1983) to capture the surface topography, an IBM PC microcomputer for data processing, and a three axis CNC milling machine to manufacture the surface. The dataprocessing included fitting a surface through the points measured by the TopoScanner, calculating the toolpath for the cutter, and translating the latter into instructions for the CNC machine. A punched paper tape was then produced to transfer the data to the CNC milling machine and the part milled.

Berelowitz (1986) produced a system with a great deal of potential but with limited accuracy. Back (1988) in an M.Sc thesis, set out to improve Berelowitz's design. He found fundamental problems with the TopoScanner and with certain assumptions in the surface fitting algorithms. Secondly, communication between the IBM PC and the CNC machine via the large amounts of paper tape were cumbersome. It also became clear that the complete system was too large a task for a single M.Sc thesis, so the task was divided into two parts; the measurement system and the milling system.

Back successfully:

- developed a mathematical algorithm to approximate a sculptured surface represented by a set of surface datapoints in the form of XYZ coordinates. These datapoints can either be measured from an existing surface or calculated from a mathematical surface equation.
- developed an algorithm to calculate the toolpath to machine the sculptured surface.
- wrote a computer program which displays the surface and toolpath in three dimensions on the computer screen.
- developed an algorithm which translates the toolpath into a program suitable for use with the CNC machine.
- developed a communications link for the direct transmission of the CNC program from the IBM microcomputer to the memory of the CNC computer.

The system is fully operational and was used to machine a variety of surfaces. An example of a mathematically defined surface that was produced is given in Fig. 1.1.

An indication of the accuracy of the milling system was obtained by milling a mathematically generated test surface whose shape is typical of that likely to be encountered by the milling system. Analysis of the data revealed an average undercutting error of

0.46 mm ± 0.20 mm over the entire surface. Although this error is large in terms of conventional machining requirements, it is acceptable for the manufacture of medical prostheses previously described.

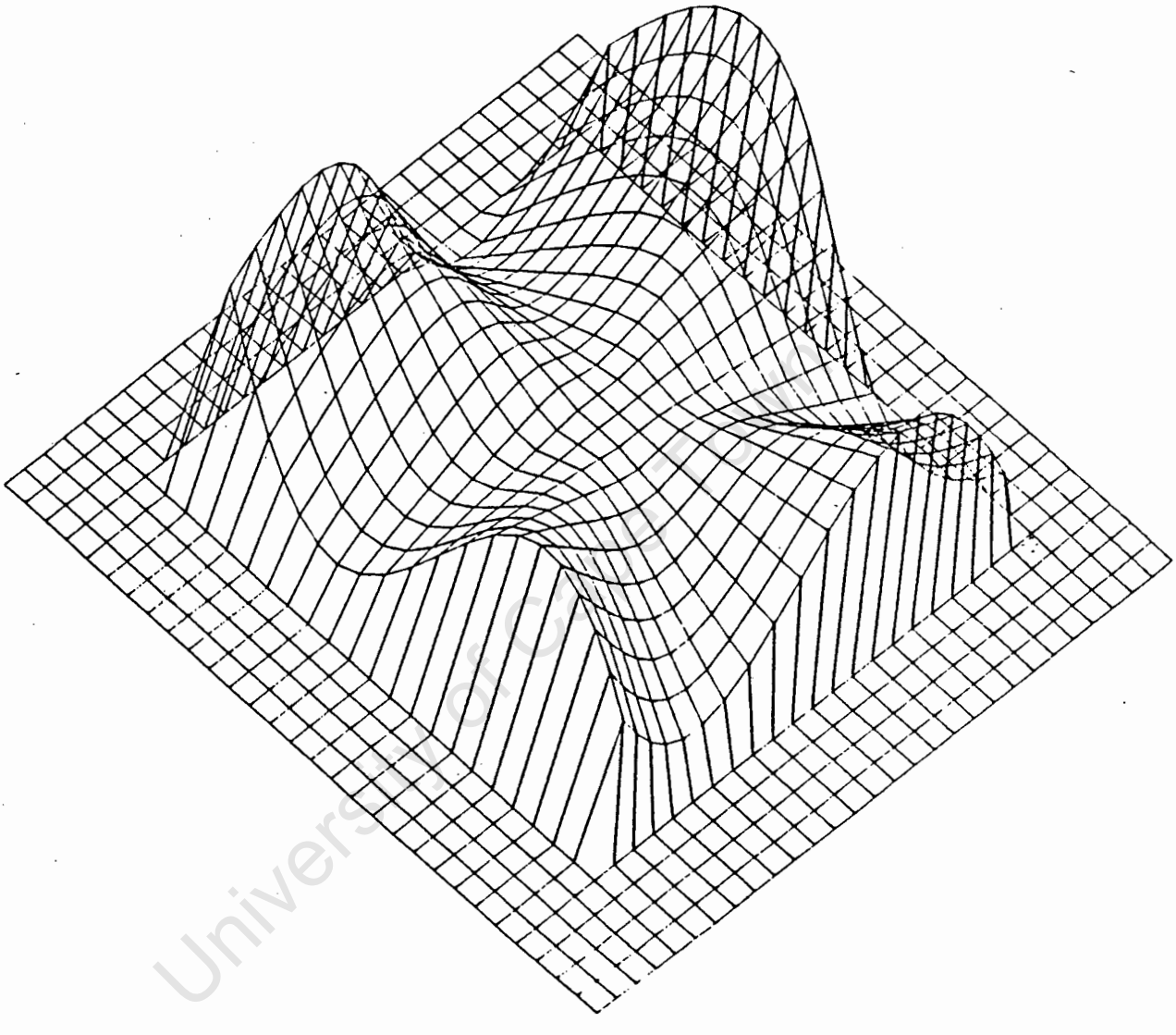

Fig. 1.1 Mathematically generated surface which was machined with the milling system

The writer undertook to investigate the measurement system, with the following objectives:

- to develop a non-contact measuring system that can be used to 'map' a sculptured surface so that it can be

represented by a set of XYZ coordinates in the form required by the milling system developed by Back (1988).

- to develop the system in such a way that it can serve as an introduction to Computer Aided Design and Manufacture (CAD/CAM) for undergraduate students who wish to further their studies in this specialised field.

The fundamental problems of the TopoScanner could not be resolved, so alternative methods were investigated. Photogrammetry seemed the most appropriate technique to start with as research work that appeared to have great potential, had just been started in UCT's Department of Surveying. Various hardware components had been purchased with the intentions to ultimately develop a real-time photogrammetric (RTP) mapping system. To the best of the writers knowledge, there are only 6 to 10 such systems operational worldwide - none on a microcomputer. Joining the research team in the Department of Surveying was thought to be an ideal opportunity to attain the primary objective and hence this path was followed.

In view of the above, a set of secondary objectives were formulated.

1. Assist in the development of the RTP system, in particular the image matching algorithms.
2. Establish the feasibility of using the system for the purpose of mapping a sculptured surface.
3. Select a test surface that can be defined mathematically and check the matching algorithm for logic and accuracy.
4. If this data proves to be suitable, use it in the milling program developed by Back (1988).

Thesis outline

Chapter 2 gives an overview of basic photogrammetry as this is a specialised field of Surveying with which undergraduate and graduate engineers are not usually familiar. The reader is introduced to the terminology commonly used in this discipline and an analytical approach for solving the photogrammetric problem is presented.

Chapter 3 begins by giving the motivations for the development of RTP systems. The design stages of such a RTP system are discussed, and a description is given of the near-real-time photogrammetric (NRTP) system being developed at UCT.

As the advent of digital cameras has made possible the development of RTP systems an introduction to the technology of these cameras is given in Chapter 4. The older Vidicon camera is also described, and the two camera types are compared.

Chapter 5 gives a review of NRTP systems with reference to the image matching algorithms used.

Chapter 6 discusses some of the concepts which were considered for developing an automatic image target detection and matching algorithm.

The image target detection and matching algorithm which was developed is described in Chapter 7.

The developed algorithm was programmed and tested in two stages on real image data. In Chapter 8 the two stages of testing are described and the results that were obtained are presented.

In Chapter 9 the limitations of the non-contact surface measuring technique which was developed, are discussed.

The final chapter outlines the conclusions which were drawn and the recommendations that were made.

CHAPTER TWO

2.0 PHOTOGRAMMETRY

2.1 Introduction and Definition

The word photogrammetry is derived from the three greek words, photos meaning 'light', gramma meaning 'something drawn or written', and metron meaning 'measurement'. Hence the original meaning of the word is 'measuring graphically using light'. The American Society of Photogrammetry (1980) defines photogrammetry as:

> "Photogrammetry is the art, science and technology of obtaining reliable information about physical objects and the environment through processes of recording, measuring, and interpreting photographic images and patterns of electromagnetic radiant energy and other phenomena."

Photogrammetry can be regarded as a branch of remote sensing which in the broadest sense is the aquisition of some physical property about an object without physical contact between it and the measuring device. Photogrammetry in turn can be divided into two categories: metrical photogrammetry and photo interpretation. In general, the first category is concerned with determining the relative locations of points in the space surrounding the object or on the object so that distances, angles, areas, volumes, elevations, the sizes and shapes of objects can be derived eg. a topographic map. In photo interpretation, on the other hand, photographs are evaluated qualitatively.

A diagramatic overview of remote sensing is given in Fig. 2.1.

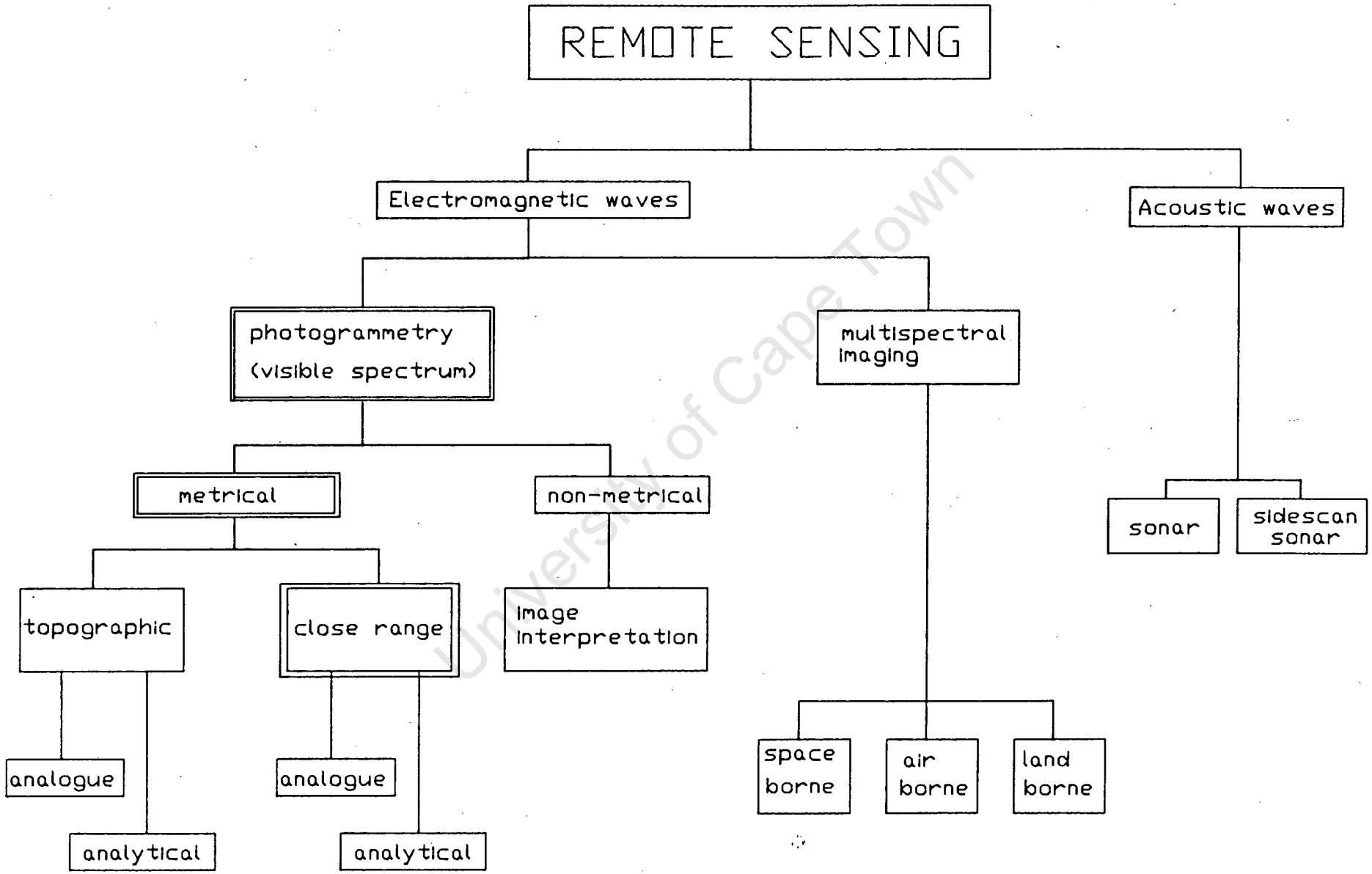

Fig. 2.1 Overview of remote sensing

As this thesis makes use of some of the tools and techniques used in metrical photogrammetry, a brief overview has been included.

Metrical photogrammetry

Metrical photogrammetry can generally be seen to consist of three stages:

1. Aquiring an image of the object to be measured.
2. Measuring the image of the object.
3. Extracting 3D information about the object from the photographs from these measurements.

Besides using conventional photographic systems to perform Stage 1, other techniques such as radar imaging and X-ray imaging are used.

Stages 2 and 3 can be accomplished by one of two methods. The first method uses complex instrumentation and is thus known as instrumental or analogue photogrammetry. A stereoscopic plotting instrument, an opto-mechanical device of high precision, is used to project and orientate two overlapping photographs in such a way that a 3D model of the original object is formed. This situation is created when all corresponding projected rays of the two photographs intersect in space which in effect means the reconstruction of the relative and absolute orientations of the camera exposure stations from where the photographs were taken.

Relative orientation refers to the correct orientation in space of the two projections with respect to one another (Fig. 2.2a). Absolute orientation refers to the correct orientation and scale of the model formed through the process of relative orientation with respect to a reference ground system (Fig. 2.2b).

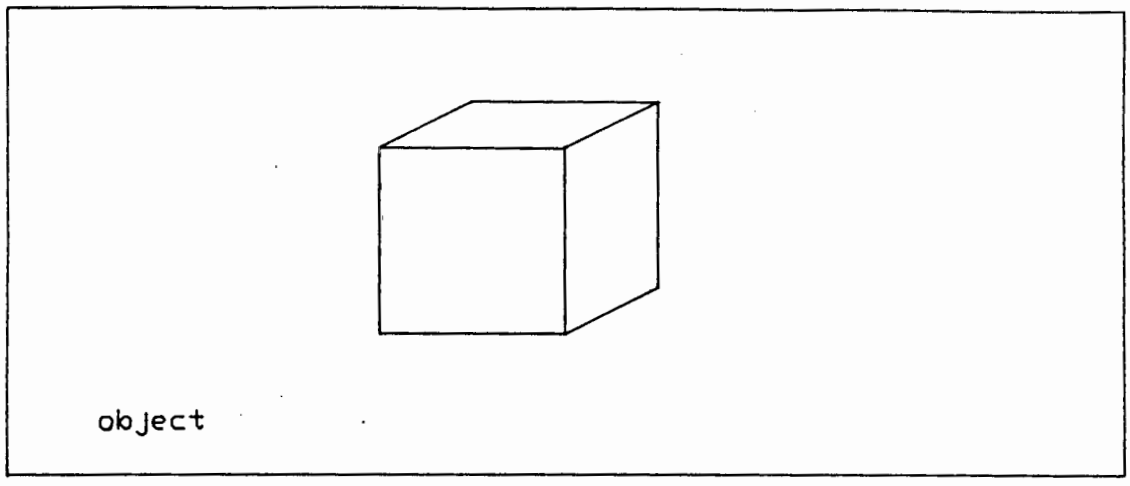

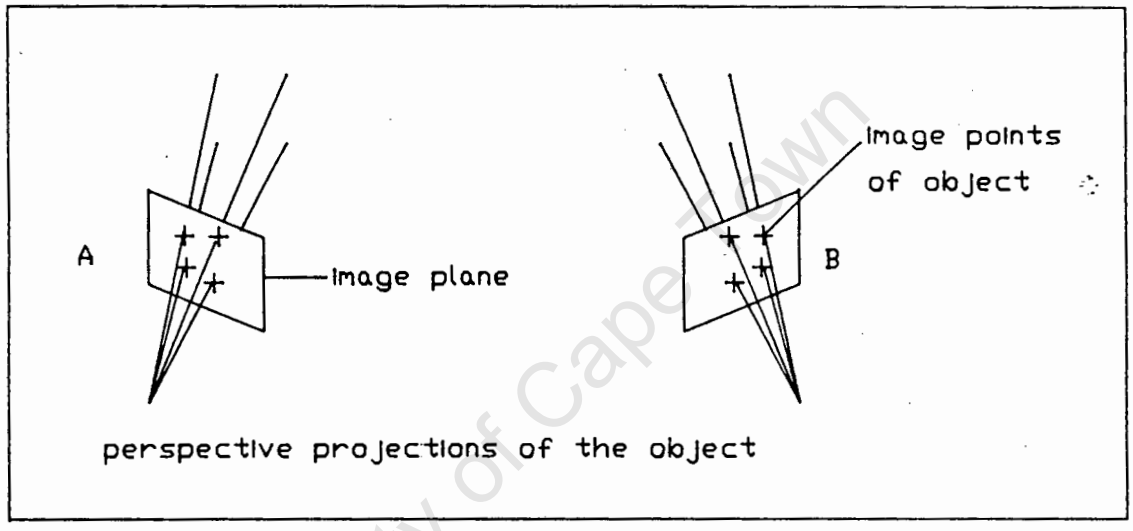

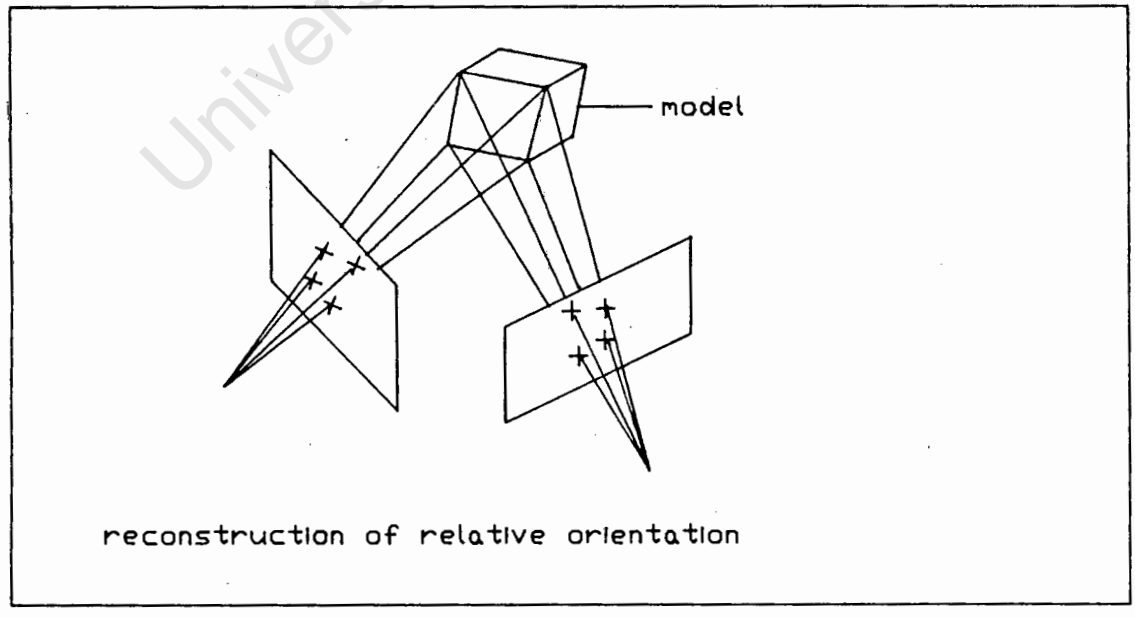

Fig. 2.2a Relative orientation

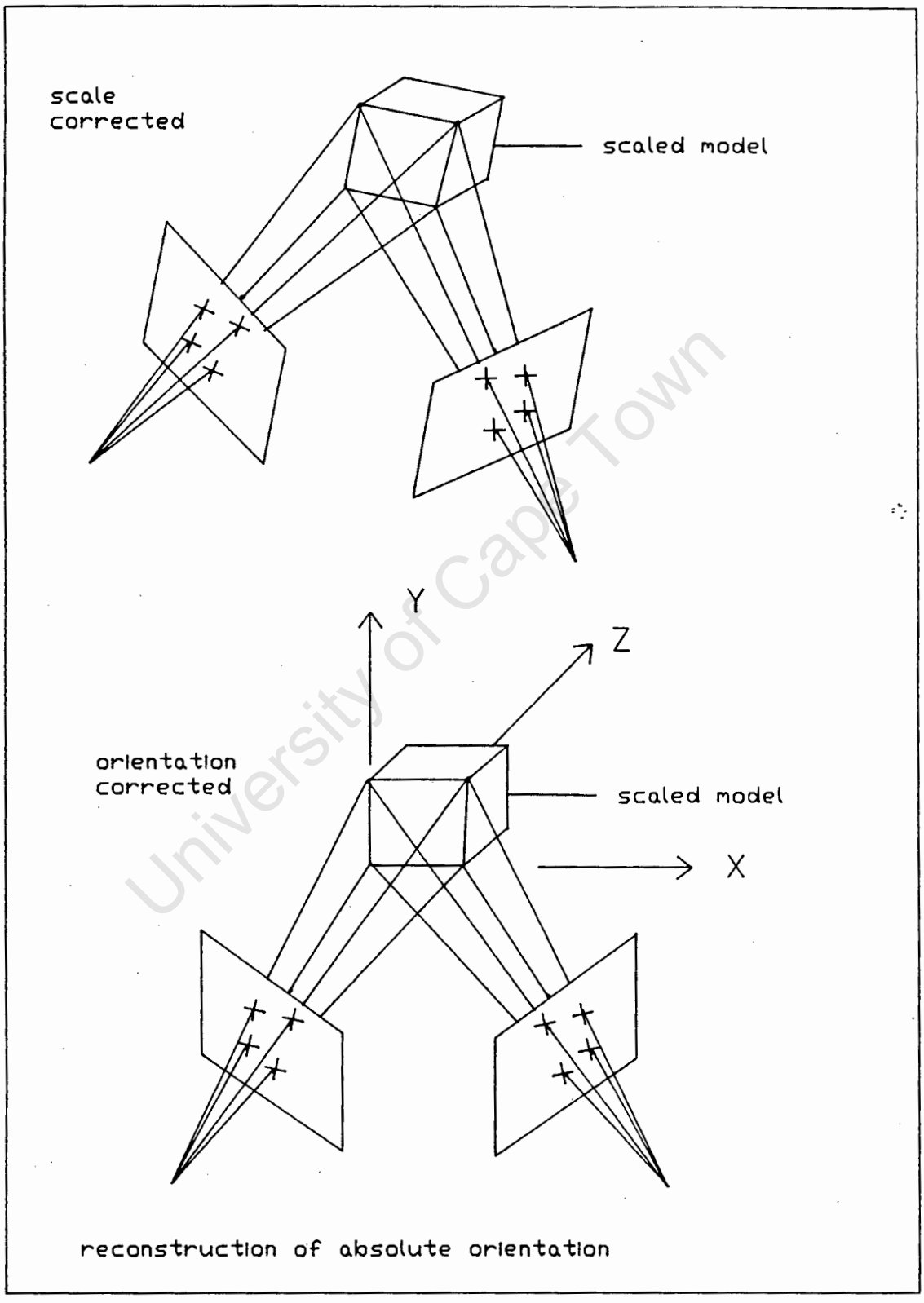

Fig. 2.2b Absolute orientation

In instrumental photogrammetry, relative orientation may either be accomplished empirically or numerically. In the first method six rays passing through the two photographs are brought to intersect in space in a repetitive, trial-and-error process. In numerical relative orientation the adjustments required are calculated from parallax measurements made with the stereoplotter after the photographs have been placed into it. Absolute orientation is then performed empirically by eliminating parallax from three control points; points with known XYZ coordinates. Subsequently, an operator can use the stereoplotter to produce a topographic map or to obtain true XYZ coordinates of a number of points on the model; this is known as a digital terrain model (DTM).

The second method, analytical photogrammetry, uses less complex but also very precise instrumentation. Measurements of x and y coordinates of common image points are made on the overlapping photographs with a comparator and used as input to a computer program to determine relative and absolute orientation. A mathematical model then used to determine the true XYZ coordinates of the object from points on the photographs. From this DTM a contour map can be produced.

The main difference between the instrumenntal method and the analytical method is that the former relies on a very precise mechanical system, whereas the latter uses an extensive mathematical model to solve the photgrammetric problem. Analytical photogrammetry is generally more accurate and easier to operate and thus, stereoplotters are progressively being used less and less.

2.2 Applications

Although photogrammetry is still principally a surveyor's tool used for the making of maps, especially topographic maps, it has

over the years found applications in many other scientific disciplines. The rapid growth of application areas started at the turn of the century when photogrammetry was first used in architecture. This became known as close-range photogrammetry: defined by some photogrammetrists as photogrammetry where the object to camera distance is less than 300 metres. All of the application areas mentioned below are examples of close-range photogrammetry.

Applications in architecture include surveys of historical monuments and sites as well as archaeological surveys. For specific examples, the reader is referred to the proceedings of the first International Symposium on Photogrammetric Surveys of Monuments and Sites, Athens (Badekas, 1974).

Applications in Zoology range from mapping the beak of a Shoebill (Adams, 1980) to measuring African Elephants (Rüther, 1979).

Applications in the medical field are also many and varied. An example is Dental-Stereophotogrammetry (Adams, 1978).

Another area which has numerous examples and a seemingly endless growth of applications in close-range photogrammetry, is in the industrial field. Today photogrammetry is used in building construction, civil engineering, mining, vehicle and machine construction, metallurgy, shipbuilding and many other areas. Some of the advantages to be gained from using photogrammetry as a measuring technique over conventional methods, are given by Knödler and Kupke (1974) in their article on production of ship propellers. These can be summarised as :

- time to measure the object is reduced by 90-95%.
- reduced material expenditure in the propeller casting manufacture through optimized moulds.
- reduced machine time for blade machining through optimization of the metal removal rate.

Knödler and Kupke (1974) also report that the photogrammetric technique "is equally suited for other industries where workpieces of a complex surface configuration are to be manufactured, which would be very time consuming to measure with conventional measuring tools".

2.3 Basic Geometry of the Single Photograph

As already mentioned there are different methods of obtaining a physical record of an object which is the first step of the photogrammetric process. Before discussing how photogrammetry is used to reconstruct the third dimension from two photographs, an understanding of the basic geometry of such photographs and of the terminology used, is required. In the literature the word photograph is sometimes used to mean "the physical record obtained by an imaging system". This can at times be misleading to the non-expert, and hence, in order to avoid any confusion, the word photograph in this chapter refers to "the positive image created through the conventional photographic process".

2.3.1 Projections

Two types of projections will be discussed here: orthographic and perspectice projections. A map or engineering drawing, usually at a reduced scale, is a reproduction of an orthographic projection of the terrain or object onto a reference datum plane (Fig. 2.3).

Distances between points (multiplied by the scale) and angles in an orthographic projection are equal to horizontal distances and angles measured in the field.

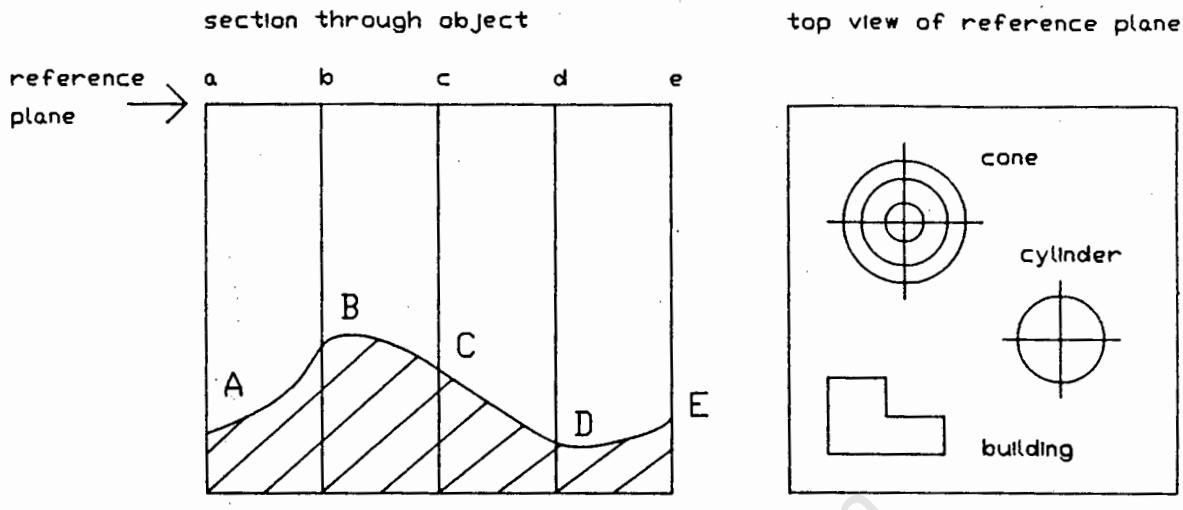

Fig. 2.3 Orthographic projections

A perspective projection is one in which all points are projected onto the reference plane through one point called the perspective centre (Fig. 2.4). In a camera system a light sensitive film or area occupies the reference plane and the perspective centre is the focal point of the lens.

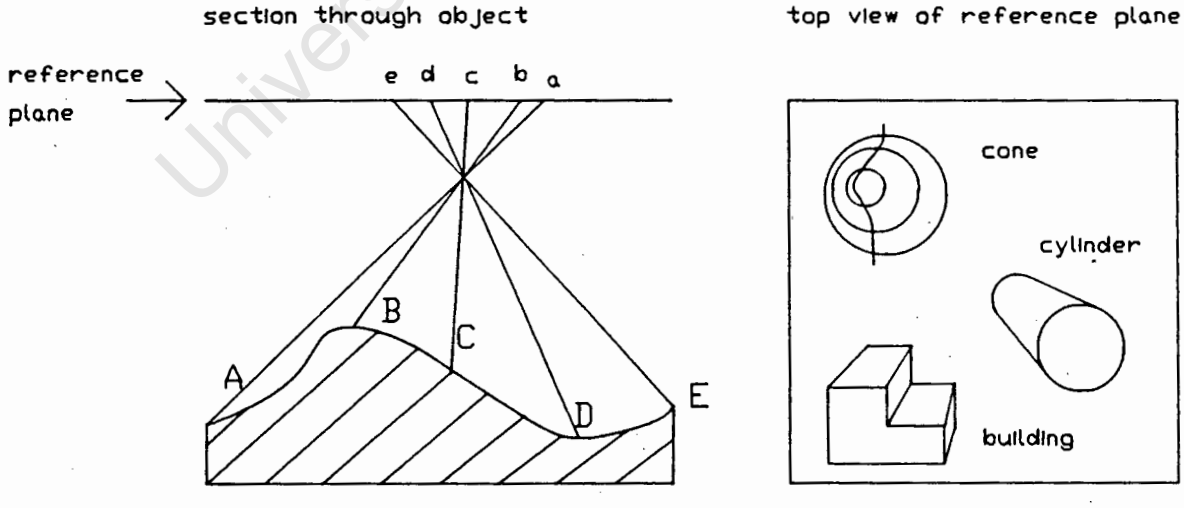

Fig. 2.4 Perspective projections

A perspective projection is only a scaled reproduction of the original points if all these lie in a plane parallel to that of the reference plane.

In this thesis the word 'projection' will always refer to a perspective projection if not otherwise specified.

2.3.2 Image and Object Space

The region between the focal point and the reference plane (image plane) of the camera is known as the image space. For convenience, it is often imagined to be in front of the focal point (positive) rather than behind it (negative). The point at the centre of the image plane is called the principal point and serves as the origin of the image space. The region occupied by the object being imaged including its coordinate system is called the object space (see Fig. 2.5).

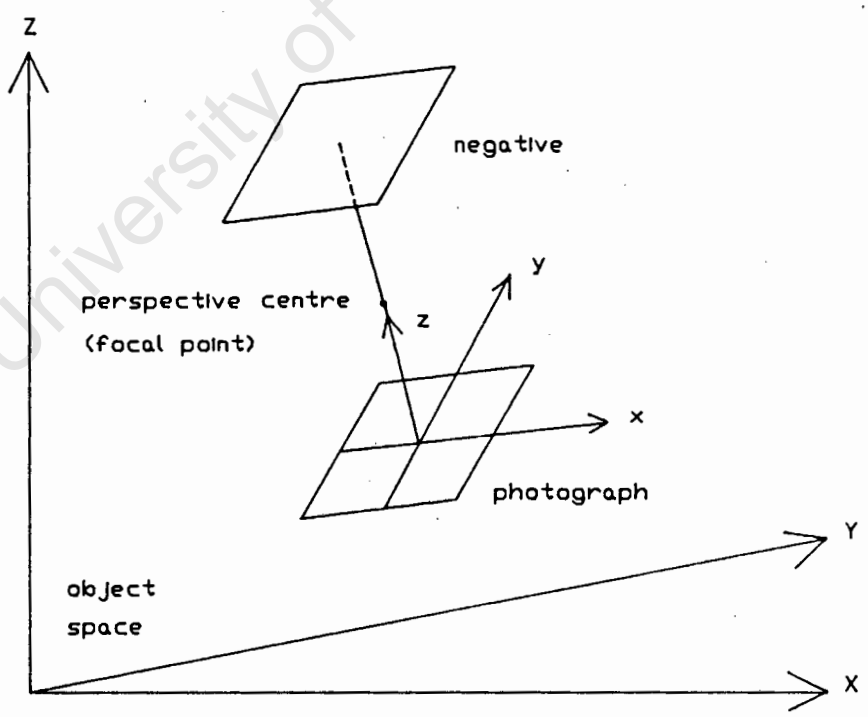

Fig. 2.5 Image and object space

In this text image space and object space coordinate systems are labelled with lower (xyz) and upper (XYZ) case letters respectively.

2.3.3 Interior Orientation

In photogrammetry interior orientation refers to the position of the perspective centre in the image space. It is given by the position of the principal point (x_o, y_o) and the perpendicular distance from the image plane to the perspective centre (f) (see Fig. 2.6).

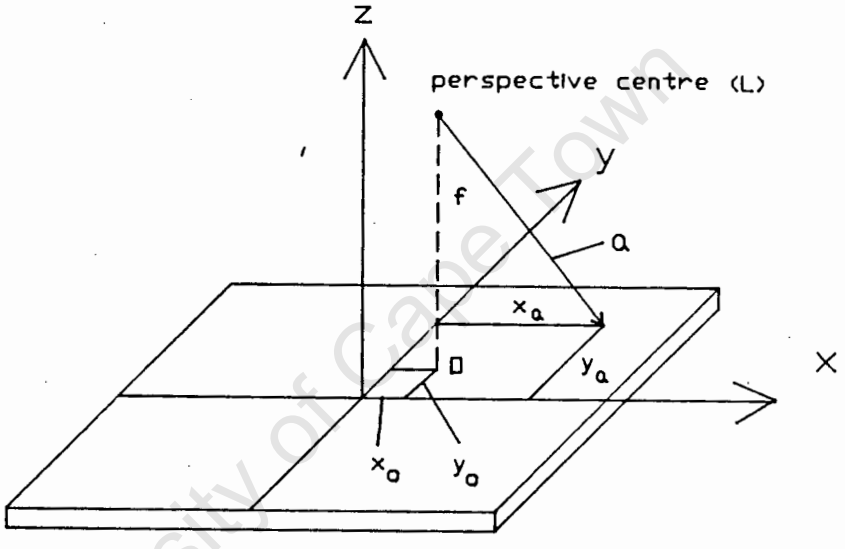

Fig. 2.6 Interior orientation

2.3.4 Exterior Orientation

The exterior orientation of a photograph defines its position and orientation in the object space (see Fig. 2.7). Usually, the position of the perspective centre is given in cartesian coordinates of the object space (X_o, Y_o, Z_o). The orientation is defined by the rotations omega, phi, kappa required about the x, y, z axes of a cartesian coordinate system parallel to that of the object, but with its origin at the perspective centre (O), so that its axes will then be parallel to those of the image space. Another common system of defining orientation in photogrammetry

is the α (azimuth), t(tilt), s(swing) system. However, in this thesis the omega, phi, kappa system has been used.

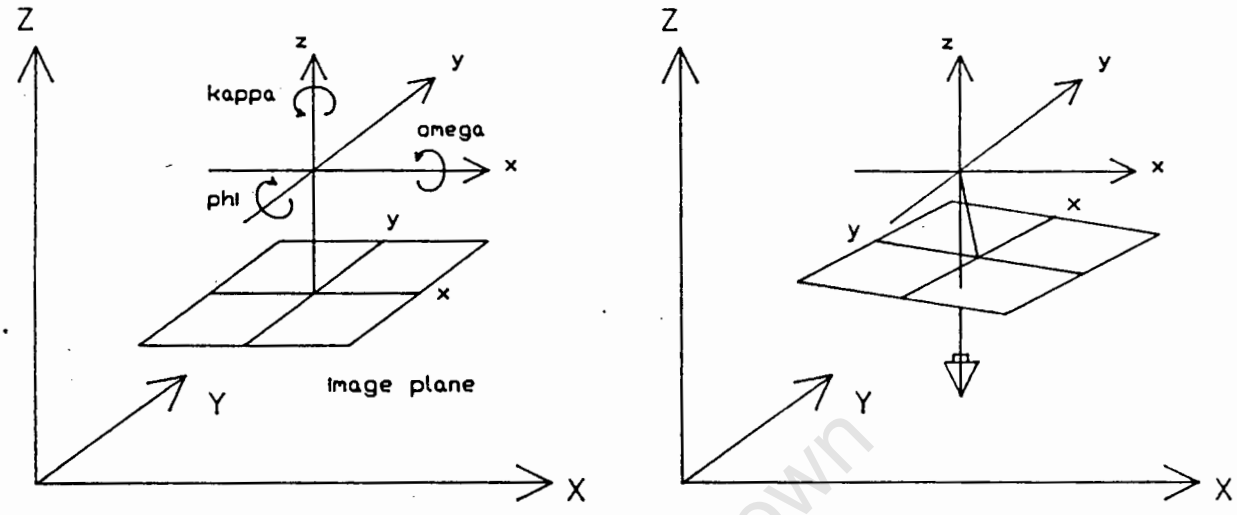

Fig. 2.7 Exterior orientation by omega, phi and kappa

The spatial relationship between the object and image space can be expressed by an orthogonal 3x3 matrix which is a function of omega, phi and kappa. By convention $\underline{M}$ is the matrix that transforms the object space into the image space.

$$\begin{bmatrix} x \\ y \\ z \end{bmatrix} = \underline{M} * \begin{bmatrix} X \\ Y \\ Z \end{bmatrix} \quad \text{and} \quad \begin{bmatrix} X \\ Y \\ Z \end{bmatrix} = \underline{M}^T * \begin{bmatrix} x \\ y \\ z \end{bmatrix}$$

For a derivation of the orientation matrix $\underline{M}$, see Appendix A.

2.3.5 The Collinearity Condition

As mentioned previously, during photogrammetric reconstruction the perspective centre, the image point and the corresponding object point must lie on one line. This is the collinearity condition and can be expressed mathematically as

$$\underline{a} = k * \underline{A} \qquad (1)$$

where $\underline{a}$ and $\underline{A}$ are vectors as shown in Fig. 2.6 and Fig. 2.8 respectively, and are expressed in the same coordinate system. k is a scalar.

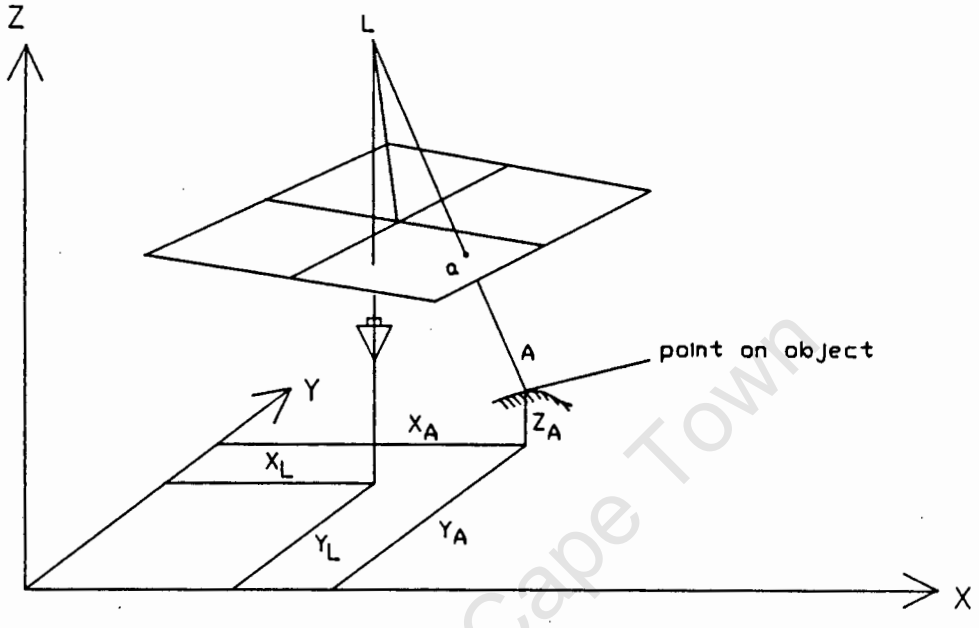

Fig. 2.8 Collinearity condition

Expressing $\underline{a}$ and $\underline{A}$ in the x, y, z coordinate system :

$$\underline{a} = \begin{bmatrix} x_a - x_o \\ y_a - y_o \\ -f \end{bmatrix} \quad \text{and} \quad \underline{A} = \underline{M} * \begin{bmatrix} X_A - X_L \\ Y_A - Y_L \\ Z_A - Z_L \end{bmatrix}$$

Hence, the equation above becomes :

$$\begin{bmatrix} x_a - x_o \\ y_a - y_o \\ -f \end{bmatrix} = k * \underline{M} * \begin{bmatrix} X_A - X_L \\ Y_A - Y_L \\ Z_A - Z_L \end{bmatrix}$$

<u>This is one form of the collinearity condition which forms the basis of all procedures in photogrammetry</u>.

2.4 Obtaining the Third Dimension from Two Overlapping Photographs

Since a photograph is a two-dimensional record of a three-dimensional object, one dimension is lost at the instant of exposure. Hence, it is generally not possible to recover all the dimensions from one photogragh. However, if the interior and exterior orientations of the photograph are known or can be determined, then the direction of a ray passing from the perspective centre through the image point can be found from a single photograph. Where on this ray the corresponding object point is situated cannot be determined. However, if this object point is present on two photographs taken from different exposure stations, then the object point is uniquely defined.

By considering the two ovelapping photographs depicted in Fig. 2.9 the reconstruction of an object point can be described. Knowing the interior and absolute exterior orientations of each photograph, the direction of the ray passing through the projective centre, the image point and the object point is found by collinearity.

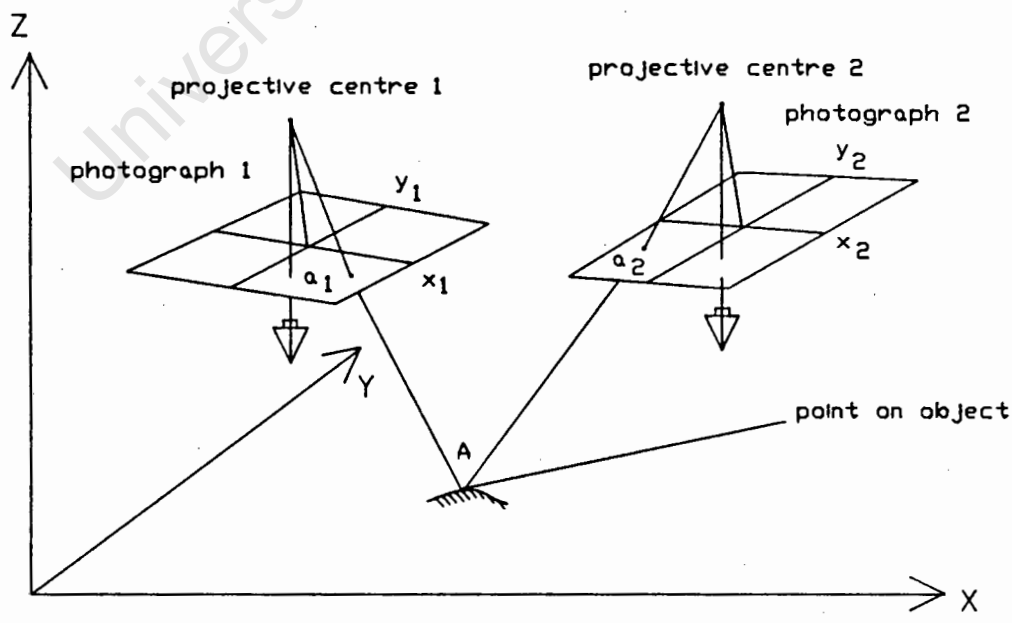

Fig. 2.9 Geometry of two overlapping photographs

The collinearity equations for both photographs can be written.

$$\underline{a}_1 = k_1 * \underline{M}_1 * \underline{A}_1$$
$$\underline{a}_2 = k_2 * \underline{M}_2 * \underline{A}_2 \qquad (2)$$

where k is a scale factor and $\underline{M}$ is the orientation matrix. Once the unknowns k and $\underline{M}$ have been determined, the XYZ coordinates of any point A can readily be calculated from measurements of the image coordinates.

In order to solve the photogrammetric problem, all the parameters of equations (2) must be known; ie. in order to solve for $\underline{A}$ given $\underline{a}$. This is the case if the interior and exterior orientation of both cameras are known.

However, more often than not, these parameters are not known. The exterior orientation is sometimes known (to a degree) but not to sufficient accuracy. The interior orientation is generally only known with metric cameras, cameras which have been designed specifically for photogrammetric purposes. These cameras have fiducial marks so that the photocentre can be accurately determined, and the camera's focal length is known to a certain tolerance. With non-metric cameras, for example amateur and professional 35 mm cameras, the interior orientation is not known.

As soon as any one degree of camera orientation is not known, one or more control points are required to solve for the resulting unknown parameters of equations (2). Control points are points which have been accurately surveyed; ie. their position with respect to ground (XYZ coordinates in Fig. 2.9) is known. In the literature, the words 'control points', 'targets' and simply 'control' are used synonymously. Ideally, control points should be evenly spaced around the perimeter of the two overlapping photographs (stereopair).

The number of unknowns determines the number of control points required. Each control point generates one pair of equations.

Finally, if more control is available than is required redundancy results. There are various mathematical techniques to solve for the 'best' solution where this occurs.

2.5 Projective Transformation - Restitution of the Object

As previously stated photogrammetric reconstruction can be done graphically, numerically, analytically, or by a combination thereof. Analytical photogrammetry tends to be more accurate than analogue or semi-analytical methods since it can more effectively remove systematic errors caused by, for example, lens distortions. However, from a practical viewpoint a computer is necessary to deal with the large amounts of data and the many computations generated by analytical photogrammetry.

Restitution of the object consists of precicely surveying ground control points and measuring their respective coordinates on two photographs to achieve relative and absolute orientation and, if necessary, to solve for these separately.

Over the years, various methods in analytical photogrammetry have evolved. However, conceptually all of them centre around enforcing condition equations on multiple photographs. The most commonly used condition equation is the collinearity equation. The various methods differ mainly in the way the condition equations are enforced or, how the resulting set of simultaneous equations are solved.

Outlined below is the projective transformation method (Adams, 1981) which uses the collinearity condition. The collinearity equation has been stated in vector form in equation (1) (Section

2.3.6). Equations (3) are merely another form of the collinearity equations for two overlapping photographs and are derived from the same condition (perspective centre, image point and object point must be collinear) as was equation (1). The derivation of the collinearity equations (3) are given in Appendix B and are repeated here for convenience.

$$x = \frac{b_{11}*X + b_{12}*Y + b_{13}*Z + b_{14}}{b_{31}*X + b_{32}*Y + b_{33}*Z + 1}$$

$$y = \frac{b_{21}*X + b_{22}*Y + b_{23}*Z + b_{24}}{b_{31}*X + b_{32}*Y + b_{33}*Z + 1} \qquad (3)$$

where x, y are image coordinates (measured from any arbitrary origin on the photograph), and X, Y, Z are space coordinates of the corresponding point.
Equation (3) can be rewritten as

$$\begin{aligned} b_{11}X + b_{12}Y + b_{13}Z + b_{14} - b_{31}Xx - b_{32}Yx - b_{33}Zx - x = 0 \\ b_{21}X + b_{22}Y + b_{23}Z + b_{24} - b_{31}Xy - b_{32}Yy - b_{33}Zy - y = 0 \end{aligned} \qquad (4)$$

Provided there are a sufficient number of control points in a stereopair, the b_{ij} terms (11 unknowns) of equations (4) can be solved for each photograph. Since two equations can be written per photograph for each control point, a minimum of six such points is required - giving one redundancy. However, the following important restrictions must be borne in mind :

1. no more than four control points should be coplanar.
2. no more than three points should be collinear.

Once the b-parameters have been solved for each photograph, it is simply a matter of backsubstitution into equations (4) and measuring the image coordinates of the points of interest on both plates. Substituting these measured coordinates (x and y)

into equations (4) generates four linear equations in X,Y,Z (the coordinates of the object space) which are easy to solve.

However, equations (3) and (4) are not linear and hence, more than one 'best' solution is possible. The 'least squares' iterative approach is popular in photogrammetry and is found in virtually every book on the subject. Adams (1981), however, argues that in certain instances a much simpler, faster approach will yield practical results. A discussion of techniques such as 'least squares adjustment' is beyond the scope of this thesis and is not needed to understand the photogrammetric process.

CHAPTER THREE

3.0 DEVELOPMENT OF A PC-BASED NRTP SYSTEM

With the advent of solid-state cameras, recent developments in image processing techniques and the ever increasing power of microprocessors, RTP measurement systems for close-range applications have become a possibility. The motivation for developing RTP systems is that photogrammetry with conventional cameras is:

a. relatively slow,
b. very tedious, and
c. requires special skills.

For many applications, especially when studing dynamic scenes, it is desirable to have an on-line, three-dimensional measuring system. This is the ultimate goal. Real-time strictly speaking implies that the system's response time must be within one video cycle (ie. < 1/25 or 1/30 second). To the author's knowledge truely real-time, 3D mensuration systems did not exist at the time of writing. However, a number of NRTP systems have already been developed. A NRT process, although longer than a video cycle practically provides immediate results. For many applications a NRT system presents a very big improvement on the conventional photogrammetric process.

RTP and NRTP camera systems already developed (Wong and Ho 1986, Haggren 1986, El Hakim 1986) typically rely on expensive mini- or mainframe type computers. However, decreasing prices and increasing processing power of PCs will change this in the future.

The stages in design of a RTP process are:

1. Image capture.
2. Target design ie. design of a suitable reference frame and targets to provide ground control.
3. Design of algorithms for target detecting, target centre extraction and target matching.
4. Design of algorithms for image matching ie. algorithms which will measure a number of object points on two or more images and then perform object point matching.
5. Design and development of photogrammetric software, more specifically, software which:
   a) receives as input pairs of matched image coordinates of the targets.
   b) solves for camera orientation (implicitly or explicitly depending on the photogrammetric method used).
   c) uses the constants determined above to transform pairs of matched image coordinates of points into 3D space coordinates.
6. Design and development of application software to make the system user friendly. The various software components that are developed and the functions performed by the bought in soft- and hardware must be integrated.

The next section describes the hardware and the software that has already been developed for a low-cost, PC-based NRTP system - PHOENICS (Photogrammetric Engineering and Industrial Camera System). Future extensions to PHOENICS are also discussed.

PHOENICS is being developed by UCT's Department of Surveying and has produced some promising results in its initial stages. Although the long term aim is to produce a real-time system, speed is of lesser importance when configuring hardware and developing software for a prototype system. The dimension of real-time or near-real-time will be added later.

Hardware Configuration of PHOENICS

The present hardware configuration of PHOENICS is shown in Fig. 3.1 and Fig. 3.2 below.

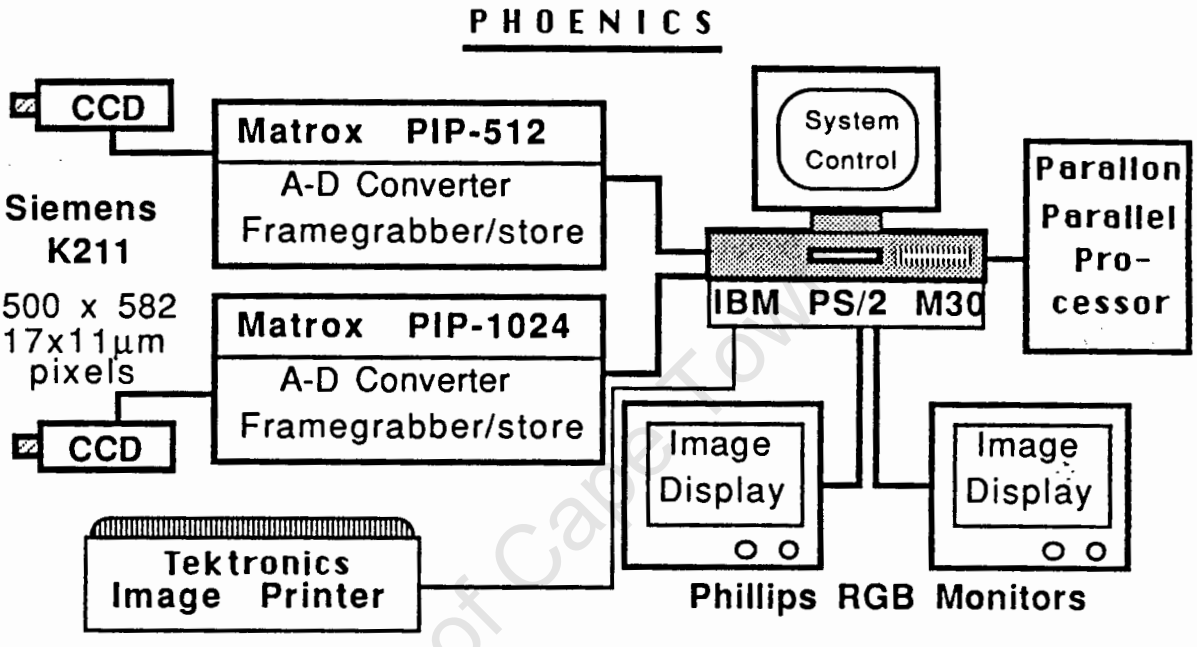

Fig. 3.1 Schematic of PHOENICS hardware configuration

The host computer is an IBM-Personal System/2 Model 30 and has a high resolution monochrome screen. Images can be displayed in formats of 640x400 with 16 grey shades or 320x200 with 64 grey shades on the PC screen, or complete images may be displayed on the two RGB monitors with 256 shades of grey. Motivations for the choice of this PC are given by Parkyn and Rüther (1988).

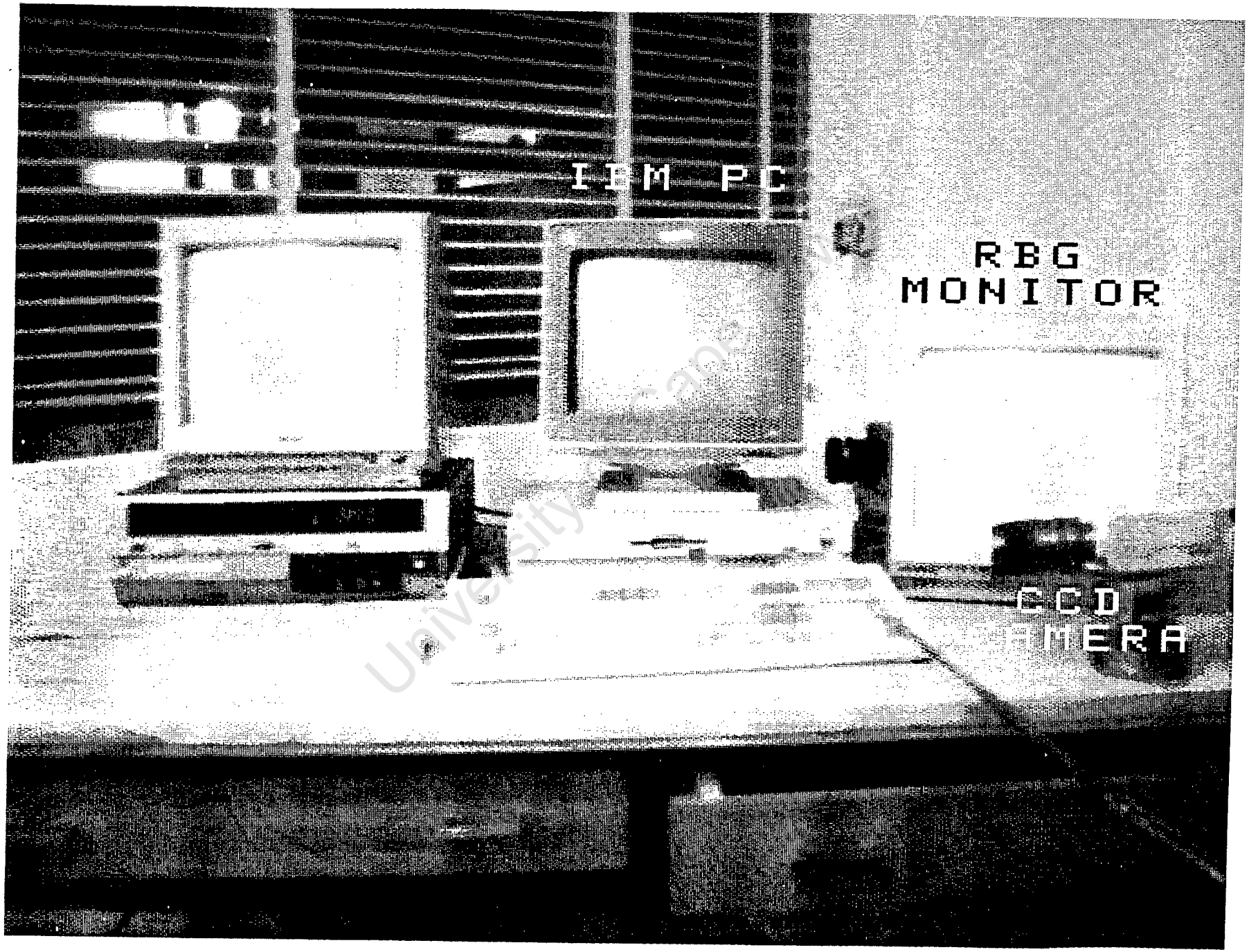

The system uses two Siemens K211 monochrome solid state charge coupled device (CCD) cameras to perform image capture. The physical size of the sensor is approximately 9 mm x 7 mm and consits of 500x582 pixels. The frame grabbing time is 1/25 second. A pixel is the smallest unit area over which the average light intensity is measured.

Although CCD's are also termed 'digital' cameras, their output is in fact a continious analogue amplitude modulated signal. An analogue to digital (A/D) converter then produces an array of intensity levels representing the image. CCD technology has made possible the development of RTP systems. Some of the fundamentals of the technology are given in chapter 4.

As mentioned earlier, the CCD cameras provide 25 frames per second as an analogue signal. Each video image is converted to an array of 8-bit pixels (representing 256 shades of grey) and then passed through look up tables (LUT), in which the grey values are transformed in a predetermined manner. The image can either be stored on disk or it can be converted back to an analogue signal and displayed. To acieve this in 1/25 second for 0,25 million bytes in the case of PHOENICS, additional hardware known as framegrabbers or video digitizers must be added to the PC. Often such video digitisers include some processing software and are then called image processing (IP) boards. Typical operations possible with an IP board are edge enhancement, noise removal, thresholding (ie. producing black and white images from 'grey' images), inverting images, changing the grey value of any pixel etc.

Phoenics has two IP boards, the MATROX PIP-512 and PIP-1024, allowing simultaneous stereo imaging. The boards fit directly into the PC and digitise the analogue signals from the two cameras into 512x512 pixels with 256 shades of grey. This means that 15% of the camera image is lost and the original pixels are

transformed in size. However, Parkyn and Rüther (1988) state that this can be dealt with in the photogrammetric solution.

Each board has a 256 kbyte buffer, enough to store one image. Once in the board-buffer, images may be stored in memory, or on a hard or floppy disk for later processing.

At present, parallel processors are being added to PHOENICS to decrease processing time. Parallel processing allows operations which must be performed on a number of pixel arrays to be done simultaneously.

Images which are generated with PHOENICS can be printed using the Tectronics image printer.

Software developed and used with PHOENICS includes automatic target detection and calculation of object coordinates of targeted object points using projective tranformation. For automatic target detection a binary image is first created with the MATROX IP. The pixels of the original image are mapped to one of two chosen values depending on whether their grey values are above or below a specified threshold value. For successful thresholding, targets should appear considerably lighter or darker than the backgound. Once targets are found, their centres are determined using a weighted mean technique (Wong and Ho, 1986) on the original image.

Experimentation with various target designs for control points revealed that the following design produced the best results (see Fig. 3.3).

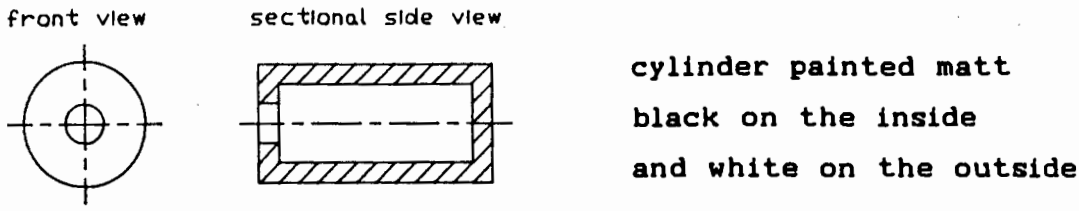

Fig. 3.3 Control point target design for PHOENICS

First results of automatic target detection and subsequent projective transformation of targeted points have revealed accuracies of 0,5 mm in X and Y, and 1 mm in Z for a camera to object distance of 1,7 m ie. 1:3400 to 1:1700.

Currently work is continuing on introducing parallel processing to PHOENICS, camera calibration and testing, and the development of image matching algorithms. The latter is the subject of a later chapter.

As was previously mentioned, many RTP and NRTP systems are dedicated systems, as truly general systems become extremely complex. The way in which PHOENICS hopes to address this, is by producing software modules which are efficient for specific applications, and allowing the operator to choose the best combination of these modules for a particular application.

CHAPTER FOUR

4.0 IMAGE AQUISITION WITH CCD CAMERAS

This chapter is intended to serve as an introduction to the technology of self-scanning solid state cameras and the older vidicon cameras. At the end of the chapter the two types of cameras are compared.

Advancements in microelectronics and semiconductor technology over the past 15 years have opened up new avenues for the data aquisition phase of the photogrammetric process. Photographic cameras can be replaced by digital ones and combined with fast data flow to a computer for further image processing. The advent of digital cameras has made possible the development of RTP systems.

There are two main reasons why RTP is not possible with film-based cameras. Firstly, there is the lead time for developing the film, and secondly, these negatives must first be digitised to perform tasks such as automatic target detection and positioning, and automatic image matching.

Apart from this, it is interesting to note some distinctive characteristics of digital (or solid state) cameras when comparing them with film-based cameras (Gruen, 1987).
Digital cameras have:

- a very small imaging area (< 100 mm^2) and hence a small image scale
- limited resolution; presently photogrammetric cameras have a better spatial resolution than digital cameras
- fixed exposure time; the integration time can not be altered
- an extremely stable image plane
- possible electronic noise.

Of these characteristics, the extremely stable image plane is the only one in favour of digital cameras.

4.1 The Vidicon Camera Tube

The vidicon tube is the basic principle on which a TV camera operates. The vidicon is a cylindrical glass envelope containing an electron gun at one end and a photoconductive target covered by a thin, positively-charged metal coating at the other (Fig. 4.1). A lens system produces an image of the scene on the photoconductive target.

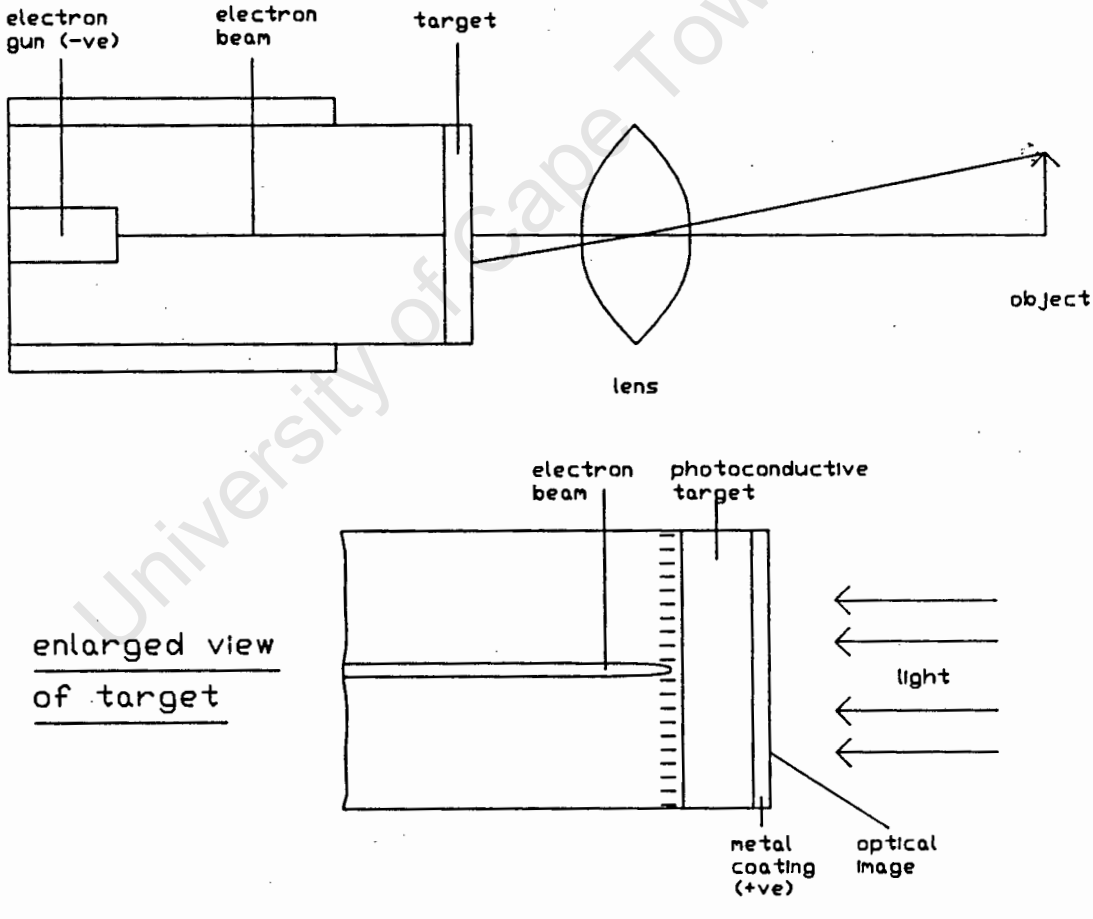

Fig. 4.1 Vidicon Camera tube

The electron beam scans across the back of the target and deposits electrons on it. When light strikes the photoconductive target the electrons flow through it to the positively charged metal coating thereby locally depleting the deposited electrons. Thus, an optical image formed on the front of the target will result in an identical electron image on the back of the target. When the beam subsequently scans the target and replaces electrons in the depleted regions a current flows. This current is proporional to the electrons required to restore the original charge which in turn is dependent on the light intensity at that point. While the electron beam continuously scans the image, the changing current flow produces the video signal of the vidicon. Control over the electron beam is exercised by an electric field surrounding the tube.

The European video standards (PAL for colour and CCIR for black and white) define 625 lines at a frequency of 25 Hz. In actual fact, the video image consists of two half images of alterate lines scanned at 50 Hz which are superimposed. This interleaving of two image 'fields' is known as the interlace principle. As a number of lines are required for syncronisation and other purposes only 575 lines remain for the image (Schild, 1988). An image thus consists of a number of lines each of which is an amplitude modulated signal. This is the big difference between a CCD and the vidicon tube - the image is only discretised in the vertical direction. In order to provide a basis for comparison of the two the following approach can be adopted: Since theoretically the smallest vertical resolution is one line we can expect/assume the same resolution horizontally ie. a square picture cell as the smallest image element. From the base to height ratio (4:3) of a TV screen this would mean that there are 575x764 (= 440 000) picture cells in a video image.

A frame rate of 25 Hz of an image with 440 000 picture cells translates to a pixel scanning frequency of 11 MHz. To increase

the resolution, a larger image is required which in turn requires a higher scanning frequency in order to comply with the video standard. Until recently larger images were not produced because of the difficulty to keep within the video standard requiring 25 frames per second. However, Japanese research dating back to 1970 has now produced High Definition Video (HDTV) with a resolution of approximately 1300x1000. At a frame rate of 25 Hz this translates to a pixel frequency of about 32 MHz. At present such frequencies can only be achieved with tube cameras (Gruen, 1987).

4.2 Solid State Sensors

Solid-state sensors use semi-conductors to transform light into an electrical signal. Unlike vidicon tubes, solid-state sensors do not have a scanning electron beam neither do they have any other moving parts. In the literature, the terms 'CCD' and 'solid state cameras' are often used synonymously. Strictly speaking, however, this is incorrect since a CCD is only one class of solid state camera making use of a particular technology. Furthermore, solid state cameras are often termed 'digital cameras'. Again, this is not necessarily correct. The output of these devices is more often an amplitude modulated, analogue signal and not a digital one. The analogue signal is digitised for computer processing, but with a separate technology.

Basic theory of semiconductors

The characteristic of intrinsic semiconductors, those that are not doped or pure, is that all their outer electrons are resident in their lowest possible energy level known as the valence band. By supplying external energy a few electrons will be able to leave the valence band and enter the conduction band, a much higher energy level. This would leave a hole in the valence band and the net positive charge of the atom will attract another electron. In this way, holes and electrons can move through the lattice (ie. the conductivity is increased). The extent to which

this phenomena occurs can be controlled by 'doping' the semiconductor with an element having fewer or more valence electrons than itself (ie. creating more holes or free electrons). Every time a hole and a free electron combine energy is liberated. This process can also be reversed by supplying energy in the form of light to produce an electron hole pair.

The photodetector

A photodetector changes light (energy) into electrical energy. If a potential difference is applied accross a doped semiconductor, the current that will flow is proportional to the amount of light falling onto it.

Through integrated circuit and recent semiconductor technology such sensors can now be built extremely small (to a few square micrometres) and positioned accurately to fractions of microns in a matrix. What remains to be done in order to record an image is to collect all the electrical signals from each sensor and process them. Solid state cameras can be classified according to the type of signal they have as output. The three categories are:

- CCD (Charge Coupled Device)
- CID (Charge Injected Device)
- Photodiodes

RTP systems normally use CCD cameras.

4.3 CCD Cameras

A CCD camera has photodetectors with a MOS structure (Metal-Oxide-Semiconductor). It consists of a doped semiconductor, an insulator (glass) and a metal electrode (Fig. 4.2). A large number (between 200 and 2000) of these photodetectors are arranged next to one another to form a sensor row.

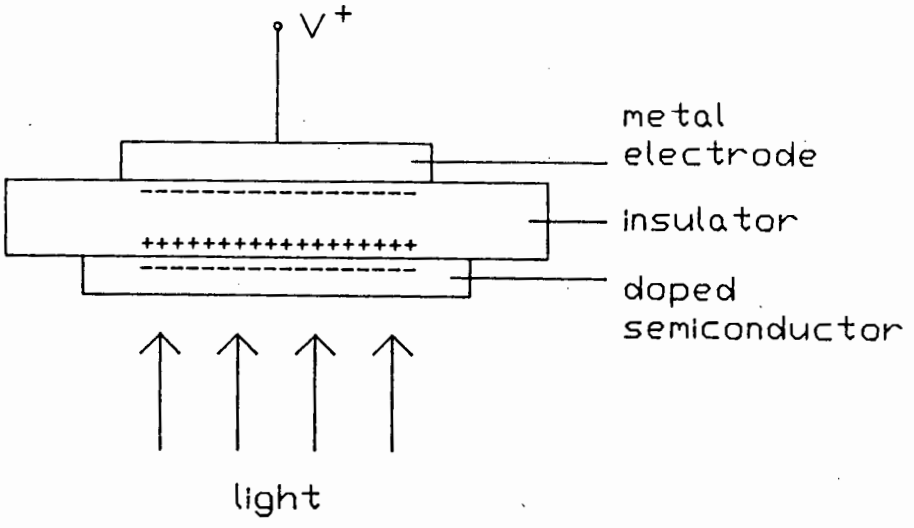

Fig. 4.2 CCD MOS structure

Applying a positive potential to the metal electrode, called a gate, will lead to a negative charge build-up on the other side of the insulator. The extent of this charge build-up depends on the amount of light falling on the detector. The more light there is, the more free electrons there are, the larger the charge. The charege build-up is also a function of the number of free electron-hole pairs in the semiconductor (this depends on the extent of 'doping' and does not vary with time).

The way in which the accumulated charge of a whole row of adjacent sensors is transported depends on whether the device is a 2-, 3- or 4-phase CCD (Dähler, 1986). In each case, however, charges are transferred along lines parallel to the row of sensors.

If a number of sensor rows are placed next to each other they make up what is known as the sensor array. It is the shiny area (less than 100mm^2) which can be seen in the image plane of a CCD.

4.3.1 Interline vs Frame Transfer

CCDs can be categorized according to how the charge transfer of the sensor array takes place. There are two methods by which this is done; interline transfer or frame transfer.

Interline transfer

The image area of the interline design consists of alternate columns of photosensitive sensors and opaque shift registers (Fig. 4.3).

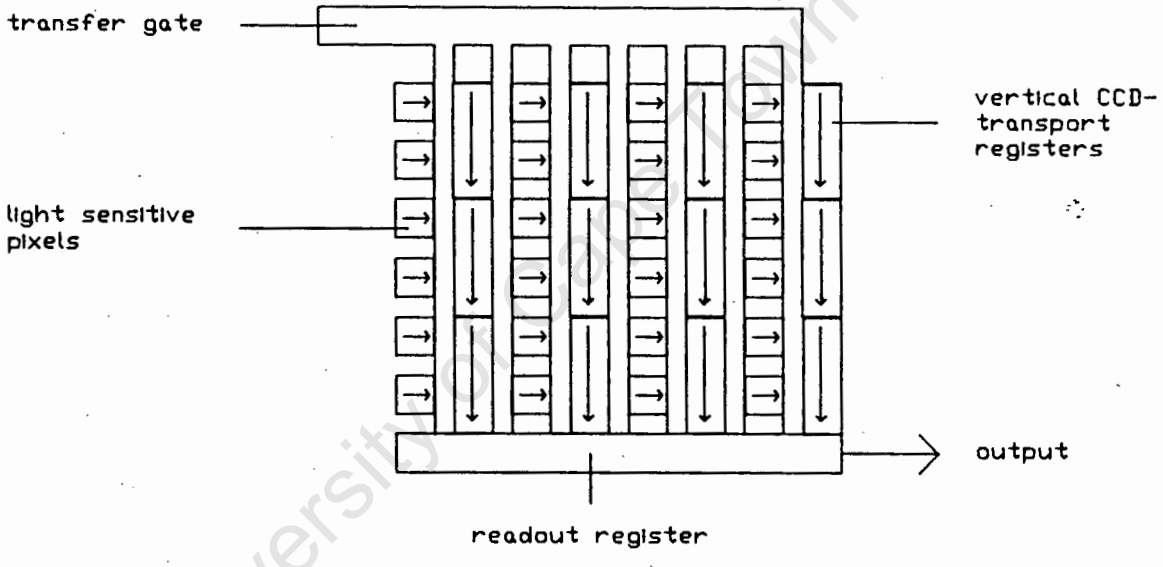

Fig. 4.3 Interline charge transfer

During the integration time ('exposure' time) charge is accumulated at the photosensors and is then passed to the adjacent shift registers for storage. From there the charges are shifted vertically to the horizontal line readout register on the next integration cycle. In this way an image, in the form of light induced charges, is sent out of the camera pixel by pixel onto one single video line. Since the number of imaging columns is the same as the number of shielded readout registers, only half of the chip area is photosensitive.

Frame transfer

In the frame transfer type image plane CCD cells are practically in contact horizontally and vertically (Fig. 4.4).

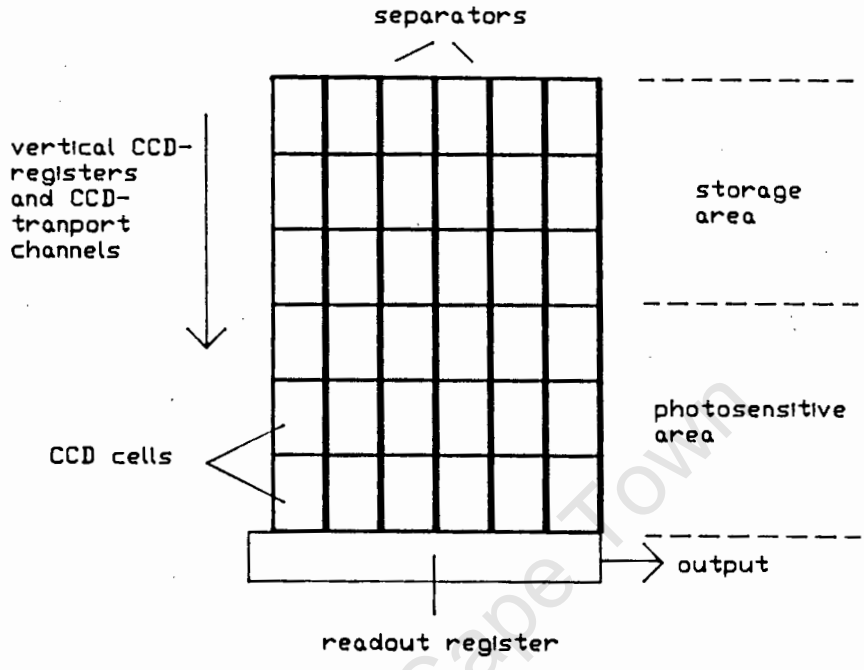

Fig. 4.4 Frame charge transfer

Half of the chip area is optically sensitive and accumulates charges during the integration time. Subsequently, the charges are transfered in parallel to the storage area which is shielded from light. The stored charges are read out through a horizontal shift register in the following integration period.

The advantage that interline has over frame transfer is the absence of smearing. Smearing occurs in frame transfer because exposure of the photosensitive areas continues during charge transfer. As a result, a charge being transfered past a very bright spot tends to pick up some additional charge. This appears as a fine, faint vertical line beginning at a bright spot on the display. The more complicated architecture of the interline concept eliminates smearing.

An important factor to consider when imaging dynamic scenes is the integration time of the device. The integration time for a frame transfer sensor is half that of an interline sensor and thus the former will record fast movements more clearly (Schild, 1988).

The main cause for differences between the two concepts is that with interline pixels are separated. This means that for a fixed total chip area and number of pixels, the lightsensitive areas are equal, merely distributed differently. However, since the light sensitive pixels in an interline design would be distributed over an area twice the size as that of the frame transfer design, the latter will have a better resolution. If, on the other hand the same number of pixels cover the same area for both designs, their resolution will be equal yet the interline sensor would only have half the light sensitivity. These observations have made frame transfer CCDs more popular with photogrammetrists (Real, 1986).

A phenomenon that an interline sensor can suffer is Moire-effect. This only occurs when imaging objects of very fine structure. Instead of showing an average intensity over an area, the image displayed has alternating light and dark bands.

One problem with all solid state cameras except CIDS (Real, 1986) is blooming. Blooming is known as that effect which causes a very bright spot in the object space to appear larger in the image than it really is. It is caused by the creation of excessive charge and subsequent overflowing of charge to adjacent pixels. Automatic aperture setting can not solve this problem as it responds to the average illumination of the whole scene. Fortunately, new technology will ensure that blooming will soon be a thing of the past (Dähler, 1986).

4.3.2 CCD Performance Features

Commercially available CCDs have area arrays ranging from 128x128 to 600x600 pixels usually covering less than 100 mm^2. The size of an individual pixel ranges from 60x60 micrometres down to 10x16 micrometres. Pixel intensity is usually converted to an 8-bit byte. This represents 256 grey scales. An exeption is the high resolution Kodak Megaplus CCD which has an area of approximately 9x7 mm containing 1320x1035 pixels.

Two current limitations of CCDs are their very small imaging areas and spatial resolution. Unfortunately, these limitations can not simply be overcome by manufacturing larger format CCD arrays. These would require improvements to the present charge transfer technology. They would also require hardware capable of processing the vast amounts of data that will be generated within one video cycle. Other approaches are mosaicked-arrays (Gruen, 1987) and zig-zag arrays (Hirschberg, 1985).

As mentioned earlier, the charge generated in a pixel is sent out of the camera in analogue form and is then digitised. However, seldom is the number of pixels in the image plane the same as those produced by the analogue to didital (A/D) converter: eg. in the case of PHOENICS a 568x468 image array is transformed to a 512x512 array by the A/D converter. The question thus arises of what happens geometrically to these pixels and what the effect is on camera resolution. This problem is specific to the particular hardware configuration and must be investigated wherever measurements on the image are to be made.

CCDs used in photogrammetric applications are usually of the black and white type. Colour CCDs do however exist. In these devices incomming light is split up into three colours (red, blue, green - RBG) with a lens system, and their intensities are recorded by three different photosensitive arrays. They are

processed separately and then displayed on an RBG monitor. The obvious disadvantage is that spatial resolution decreases since an object space represented by one pixel in a black and white image, now requires three or sometimes even four pixels depending on the CCD design.

4.4 CCD vs Vidicon Tube Cameras

Although both solid state and vidicon tube cameras may be used for real-time photogrammetric applications, vidicon cameras are not expected to be used for this purpose in the future because they suffer from large geometric distortions. Real-time systems currently being developed (Haggren, 1986; Gruen, 1986; Wong, 1986) largely use CCD cameras. CCDs are preferred over Vidicons for the following reasons:

- high geometric fidelity of array picture elements in space and time
- small, lightweight and rugged
- low power consumption
- high dynamic range
- maintenance free
- no damage through overlighting
- low cost

Factors in favour of Vidicons are:

- better operation at lower light level
- higher resolution and less Moire
- faster image capture

The overriding factor responsible for photogrammetrists turning to CCD cameras for real-time applications is their metric stability.

The higher resolution of Vidicon tubes applies to comercially available cameras. It was pointed out earlier that the average TV

has an equivilent of approximately 440 000 pixels whereas for an average CCD the figure is below 350 000. Especially with the development of comercial HDTV with around 1000 lines (equivalent to 1,3 million pixels) the better resolution of electron tube imagers is emphasized. Nevertheless, CCD resolution is good enough for many photogrammetric applications.

The limiting factor preventing larger photosensitive chips with more pixels is charge transfer efficiency (CTE). The CTE is the efficiency with which a charge can be transferred from one photocell to the next. It depends on the available charge transfer time which in turn is dictated by the frame rate. At present CTEs of 99,9999 % are being achieved with comercial CCDs that comply with the video standards (frame rate of 25/second). The effect of increasing array sizes, is a decrease in charge transfer time since more charges must be transferred in the same time. Since the time allowed for charge transfer is less, the CTE will also decrease. This results in a generally poorer image being displayed. However, larger format CCDs with higher resolution are possible as the frequency of charge transfer in todays cameras is only between 1% and 10% of the theoretically possible value.

CHAPTER FIVE

5.0 A REVIEW OF NRTP SYSTEMS WITH REFERENCE TO THE IMAGE MATCHING TECHNIQUES USED

One of the most difficult operations in photogrammetry to automate is image matching. As explained in chapter 2, after having solved for camera orientation using control points it is necessary to identify a sufficient number of corresponding object points on the two images that will enable reconstruction of the surface from these points.

Keefe and Riley (1986) state that this becomes particularly difficult on relatively featureless surfaces like a human face. According to Wong (1987) present algorithms for digital image correlation can not match the capability of an experienced human operator. This applies in particular to close-range applications because of the large difference in perspective from one camera position to another. El-Hakim (1985) gives some of the factors which complicate automatic matching. Some patches may appear with different brightness in the two images. For surfaces with a certain shape or texture, where the light intensity is the same for all surface points or follows a periodic pattern, there will be no unique solution. Further, clarity and contrast of special features such as edges or targeted points varies from one scene to the next, because pixel grey values are affected by surface material, intensity and angle of illumination, camera location and orientation, and atmospheric conditions. It is very difficult to predict the influence these parameteres will have. Some of these problems could even be of great obstacle to a human operator.

A number of techniques for solving the matching problem have evolved over the years. Most of these methods were established whilst developing a NRTP or RTP system. As a result they are usually part of a dedicated system and hence rely on specific equipment and/or a controlled enviromental condition. Presently,

matching is solved using stereopairs consisting of parallel or convergent digital images and algorithms which find corresponding points. In some cases one of the two images of the stereopair is replaced by a structured light projector with known perspective geometry to simplify the matching process.

The following sections briefly describe some NRT systems which employ automatic and semiautomatic image matching. Digital image correlation, a general image matching algorithm, is discussed at the end of this chapter.

5.1 Isis Scanner

In an effort to gain some quantitive record of the shape of a human back in order to assess various spinal disorders, Turner-Smith and Harris (1986) developed the Isis Scanner. It consists of a projector producing a plane of light and a vidicon camera (see Fig. 5.1).

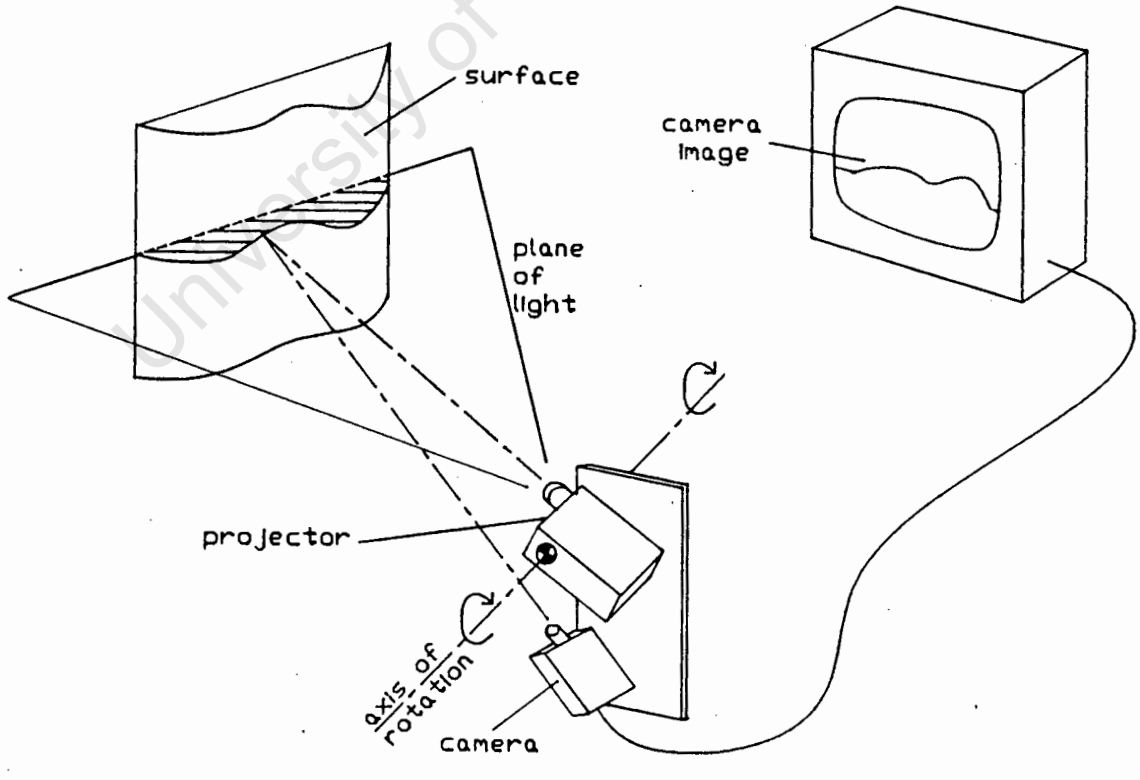

Fig. 5.1 Principle of operation of the Isis Scanner

The position and orientation of the camera with respect to the projector is known and fixed. This assembly, camera and projector, can be rotated so as to move the plane of light across the surface. As the assembly rotates, camera images are stored at known degrees of rotation. The line of light on the surface is seen by the camera as a profile. Once the scan is complete the three-dimensional coordinates along the profile lines can be determined by considering the geometry of the system.

The RMS errors of relative measurements made through a volume of 350x750x100 mm were reported as ±1.1 mm in X, ±1.5 in Y and ±1.7 in Z. These RMS values translate to accuracies of approximately 1:300, 1:500 and 1:60 in the X, Y and Z directions.

The Isis Scanner is similar to the TopoScanner used by Berelowitz (1986) which also solves the matching problem by capturing a large number of images which contain a small amount of information. Since the pattern is simple, there is no ambiguity when calculating coordinates. However, the accuracies achieved with the Isis Scanner are not accepable for the applications intended here.

5.2 Mapvision

Mapvision is a commercially available, RTP machine vision system developed at the Technical Research Centre of Finland (Haggren, 1986). Mapvision uses up to four CCD cameras and an 'especially developed photogrammetric microprocessor'. In order to extract 3D information from a surface, individual points on the object must either be targeted or pointed at with a laser beam. In a way, this approach is similar to the Isis Scanner system of simplifying the matching problem by processing a number of images containing a small amount of information about the surface. Since only one object point appears in each set of images, matching is easy.

Developing algorithms to recognise a well targeted point or spot of light on the object is a relatively simple matter.

To measure a surface with Mapvision necessitates targeting or pointing to a large number of points on the object. Haggren (1986) reports a relative accuracy of 1:5000 which means that a point on the object 5 meters from the camera is measured with an accuracy of 1 mm. In order to measure with this accuracy, assumed to be under ideal conditions, each point requires one second of processing time.

5.3 A RTP System for Object Measurement at the National Research Council of Canada

A system for automatic measurement of 3D coordinates of targeted points has been developed at the National Research Council of Canada, Ottawa (El-Hakim, 1986 and 1985). This RTP system uses a program which combines image processing, pattern recognition and photogrammetric algorithms to automatically map targeted points. These points take the form of filled circles or grid intersections on a highly contrasting background. Points are recognised and accepted as targets by comparing their geometric characteristics with a set of parameters of an ideal target. No information is given by the authors as to how a grid point is recognised or how its centre is determined.

Once the position of control and targeted object points in both images has been determined, matching commences. The a priori knowledge about the number and arrangement of control points is used to validate and identify the control points in each image. El-Hakim (1986) suggests having control points with different shapes to uniquely define them as an alternative for easy matching.

Subsequently, epipolar geometry is used to match targeted object points in the two images. For each targeted point appearing in

the one image, the corresponding epipolar line in the other image is calculated. The point in the second image which best satisfies this line is the matching point. For an explanation of how epipolar geometry can be used as a matching technique, see Appendix C.

Highly contrasting targeted object points were measured with an accuracy of 0.15 mm. Since the distance over which the results presented were obtained is not given, the resolution of the system cannot be quoted here. However, if the assumption is made that the object's image covered the entire active area of the CCD cameras which were used (illustrations in the article suggest that this was the case), then it can be said that a relative accuracy of approximately 1:2000 was achieved.

5.4 A Close-Range Mapping System at the University of Illinois

A close-range mapping system using solid-state cameras developed by Wong and Ho (1986) is described below. The object, a toy moose, was imaged at a distance of 0.9 m. First, the coordinates of the control points (6 mm black dots on a white background) on the digital image were located as follows. Manual indication of the approximate control point position was followed by automatic thresholding of a window containing the control point. The weighted mean technigue was used to determine the centre, and various shape, size and location criteria are applied to check the validity of the target. The position of these control points was determined with an error of ±0.2 mm in X and Y and ±0.4 mm in Z. This is equivalent to a relative accuracy of approximateley 1:2000.

Wong and Ho (1986) use a correlation function to match a search array in the second image with the target array of the first image. These arrays are typically 7x7 pixels. To guide the search the position of pairs of epipolar lines are computed. The position

of the probable matchpoint is estimated using sets of previously determined matchpoints and the search is performed along the direction of an epipolar line (Fig. 5.2).

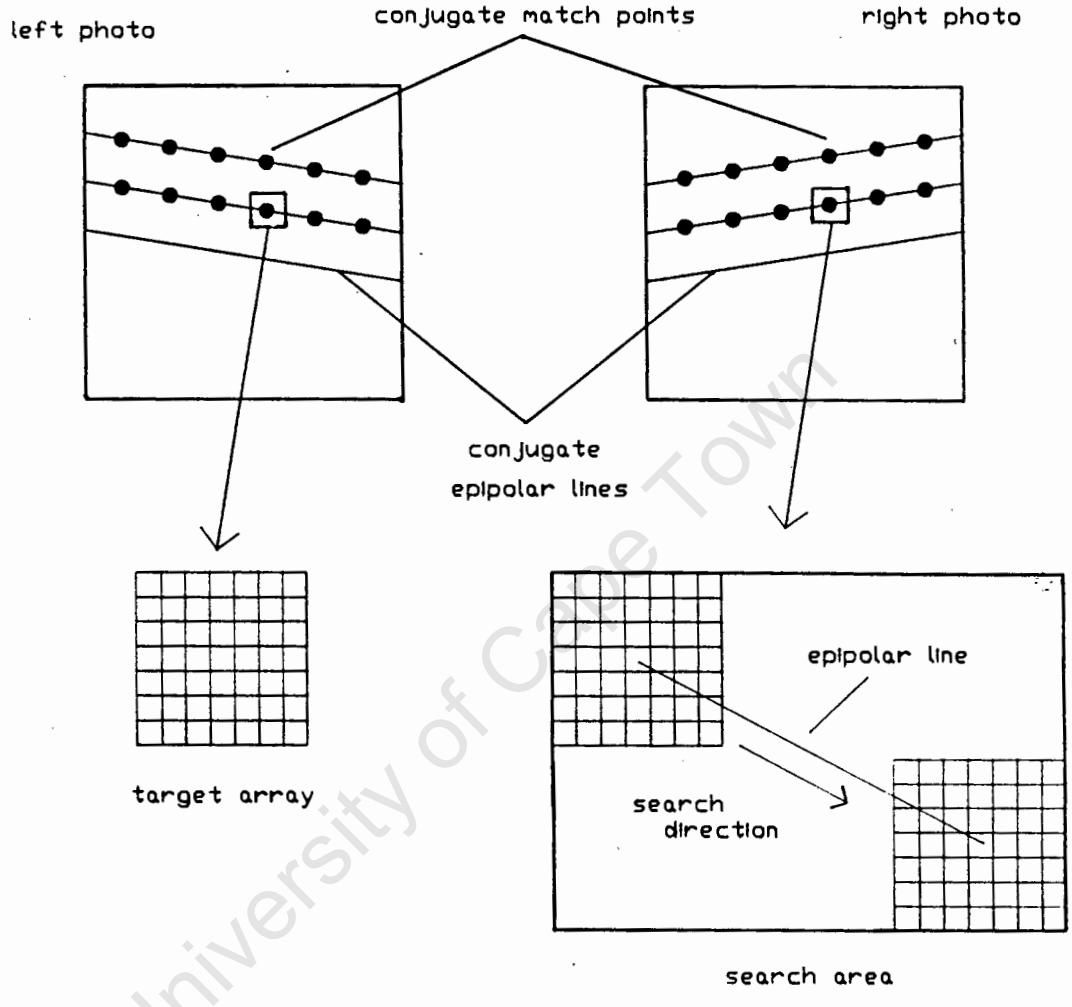

Fig. 5.2 Image correlation along epipolar lines

Tests done with a number of one and two dimensional target array sizes revealed that although larger arrays gave consistently higher success rates of finding a matchpoint, the position accuracy did not improve in the same manner. A 1x9, 1x5, 5x5, and an 11x11 array produced similar accuracies, but CPU time increased markedly for arrays larger than 5x5.

5.5 Robot Vision at the National Research Council of Canada

El Hakim (1985) presents a vision system based on a light strip-sensing technique which in principle is similar to the Isis Scanner system (Turner-Smith and Harris, 1986) described earlier.

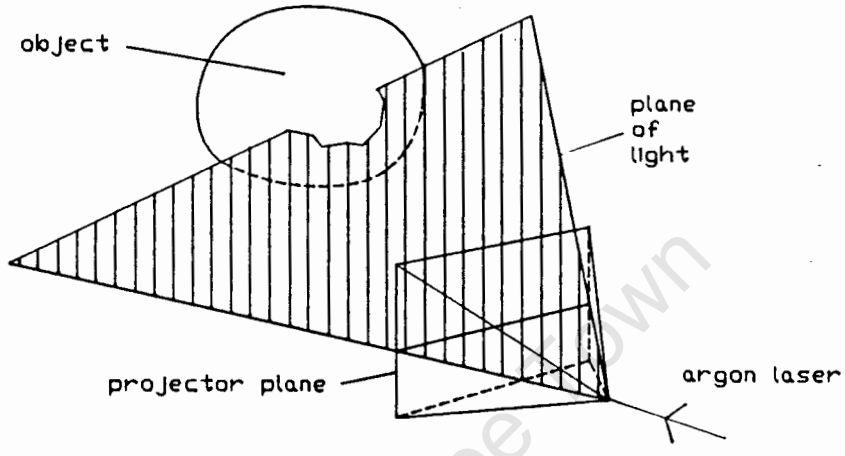

Fig. 5.3 Optical beam deflection assembly

An optical beam deflection assembly (Fig. 5.3) produces a single line of light on the object from an argon laser. The object is scanned with the plane of light (1 second for simple objects) and at predetermined intervals the assembly accurately determines the line position on the projector plane. A control unit syncronizes camera (CCD) activation at the same intervals. Image processing removes noise from the images, and then a number of points on each line are extracted. Accurate x and y coordinates of these line points are determined using thinning techniques (Kreis et al, 1982 in El Hakim, 1985).

Before measuring an object, the camera and light source are calibrated. This is done via a test object with a series of precisely measured control points. Briefly, the calibration process proceeds as follows. First, the unknown orientation parameters of two cameras are determined using the control points in the usual

way. For the light source the interior orientation is known and fixed and the parameters of exterior orientation are determined as follows. The light plane is projected onto the object and the image coordinates of a number of object points on the light strip are used to determine their true XYZ coordinates. This is repeated for different line positions on the projector plane. In a sense, the two cameras are used to generate a set of control points with which the light source is calibrated. From the collinearity equations for the light projector, its orientation parameters can be determined. The light source-camera system is now calibrated.

Knowing all the orientation parameters, the true object coordinates of any object point can be derived from the x, y image coordinates and the position of the light strip (one coordinate on the reference plane).

The system was used to recognize, in real time, shapes and positions of simple objects such as cylinders for robot manipulation.

No indication of system accuracy is given.

5.6 Rasterstereography

Rasterstereography is quite similar to conventional stereophotography except that one of the two cameras is replaced by a projector with a raster diapositive. This approach, of projecting structured light onto the object, is essentially the same as that presented by Turner-Smith and Harris (1986) and El Hakim (1985) described earlier. The only significant difference is that in rasterstereography a pattern is projected over the entire surface and only one image of the camera is processed.

The pattern projected is either a grid, a series of crosses, or a set of parallel lines (Fig. 5.4).

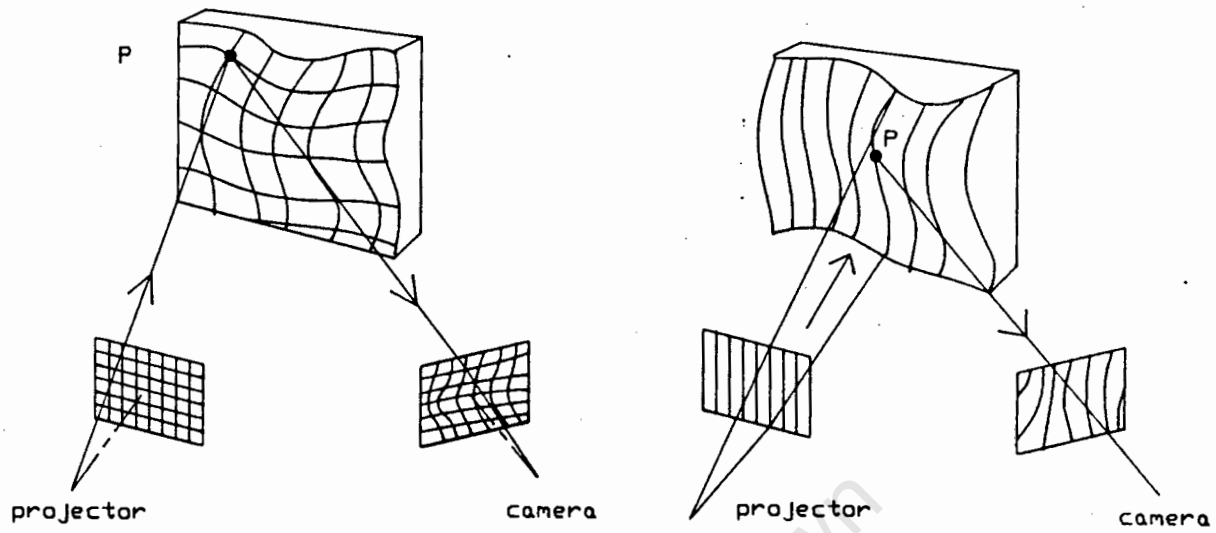

Fig. 5.4 Cross- and line rasterstereography

In cross-rasterstereography only raster intersections are evaluated for the reconstruction of surface points. In order to perform photogrammetric reconstruction of these points the column and row numbers of a raster intersection must be known (defining the 'image point' in the projection plane) as well as the x, y coordinate in the camera image. Although this appears to be relatively simple to do, it does not lend itself to automatic image processing (Frobin and Hierholzer, 1981).

Line-rasterstereography, however, is suitable for image processing. Knowing the raster line number and the position of any arbitrary point along this line leads to a unique solution of the XYZ coordinates of the object point. However, since there is one degree of redundancy in a cross-raster image and none in a line-raster image, the former will enable more accurate results. Algorithms for automatically analysing line rasters have been developed and tested (Frobin and Hierholzer, 1983a, 1983b).

As with any photogrammetric system, control is required to solve for unknown orientation parameters. Methods of extracting

control points from rasterstereographic images are given by Frobin and Hierholzer (1981, 1982, 1983a, 1985).

Frobin and Hierholzer (1983b) report processing times of 30-40 minutes for complete evaluation of a rasterstereograph of a human back. No quantitive information of system performance is presented.

5.7 A system for Capturing Facial Surface Information at the University of Minesota

Keefe anf Riley (1986) have developed a system that semi-automatically generates 3D surface information of a human face. The system setup is a conventional one with two cameras (not digital) and a control frame to solve for camera orientation.

Automatic image matching has been effected as follows. A single line of dots is projected onto the human face by passing a single low-power laser beam through a collimator, a cylindrical lens and an opaque barrier containing small holes. This produces an 80 dot, 140 mm long line segment in the object space. The laser line of dots is projected onto the subject and photographed. To capture the entire surface multiple stereopairs with the beam in different positions are necessary. After the film has been developed it is digitised and the dot patterns for each stereopair are matched. This is done by determining the position of the dots closest to the control frame and comparing the spacing between adjacent data spots. Image processing algorithms determine whether any data points are hidden in one view, and if that is the case, will discard their corresponding points in the other view.

Photgrammetric algorithms are then used to determine the XYZ coordinates of the dots which were matched in the various stereopairs. From these XYZ coordinates, the surface is

reconstructed. Finally, the system has computer graphics software which enables the user to view the reconstructed surface.

5.8 Digital Image Correlation

Digital image correlation is an approach to image matching in which corresponding pixel arrays of overlapping digital images are searched for. Only once a matching pair of arrays has been found, are the respective image coordinates of the match points determined. This is different to the methods discussed previously in which the precise position of a targeted point or distinct pattern is first determined in each image.

The method frequently used to find the approximate position of the array to be matched in another image is the use of epipolar geometry (Wong and Ho, 1986). Up until recently the most commonly used algorithm to match two image windows tries to maximise the cross-correlation coefficient of the two arrays by moving one relative to the other in a systematic trial and error procedure. However, a number of fundamental aspects that crosscorrelation cannot address, have caused a slow-down in the development of operational automated correlation systems (Gruen, 1985). Conjugate images may differ condsiderably from each other due to a number of reasons. Some of these are differences in height, positional and attitude differences of cameras which cause geometrical distortions, and illumination and reflectance conditions which distort images radiometrically. Furthermore, noise from electrical components may influence image appearance. Crosscorrelation only works well "if the patches to be matched contain enough signal without too much high frequency content and if geometrical and radiometric distortions are kept to a minimum" (Gruen, 1985).

As these phenomena are often present in typical images, efforts in recent years have been directed at developing alternate correlation algorithms. Ackermann (1984) adopted an approach in

which an array pair with minimum grey value differences qualifies for the optimum match. An iterative least squares solution is used to determine parameters to rectify geometric and radiometric distortions in the process of array matching. Another approach, also making use of the least squares technique, is presented by Gruen (1985).

5.9 Conclusions

In the 3D vision systems described above, the different approaches to solving the matching problem can be summarized as follows:

1. One approach simplifies matching by evaluating a number of stereo image pairs taken from the same camera position, each of which contains information about part of the object. As image scanning takes a few seconds, this method can only be applied to perfectly static scenes. Expensive, specialised equipment is required.
2. One of the cameras is replaced with a structured light projector with known perspective geometry. Expensive, specialised equipment is required.
3. Epipolar geometry.

The methods of image matching which fall into categories 1 and 2 above require expensive hardware which is not part of PHOENICS.

CHAPTER SIX

6.0 DEVELOPING AN AUTOMATIC IMAGE MATCHING ALGORITHM

After reviewing a number of image matching algorithms used in existing and developing photogrammetric systems it was concluded not to adopt any of these approaches (chapter 5), but rather to develop one in-house. After having designed a suitable algorithm it had to be programmed and tested on real image data.

One of the principal objectives of the thesis was to obtain a number of spotheights of the object surface to be measured, or in photogrammetric terms, XYZ coordinates in the object space. As it was intended to use the XYZ values as input data for the milling program developed by Back (1988), the measured object points had to be in an approximately grid-like structure.

6.1 Problem formulation

The need for a general, automatic image matching algorithm is the long term requirement of PHOENICS. To start with it was decided that a less general algorithm had to be developed. The problem definition was as follows.

6.1.1 Problem Statement

Develop, program and test an algorithm to be used with PHOENICS for matching conjugate object points which are approximately in a grid-like pattern.

6.1.2 Requirements

The problem specific requirements were:

(i) The matching algorithm had to have an accuracy of better than 0.5 pixels (this was considered sufficient for the prototype).

(ii) The program input be resticted to the image name and the starting point of the image search.

(iii) The program output be a set of matched image coordinates (ie. x and y coordinates in the left and right images).

(iv) The measured points on the object to be in a grid-like pattern suitable for the milling program.

(v) Physical contact with the object for targeting purposes not be allowed ie. the measuring technique to be "non contact".

6.1.3 Constraints

(i) The programmed algorithm be be executable on an IBM microcomputer (part of the PHOENICS hardware) with 640 kB RAM; apart from memory limitation, this constrains the number of instructions that can be programmed as the program should run to completion within a reasonabe time.

6.1.4 Criteria

(i) As the image processing card only supports the Microsoft (MS) 'C' and MS-Fortran computer languages, no other computer languages allow direct access to the IP. With MS-'C' and MS-Fortran the PIP card's soft- and hardware routines and libraries may be directly used in a program. This has speed and convenience as an advantage. TRUE BASIC is the next preferred choice.

(ii) Fast program execution.

(iii) Efficient algorithms and computer programs.

(iv) Well structured programs so they can be understood by subsequent researchers.

(v) User-friendly programs.

Before some of the concepts which were considered are described, some background is given on the images to be analysed.

With the PIP image proccessing software an image is displayed on a TV monitor as a 512x512 array of pixels each having an intensity level between 0 (black) and 255 (white) ie. there are 256 'shades of grey' or 'grey levels'. An example of such an image is shown in Fig. 6.1 and the grey levels of a portion of it are shown in Fig. 6.2. These images will henceforth be referred to as a 'grey' images.

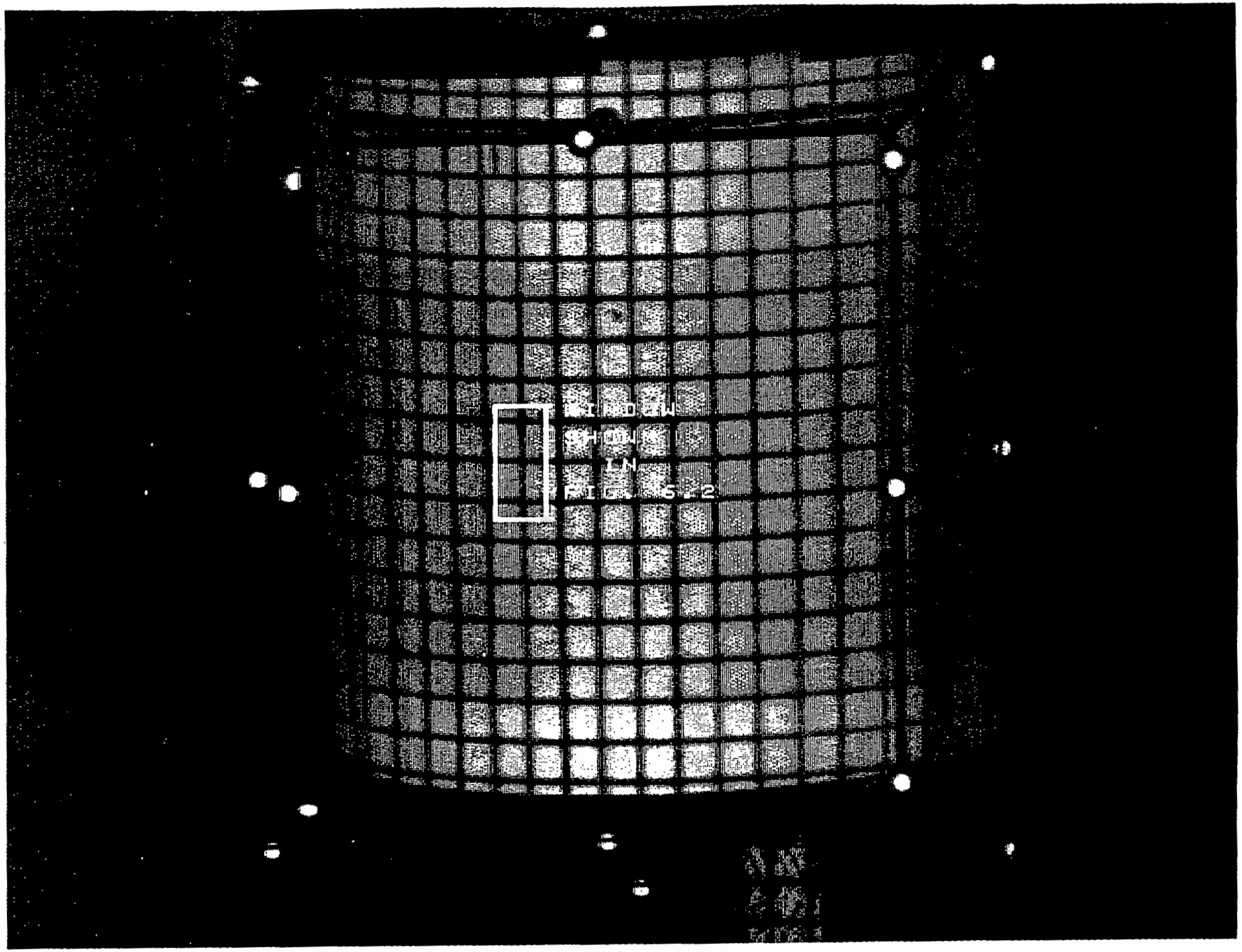

Fig. 6.1 Example of a grey image

158	155	153	156	157	157	156	149	123	92	92	123	151	160	159	159	166	166	164
152	151	151	152	158	161	153	139	113	87	89	116	142	155	160	163	167	165	163
154	153	153	155	155	154	150	137	111	86	86	112	138	153	160	161	159	157	161
140	143	143	147	151	153	148	138	112	81	78	103	128	144	153	155	155	154	155
126	128	133	136	140	140	130	119	94	75	75	94	119	134	141	140	143	149	152
83	85	91	98	99	99	96	92	78	64	64	75	93	106	112	118	125	125	125
66	64	64	67	68	64	61	62	60	58	57	59	65	69	71	72	74	73	77
76	73	74	72	67	66	66	65	62	61	62	61	63	69	69	70	73	70	71
121	118	113	113	113	105	96	89	76	67	66	73	84	91	94	96	95	94	97
148	144	139	141	143	140	134	127	104	78	70	89	117	128	135	135	134	136	138
154	152	150	150	151	153	149	137	111	84	79	104	135	148	148	149	152	154	157
157	156	154	154	153	151	145	138	118	89	82	109	145	158	155	154	157	159	160
157	157	158	157	156	156	151	140	117	91	89	117	147	160	163	164	165	161	162
159	160	159	153	149	149	148	141	120	91	83	108	137	153	158	157	160	159	160
156	156	156	154	155	155	151	149	128	97	87	114	145	157	158	156	157	163	164
151	154	157	159	158	156	154	150	127	96	86	110	140	157	163	163	165	164	162
156	159	158	155	156	155	155	152	128	99	90	114	142	156	163	164	165	165	164
159	160	155	152	155	161	158	150	130	106	92	113	144	160	165	165	164	163	164
155	158	158	160	162	160	155	152	134	104	86	110	145	158	161	165	167	167	168
159	159	162	164	164	165	161	156	138	110	92	111	143	159	165	167	169	167	168
158	161	158	156	160	163	160	155	136	106	87	108	141	157	159	163	169	171	171
156	159	158	157	158	159	154	151	133	101	87	111	143	157	160	161	164	165	167
148	149	155	157	153	154	156	152	128	100	86	110	141	154	154	156	162	160	160
148	150	151	151	153	156	155	153	133	102	85	106	138	152	156	157	158	158	160
147	148	146	145	147	151	150	144	125	95	85	108	134	146	153	156	158	159	161
142	140	142	145	144	140	136	131	117	89	75	95	125	136	139	144	149	151	157
119	123	128	131	136	136	128	123	105	81	71	90	118	126	128	135	138	140	147
79	80	87	91	91	93	91	87	80	71	66	74	88	97	104	109	114	118	122
66	67	67	64	63	64	66	66	60	61	63	60	63	70	72	72	77	76	76
82	81	78	75	71	69	72	74	66	62	64	67	71	75	77	77	77	75	72
123	121	120	119	118	119	115	106	90	73	66	78	94	104	110	113	111	107	105
144	143	143	140	135	144	145	134	117	91	75	90	122	137	141	144	144	146	150
144	145	147	147	145	145	140	140	127	97	81	101	129	143	149	156	159	157	159
140	145	148	151	150	148	150	147	129	107	87	99	127	145	155	159	160	158	162
143	142	148	151	146	145	148	146	128	104	87	106	137	150	154	159	163	167	167
149	149	149	154	154	152	152	155	139	109	88	103	135	154	160	164	166	168	168
154	151	152	157	154	154	154	146	127	101	85	108	140	155	162	165	165	169	172
154	155	156	158	157	153	150	147	132	107	85	100	133	152	159	163	161	161	163
148	152	153	151	151	150	147	146	131	104	87	110	145	157	162	169	168	164	165
141	143	145	147	145	139	134	138	129	103	82	99	130	147	156	164	168	169	167
152	148	147	148	143	137	139	143	128	100	86	110	140	151	155	164	170	172	171
147	150	148	148	149	147	144	145	134	110	87	103	138	157	163	165	161	162	171
148	148	145	145	148	150	150	149	136	109	83	95	128	149	157	161	162	164	172
140	142	143	147	151	155	154	152	142	114	85	97	128	145	149	155	161	162	163
140	145	148	146	145	151	150	146	132	108	86	100	131	146	152	158	157	160	168
144	147	147	148	147	150	151	149	136	108	83	95	128	149	156	160	164	164	164
140	144	149	151	147	145	143	140	128	104	84	99	132	151	155	161	164	159	159
135	139	141	142	141	141	139	136	128	109	84	90	121	141	148	158	165	160	157
119	123	126	127	126	128	128	127	114	91	76	85	112	129	141	149	153	151	151
83	87	92	93	90	91	94	96	89	76	65	69	88	104	115	121	127	128	128
69	69	68	67	67	69	68	68	68	67	62	61	66	69	73	74	77	81	83
74	74	75	76	75	73	68	66	65	64	62	63	63	64	69	69	71	70	69
116	117	119	115	110	110	104	98	89	78	69	67	75	85	95	99	98	95	96
131	138	142	140	138	139	135	128	119	99	78	81	102	121	133	138	142	142	141
140	142	144	145	148	149	146	147	138	114	84	82	109	132	144	148	156	159	158
140	139	143	151	150	149	149	151	140	114	87	89	120	145	151	155	162	159	159
146	150	148	152	155	152	148	149	141	117	89	89	121	148	159	161	164	165	165
149	152	155	156	154	154	155	151	132	109	86	92	125	152	160	161	165	168	170
150	152	155	158	157	158	154	149	140	118	91	92	123	148	158	160	163	162	164
151	154	153	156	158	155	148	147	138	113	89	94	123	150	161	159	162	165	169

Fig. 6.2 Pixel intensities of a grey image

A grey image may be converted to a black/white image by thresholding. A black/white image is normally referred to as a binary or thresholded image. Thresholding is a common technique used to simplify image processing algorithms. A binary image only has two pixel intensity levels (usually 0 and 255). Binary images are created by PIP after a threshold value is specified; all pixel intensities above this value are mapped to a single higher grey value and those below are mapped to a single lower value (eg. Fig. 6.3).

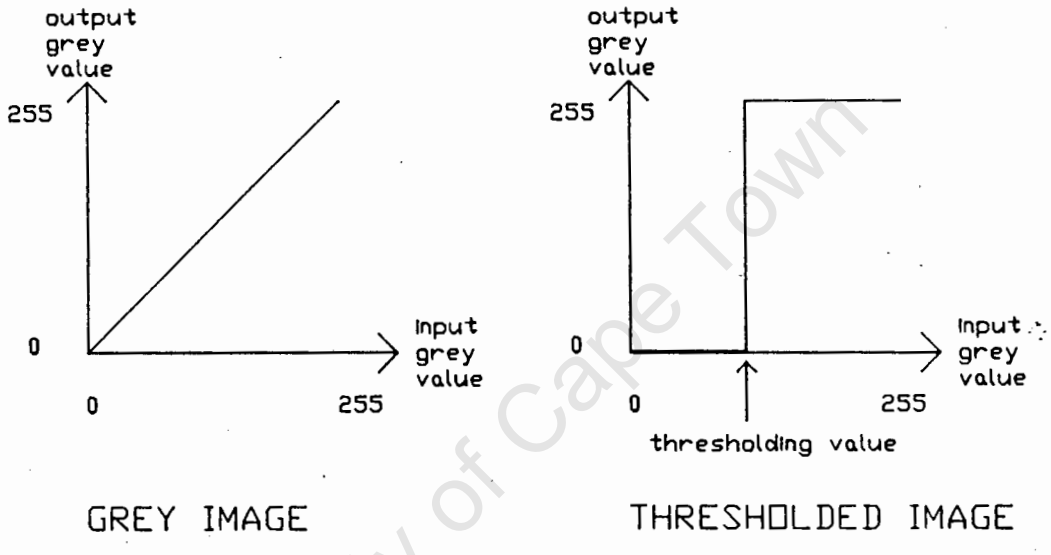

Fig. 6.3 Thresholding

In real-time photogrammetry, the binary image is often used for initial search or positioning operations, and only then is the grey image processed. An example of a binary image is shown in Fig. 6.4 and the grey levels of a porion of it are shown in Fig. 6.5. Fig. 6.5 depicts the grey image shown in Fig. 6.2 thresholded at a grey level of 105. It should be noted that the terms 'binary image' and 'thresholded image' are used synonymously in this thesis.

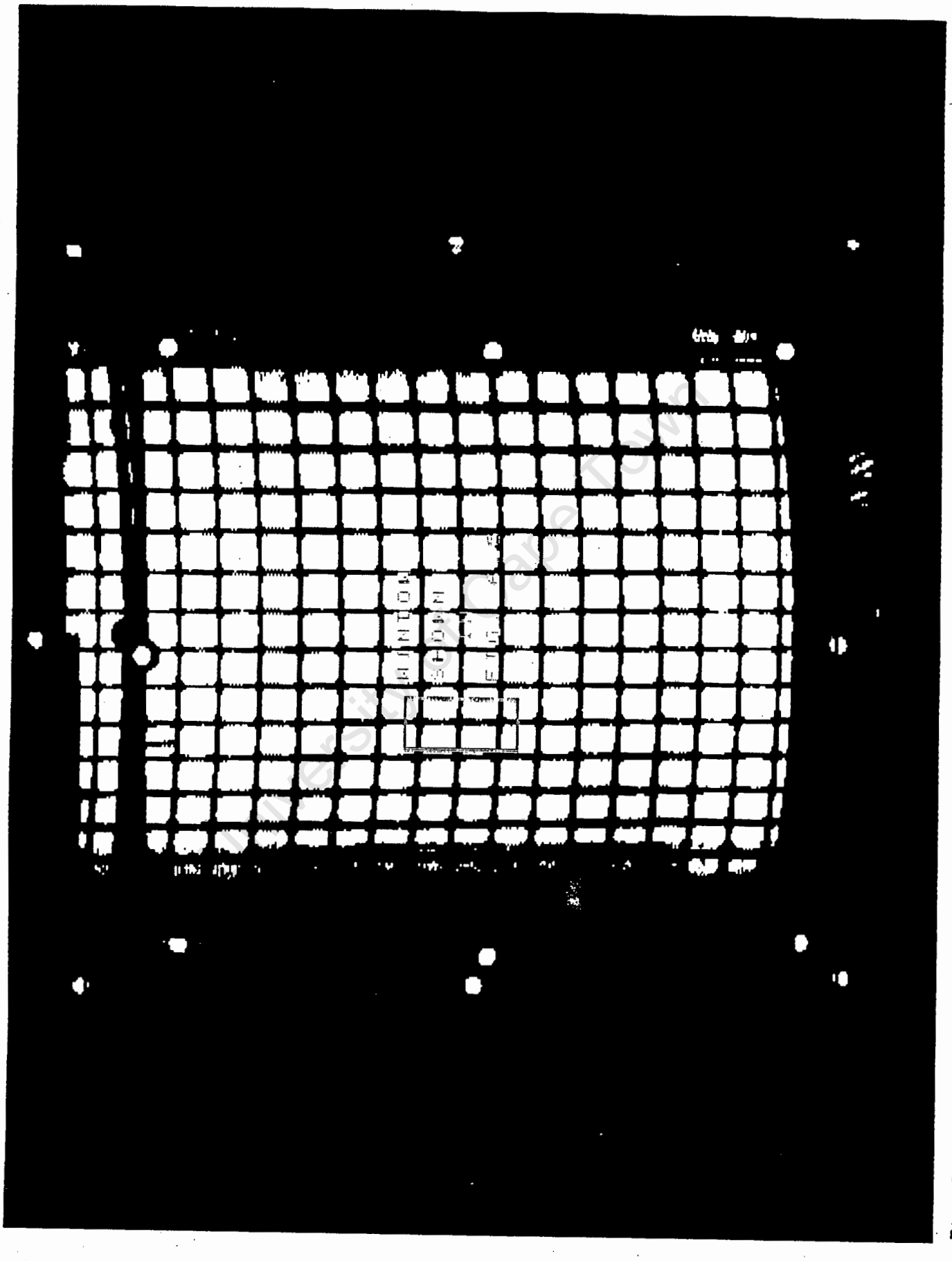

Fig. 6.4 Example of a binary image

255	255	255	255	255	255	255	255	255	0	0	255	255	255	255	255	255	255	255
255	255	255	255	255	255	255	255	255	0	0	255	255	255	255	255	255	255	255
255	255	255	255	255	255	255	255	255	0	0	255	255	255	255	255	255	255	255
255	255	255	255	255	255	255	255	255	0	0	0	255	255	255	255	255	255	255
255	255	255	255	255	255	255	255	0	0	0	0	255	255	255	255	255	255	255
0	0	0	0	0	0	0	0	0	0	0	0	0	0	255	255	255	255	255
0	0	0	0	0	0	0	0	0	0	0	0	0	0	0	0	0	0	0
0	0	0	0	0	0	0	0	0	0	0	0	0	0	0	0	0	0	0
255	255	255	255	255	0	0	0	0	0	0	0	0	0	0	0	0	0	0
255	255	255	255	255	255	255	255	0	0	0	0	255	255	255	255	255	255	255
255	255	255	255	255	255	255	255	255	0	0	0	255	255	255	255	255	255	255
255	255	255	255	255	255	255	255	255	0	0	0	255	255	255	255	255	255	255
255	255	255	255	255	255	255	255	255	0	0	255	255	255	255	255	255	255	255
255	255	255	255	255	255	255	255	255	0	0	0	255	255	255	255	255	255	255
255	255	255	255	255	255	255	255	255	0	0	255	255	255	255	255	255	255	255
255	255	255	255	255	255	255	255	255	0	0	255	255	255	255	255	255	255	255
255	255	255	255	255	255	255	255	255	0	0	255	255	255	255	255	255	255	255
255	255	255	255	255	255	255	255	255	0	0	255	255	255	255	255	255	255	255
255	255	255	255	255	255	255	255	255	0	0	255	255	255	255	255	255	255	255
255	255	255	255	255	255	255	255	255	255	0	255	255	255	255	255	255	255	255
255	255	255	255	255	255	255	255	255	0	0	0	255	255	255	255	255	255	255
255	255	255	255	255	255	255	255	255	0	0	255	255	255	255	255	255	255	255
255	255	255	255	255	255	255	255	255	0	0	255	255	255	255	255	255	255	255
255	255	255	255	255	255	255	255	255	0	0	0	255	255	255	255	255	255	255
255	255	255	255	255	255	255	255	255	0	0	0	255	255	255	255	255	255	255
255	255	255	255	255	255	255	255	255	0	0	0	255	255	255	255	255	255	255
255	255	255	255	255	255	255	255	0	0	0	0	255	255	255	255	255	255	255
0	0	0	0	0	0	0	0	0	0	0	0	0	0	0	0	255	255	255
0	0	0	0	0	0	0	0	0	0	0	0	0	0	0	0	0	0	0
0	0	0	0	0	0	0	0	0	0	0	0	0	0	0	0	0	0	0
255	255	255	255	255	255	255	0	0	0	0	0	0	0	255	255	255	0	0
255	255	255	255	255	255	255	255	255	0	0	0	255	255	255	255	255	255	255
255	255	255	255	255	255	255	255	255	0	0	0	255	255	255	255	255	255	255
255	255	255	255	255	255	255	255	255	0	0	0	255	255	255	255	255	255	255
255	255	255	255	255	255	255	255	255	0	0	0	255	255	255	255	255	255	255
255	255	255	255	255	255	255	255	255	0	0	0	255	255	255	255	255	255	255
255	255	255	255	255	255	255	255	255	0	0	0	255	255	255	255	255	255	255
255	255	255	255	255	255	255	255	255	0	0	0	255	255	255	255	255	255	255
255	255	255	255	255	255	255	255	255	0	0	255	255	255	255	255	255	255	255
255	255	255	255	255	255	255	255	255	0	0	0	255	255	255	255	255	255	255
255	255	255	255	255	255	255	255	255	0	0	255	255	255	255	255	255	255	255
255	255	255	255	255	255	255	255	255	255	0	0	255	255	255	255	255	255	255
255	255	255	255	255	255	255	255	255	0	0	0	255	255	255	255	255	255	255
255	255	255	255	255	255	255	255	255	255	0	0	255	255	255	255	255	255	255
255	255	255	255	255	255	255	255	255	0	0	0	255	255	255	255	255	255	255
255	255	255	255	255	255	255	255	255	0	0	0	255	255	255	255	255	255	255
255	255	255	255	255	255	255	255	255	0	0	0	255	255	255	255	255	255	255
255	255	255	255	255	255	255	255	255	0	0	0	255	255	255	255	255	255	255
255	255	255	255	255	255	255	255	255	0	0	0	255	255	255	255	255	255	255
0	0	0	0	0	0	0	0	0	0	0	0	0	0	255	255	255	255	255
0	0	0	0	0	0	0	0	0	0	0	0	0	0	0	0	0	0	0
0	0	0	0	0	0	0	0	0	0	0	0	0	0	0	0	0	0	0
255	255	255	255	255	255	0	0	0	0	0	0	0	0	0	0	0	0	0
255	255	255	255	255	255	255	255	255	0	0	0	0	255	255	255	255	255	255
255	255	255	255	255	255	255	255	255	255	0	0	0	255	255	255	255	255	255
255	255	255	255	255	255	255	255	255	255	0	0	255	255	255	255	255	255	255
255	255	255	255	255	255	255	255	255	255	0	0	255	255	255	255	255	255	255
255	255	255	255	255	255	255	255	255	0	0	0	255	255	255	255	255	255	255
255	255	255	255	255	255	255	255	255	255	0	0	255	255	255	255	255	255	255
255	255	255	255	255	255	255	255	255	255	0	0	255	255	255	255	255	255	255

Fig. 6.5 Pixel intensities of a binary image

would in any event be computationally too expensive for a PC. Systems which do match entire images, typically make use of mini computers and dedicated hardware components. If only targeted points are matched, the complexity of the algorithms required is greatly reduced. Targeting is done by, for example, pasting or drawing solid black circles with a white perimeter onto the object. As this is not allowed for this application because the whole measuring process must be 'non-contact', it was decided to project a pattern onto the object using an overhead or slide projector.

Furthermore, as image coordinates were required in a 'grid-like pattern' it seemed logical to project target points in a similar pattern.

The matching process can be seen to consist of two parts. In the first part, the position of the targeted points in the images are determined accurately. In the second part, a particular target point is matched with the corresponding one in the other image.

Gruen and Beyer (1987) identify this part of the RTP process as the recognition phase and state:

> "The recognition phase of the RTP process involves the detection and location of features that are relevant to the determination of the location of points or structures in the object space. ..... The development of efficient, reliabe and precise methods for this phase might prove to be the most difficult part in the development of a fully automated and general real-time photogrammetric system."

6.2.1 Finding Corresponding Points

The simplest but not very efficient way to find corresponding points is to target them one at a time. Haggren (1986) uses this

approach when requiring high accuracy by targeting points individually with a laser beam. The obvious disadvantage of this method is that the object must be very stable with time and that the process is tedious.

Another approach to finding conjugate points is to have targets with different shapes. In this method a number of moments, depending on how complex the shape is, are calculated for each target. Here, the definition of a n^{th} order moment is the following:

$$M_n = \Sigma_{ij} (x^i * y^j * f(x, y))$$

where: $i, j = 1, 2, 3, ...$
$n = i + j$
x, y are pixel positions
f is the pixel grey value

The second order moment with $i = j = 1$ is analogous to the centre of mass, or weighted mean. As each shape has a set of characteristic moments, targets with a common shape can be identified and matched. This method of using moments to characterise a shape is used extensively in character recognition.

Although this approach appears simple, it has some disadvantages for application to PHOENICS. Firstly, the moment equations required to describe a shape other than a simple geometric one (eg. circle, square, triangle) become complex and increase in number. Secondly, since the targets should not appear too large on the object, a high resolution camera is required to record subtle differences in shape. Further, it is difficult to define the position and orientation of non-symetrical shapes.

Alternatively, epipolar geometry may be employed to identify corresponding targets in two or more images. A large number of similar, geometrically simple targets can be matched. In order to apply this method, it is necessary to program extensive photogrammetric algorithms. These algorithms are complex and

computationally too expensive for a PC, and hence it was decided not to implement them. Furthermore, in NRTP there are often complications which must be dealt with which do not occur in photogrammetry with conventional cameras. eg. different image scales in the x and y directions which is the case with PHOENICS.

It is ideal to use similar, geometically simple object targets since this simplifies target centering. If all the targets are joined together in a manner such that their positions relative to each other are uniquely defined, corresponding targets can be identified in other images. One way of doing this is to position targets at the intersection points of a regular grid. The position of a target is uniquely defined by the row and column number from a reference point common in all the images (Fig. 6.7a).

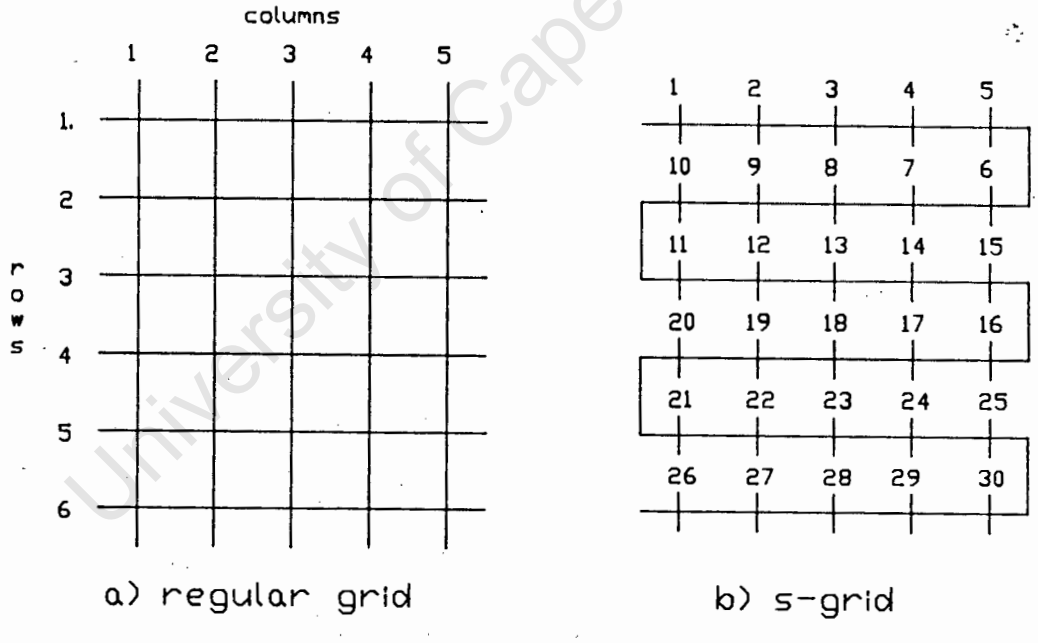

Fig. 6.7 Grids for object tartgeting

Targets in a grid pattern can also be joined as shown in Fig. 6.7b. This pattern is referred to as a s-grid. Target positions are numbered from the top down, row by row.

For this approach for target matching, a line following algorithm has to be developed to move from target to target.

The advantage of joining target points is that the matching algorithm can readily be adapted to a multi camera photogrammetric system since images are processed independently. Although more than two images may be matched when using epipolar geometry, this would be cumbersome.

Conclusion

It was decided to adopt the approach outlined last; ie. determining the precise position of interconnected targets and identifying conjugate points by virtue of their relative position to a reference point common in all images. The decision on whether to use a regular grid or a s-grid to join the targets has to be made in conjunction with the choice of target type and centering technique.

6.2.2 Target Recognition and Centering

The next step is to recognise a target when moving along a line and then to find its position accurately. A few of the target designs and centering methods which were considered are described below. The targets described may be divided into two groups: circular- and cross shaped targets.

Circular targets

Circular targets are popular for automatic detection and centering because they are rotation symmetrical. As a result, the simple weighted mean technique, also referred to as the first order moment or centre of gravity technique, can yield good results for finding the centre. There are however more sophisticated methods for locating the exact centre which are generally more accurate. One approach is to precisely locate the edges of the target using well established mathematical

techniques such as Fourier Analysis and then to find the centre of the best-fitting ellipse through these points.

Three variations of circular targets which can be used with either the regular grid or the s-grid are shown in Fig. 6.8. Although the target shown in Fig. 6.8a at first appears to be suitable for the weighted mean technique, this is only the case if the lines passing through it are perfectly straight. However, this ideal situation does not necessarily always prevail in practice. The target shown in Fig. 6.8a is also not suited to more sophisticated centering methods as these require the circle to be free-standing as shown in Fig. 6.8c. Developing and programming an algorithm which can determine where the junction point between a circle and a line is positioned (in order to isolate the target), is far too problematic if not impossible.

Two alternatives of target/line design which attempt to isolate the target from the lines so that centering algorithms can be employed are depicted in Fig. 6.8b and c. The problem with the alternative shown in Fig. 6.8b1 is that there is not sufficient background area surrounding the target. The writer suspects that background area is necessary for any centering algorithm to be effective. If a black background were introduced around the target (Fig. 6.8b2), the size of the target would become undesirably large. Further, it would become too detached from the line thus making target detection algorithms more complex. This also applies to alternative shown in Fig. 6.8c. Again, a considerable gap is required between the line and the target which to a certain degree contradicts the idea of joining targets to simplify target detection and matching.

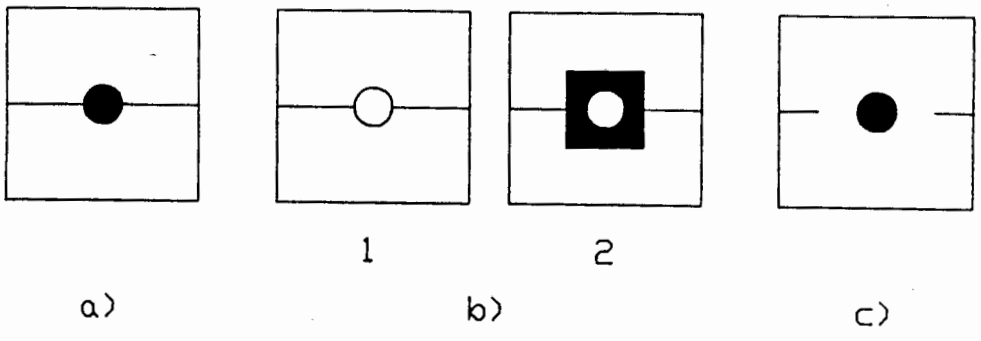

Fig. 6.8 Circular targets

Cross shaped targets

Crosses are a logical choice for targets which are to be linked together. Since a cross is defined by the intersection of two lines, it forms part of the line pattern. This means that cross targets (unlike circular or any other shape targets) must not be isolated from the line pattern so that their centre may be found.

A number of approaches to finding cross centres which have been investigated are described below. It must be borne in mind that crosses in real images are not ideal ie. the arms of the cross do not have a constant thickness and the angle between them is not fixed.

The weighted mean technique is not suitable for accurate cross centering since the targets are not symmetical. This was verified with tests on real images. However, the results obtained showed that this technique is accurate enough for obtaining a first approximation to the cross centre. It has the advantage that it is simple to program.

An alternative to centering the cross is to find the position of a hollow square which when placed over the cross will enclose equal areas between its borders and two adjacent cross arms. Again, this only works for ideal crosses.

It was mentioned earlier that shapes may be described by a set of moments. This can also be applied to a cross by modelling it as shown in Fig. 6.9.

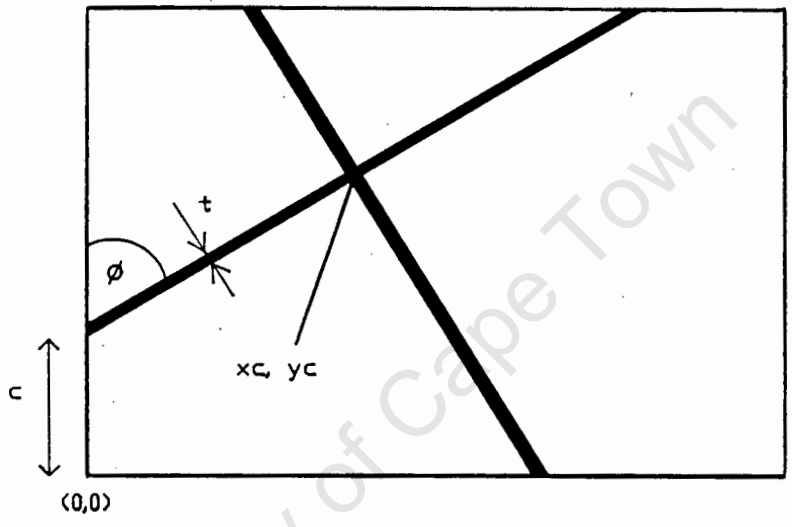

Fig. 6.9 Cross centering with higher order moments

For purposes of derivation, it is assumed that the arms of the cross are at 90°, that both lines are straight and have the same, constant thickness t. As there are four unknowns (xc, yc, θ, t), four moment equations are required to solve for the cross centre. For example, the zeroth, two first and one second order moment equation can be used. The resulting set of non-linear equations are then solved. This approach was not investigated further since a priori knowledge is required about the angle of intersection of the two lines. Of course, this angle could be made a variable and the two lines could be modeled with different thicknesses. Then, however, the resulting equations would become extremely difficult to solve. Whether there would be any value in doing this is

doubtful, as the assumption that the lines are straight anyway introduces inaccuracies. It would be interesting to compare the accuracy of this method with that of the weighted mean technique offset against computation time.

From the above discussion it becomes clear that more sophisticated methods must be pursued to determine the exact position of cross shaped targets.

As the definition of a cross is "the intersection of two lines" it was thought that modelling a cross in this way would yield good results. To do this, a number of points on each line are required to which a polynomial can be fitted using least squares. The point where the two polynomials intersect represents the cross centre. This approach was tested using data from a real image and third order polynomials to fit the lines. At the immediate area of intersection of the two lines no data points were sampled. Results obtained from crosses formed by lines with little or no irregularities were satisfactory. When the algorithm was tested for crosses formed by lines as shown in Fig. 6.10, poor results were obtained.

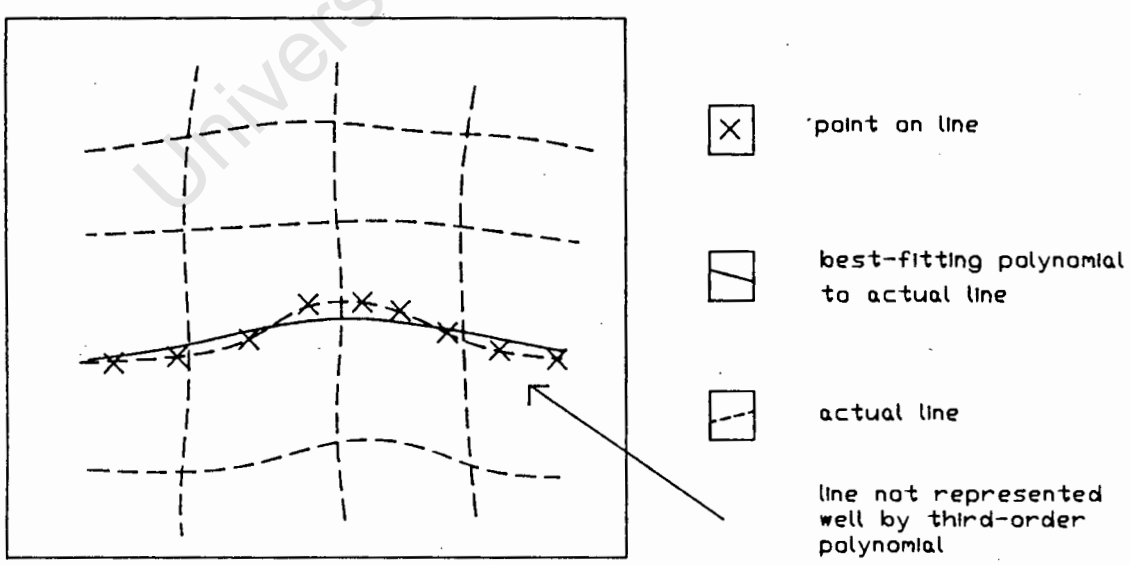

Fig. 10 Modelling a cross as the intersection point of two lines

The reason for this is that third order polynomials cannot represent/contend with such lines very well. Although higher order polynomials would fit the points better, they are not more suitable because they are unstable in the region where there are few data points - in the region of a cross.

As a result of this problem the writer decided to only use points in the vicinity of the cross. Two points on each cross arm were determined and third order polynomials used to fit the points on the lines (Fig. 6.11).

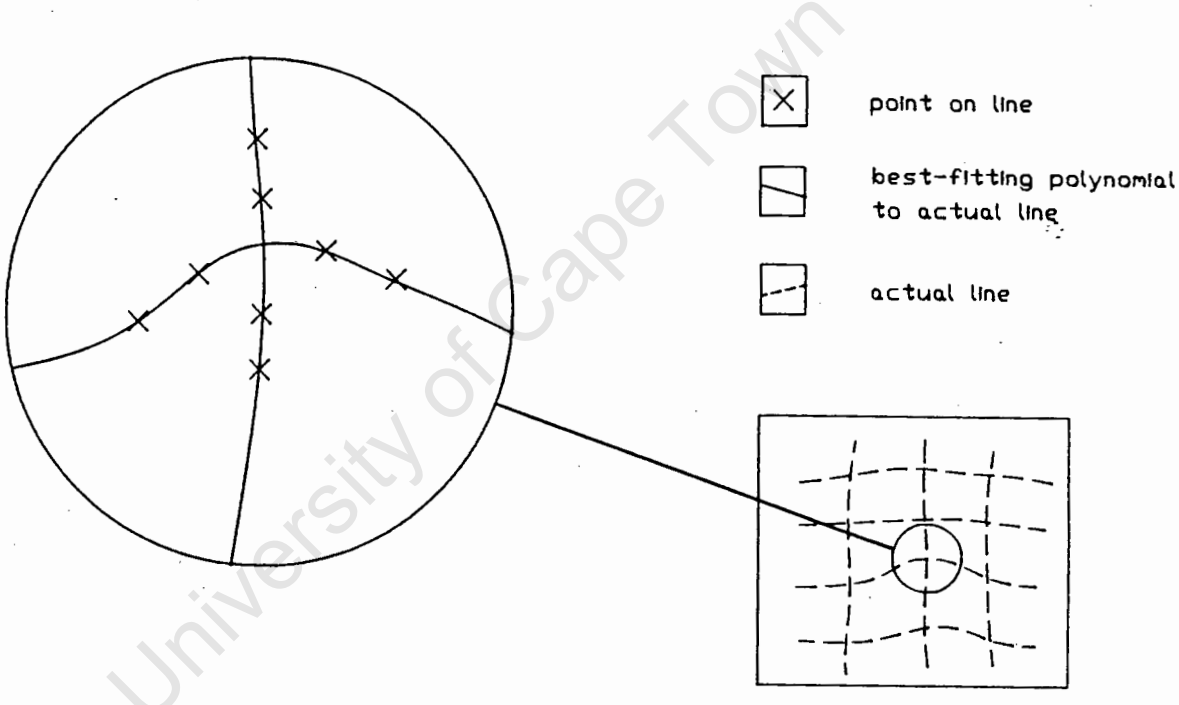

Fig. 6.11 Modelling a cross as the intersection point of two line segments

This method was tested for a number of crosses and gave consistently good results. This approach is similar to the algorithms developed by Luhmann (1986a, b) for precise point determination of ring- and cross shaped targets of the résau scanning imaging system Rolleimetric RS1 (Luhmann and Webster-

Ebbinghaus, 1986). The authors report accuracies of 0.1 to 0.2 pixels.

Conclusions

1. Of the target types investigated, intersecting lines proved to be the most suitable for a network of interconnected targets. Crosses require less complex algorithms for detection and have potential for precise target centering.

2. It is appropriate to state two facts about the weighted mean technique here.
   - It should only be used when the target background is uniform and appears similar in both images. This is not often the case with all the target points.
   - The method is not suited to non-symetrical target shapes.

A point of practical relevance is that grey values must be subtracted from 255 when computing the weighted mean of a black target on a white background (this is usually the case), as darker areas have lower grey values than lighter areas. Otherwise, the centre of mass of the light area will be calculated which may often be close to but usually not equal to that of the dark area.

6.2.3 Line Following

In order to move from target position to target position, a general algorithm capable of following a line in any direction as well as around corners had to be developed. To the author's knowledge none of the digital photogrammetric systems being currently developed utilize such algorithms since they employ alternate target searching techniques.

Two approaches to line following were considered. The first one is based on a region growing algorithm. For this application, pixels

which define the line represent the 'area' which is grown. Once a pixel is found which is on a line, pixels adjacent to it are examined to decide whether they are also on the line. This is be done on a thresholded image where the line for example is white (255) and everything else is black (0). If a neighbouring pixel is also on the line it is added to the first and the process is repeated. If on the other hand it is not, it is discarded. Such region growing techniques are used in many computer graphics applications (eg. region filling/flooding).

In the other approach (see Fig. 6.12), pixels on the perimeter of a circle which has its centre point on the line are tested to establish whether they are on the line or not. The point where the line intersects the circle becomes the centre of the next 'search-circle'. A circle was chosen as the search array because of its symmetry. This ensures that line following is independant of direction. In a sense using a 'search-circle' is similar to moving a mask from point to point and evaluating it. A mask is a square or rectangular area within which all the pixel grey values are determined. For line following it is not necessary to read in as many points.

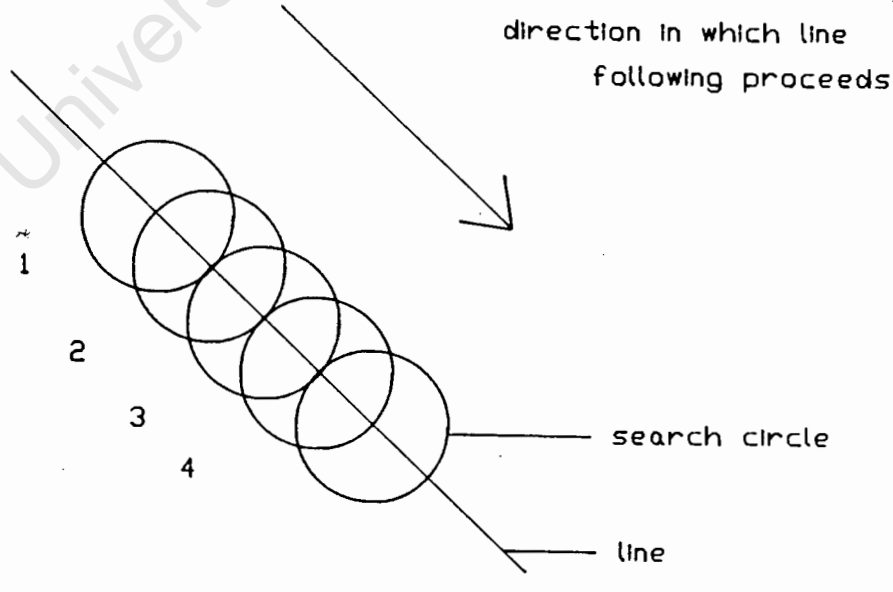

Fig. 6.12 Line following using a search-circle

A major advantage that the 'search-circle' technique has over the line 'growing' approach for line following is that the circle may simultaneously be used for cross detection. As the circle is moved along a line, two intersection points characterise a line and four intersection points characterise a cross. This algorithm was programmed and then tested on real images. The basic concept proved to be sound and was thus adopted for the final solution.

6.3 Summary and Conclusions

1. In section 6.2.2 above it was decided to use crosses to target object points. The crosses are the intersection points of a regular grid which is projected onto the object. A slide projector was used for this as an overhead projector does not produce an image suitable for thresholding purposes (ie. there is not enough contrast between the lines and the background). In fact, object targeting via slide projector produces better images than any of the methods which have been used for prototype studies with PHOENICS.
2. It was decided to use a regular grid rather than a s-grid as the former is more adaptable. The major disadvantage of the latter is that any one particular s-grid can only be used for a limited range of object sizes.
3. The cross centres are determined from the intersection point of the best fitting third-order polynomials to the line segments which form the cross as shown in Fig. 6.11

The next chapter describes in detail the computer program which was written to implement these algorithms.

CHAPTER SEVEN

7.0 DISCUSSION OF SOLUTION

A general algorithm which automatically detects and finds the accurate positions of crosses on a line has been developed and is described in the first part of this chapter. This algorithm was then extended from finding the crosses on a line, to finding all the intersection points of a grid and was specifically adapted for use with PHOENICS as an object point matching tool. The computer program (named CROSS) which implements this algorithm has been programmed in TRUE BASIC and is described in the second part of this chapter. In addition to CROSS, a number of computer programs have been written for use with PHOENICS. A list of these programs and a brief explanation of thier use is given in Appendix F.

7.1 A General Line Following and Cross Detection Algorithm

The development of this algorithm was done in three parts:

1. line detection
2. line following and cross detection
3. accurate positioning of a cross

Fig. 7.1 shows how these three parts are linked together. The following sections explain the algorithm assuming a given situation in which black lines and crosses must be detected on a white background. This condition can easily be realised by an inversion procedure with the IP should the opposite situation occur.

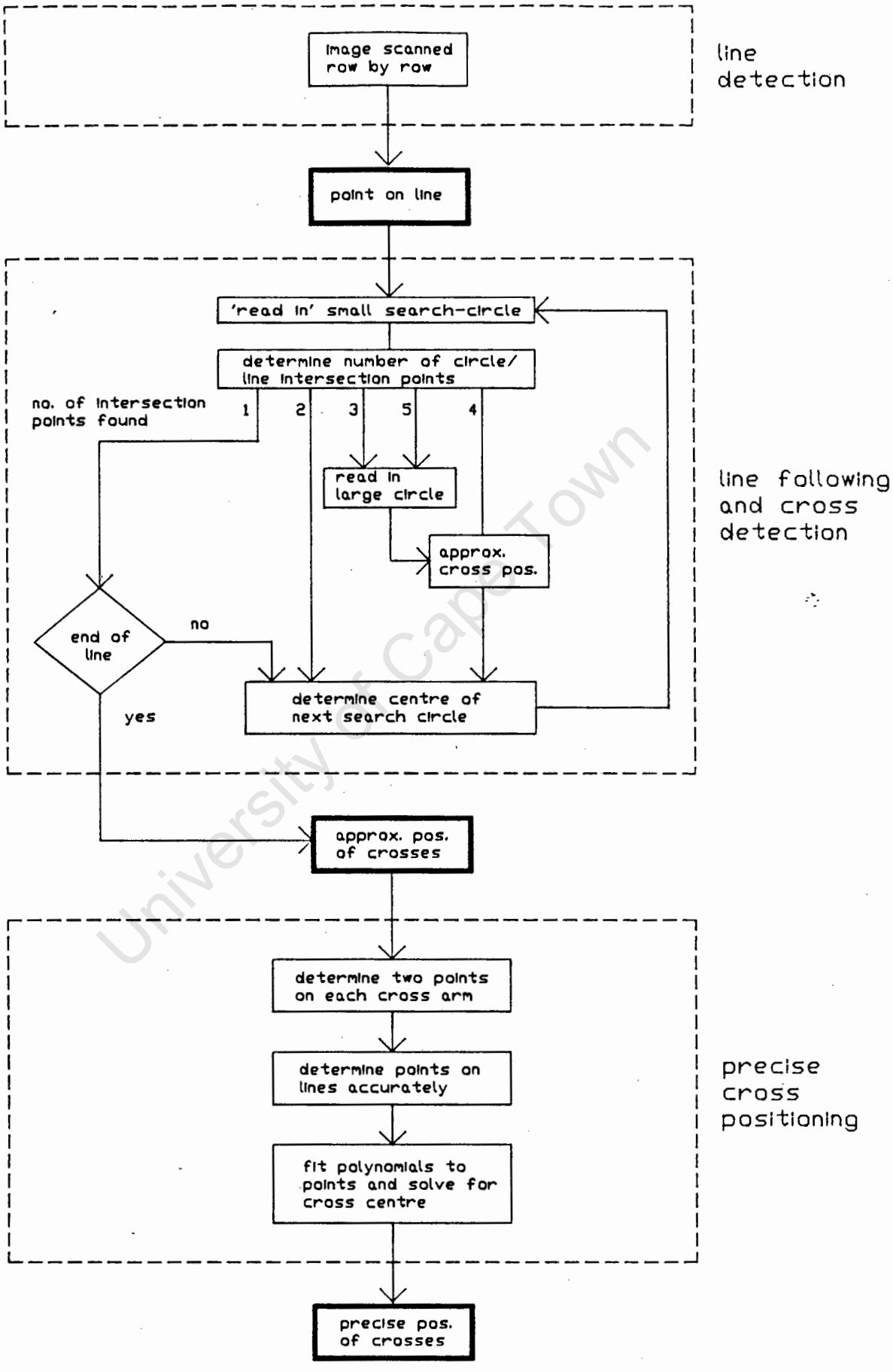

Fig. 7.1 Flow diagram of a general line following and cross detection algorithm

7.1.1 Line Detection

Line detection is done on a binary image and is implemented as follows. From an operator selected starting point, the image is scanned row by row if vertical lines are to be found. If horizontal lines are to be found, the image would be scanned column by column. Each row is tested for black pixels, and when a row contains a number of adjacent black pixels a line has been found. Once such a line is detected, its approximate centre is found using the weighted mean technique.

Thus the line detection phase requires as input a point where the search should start, and produces as output a point on the line.

7.1.2 Line Following and Cross Detection

In section 6.2.3 it was decided to use a search-circle for line following and cross detection. A flow diagram showing how this is accomplished is given in Fig. 7.1.

The image coordinates output of the line detection phase are used as the centre of the first search-circle. Pixels in a circle are read from the binary image and stored (Fig. 7.2).

The next step determines the position and number of intersection points the search-circle has with the line. This is done in a similar way to line detection. Any single pixel or group of adjacent black pixels on the circle is classified as a intersection point. The approximate position of the intersection point is determined using the weighted mean along the circle's perimeter. The position of a circle intersection is defined by its position along the perimeter measured from 12 o'clock.

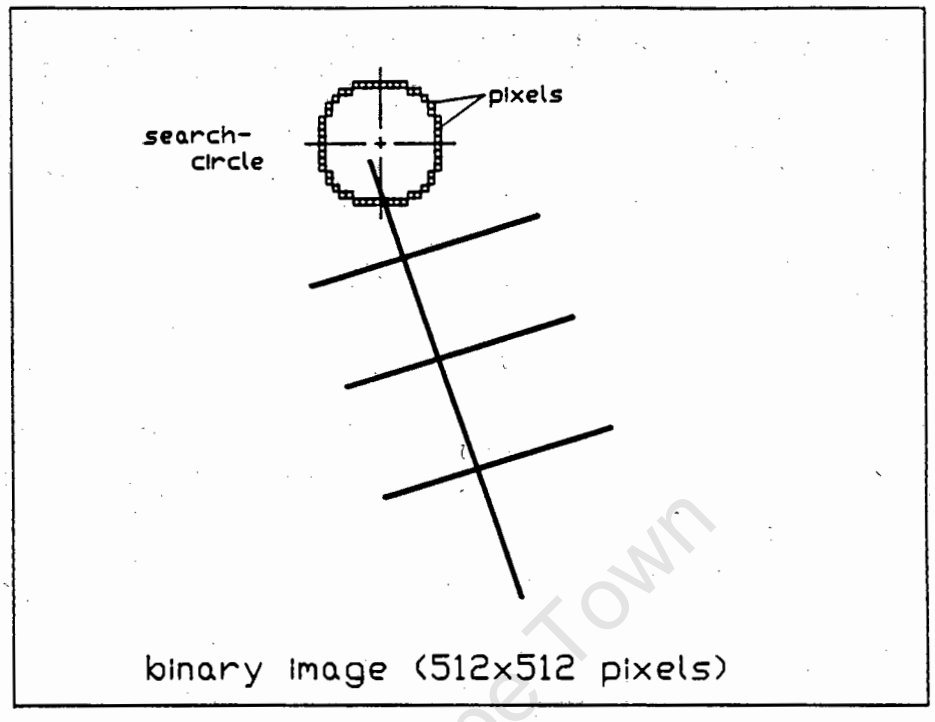

Fig. 7.2 Search-circle used for line following and cross detection

Once all the circle/line intersection points on one search-circle have been established, the direction in which line following should continue is determined. Direction is to be understood as "position on the search circle's perimeter". The circle position of the intersection point closest to the previously determined line direction, defines the direction in which line following proceeds. At the beginning of the program, when this information is not established, the initial line following direction must be defined. This would normally be vertically downwards.

The number of intersection points which are found will vary between 1 and 4 as the search-circle is moved along the line. These four cases are shown in Fig. 7.3.

Case a: Only one intersection point is found. The search-circle is at the beginning or at the end of a line (Fig. 7.3a). The search-circle is considered to be at the beginning of a line if the intersection position is close to the previous line following direction (eg. within 1/4 of the search-circle) - in this case to the value initialised at the beginning of the program. If, however, the intersection position is not close to the previous direction, then the end of the line has been reached.

Case b: Two intersection points are found. The entire circle is on a line (Fig. 7.3b).

Case c: Three intersection points are found. This situation which can occur due to the pixeling effect and non-ideal crosses and/or lines (Fig. 7.3c). In this case a second, larger search circle is read from the image and the intersection points determined once more. The same procedure is followed if five intersection points are found (not shown). If other than two or four intersection points are found on this large search circle the program is terminated.

Case d: Four intersection points are found. A cross has been detected (Fig. 7.3d).

If none of the above cases is true the program is terminated. This can for example occur when the search circle has 'lost' the line and no intersections are found.

When a cross is detected its approximate centre is found as follows. First, the opposite intersection points on the search-circle are joined with straight lines and their intersection point found. This first approximation is then used as the centre of a square window of which the weighted mean is computed in the binary image. The window's centre is moved to this point and the weighted mean recalculated until convergence occurs. The second

approximation is stored and recalled later when the precise position of the cross is determined.

After the approximate position of the centre has been found the small search-circle is read in and the four intersection points are established. The new direction of line following is determined in the usual way. Experimentation has shown that if the original intersection points are used to determine the line following direction, the centre of the next search-circle does not always fall onto the line. This can be critical when dealing with a dense grid as the circle may intersect an adjacent line. The original intersection points are those circle/line intersection points which were found when the cross was detected with the search-circle.

Unless the end of the line is reached or the program terminates due to an error condition, the centre of the next search-circle is calculated. If two intersection points were found, the centre is moved ahead one radius. It is not advisable to move more than this at a time since then the chance exists that a cross may be missed - especially in the case where line and cross elements are thick. If a cross has been detected then the centre should be moved more than one radius in order to avoid "finding" the same cross twice. If adjacent crosses are closer to one another on a line than one search-circle radius, the distance moved should not exceed 1.25*radius. For crosses spaced further apart this distance may be increased for faster line following.

The process is repeated until all the crosses on the line are found and the end of the line is reached. This completes the target detection phase.

7.1.3 Accurate Cross Positioning

In the approach to cross centering which was decided upon and described in the previous chapter, the line segments which form the cross are modelled as third order polynomials. This requires two points on each cross arm which are three pixels apart and close to the cross centre to be precisely located. A separation of three pixels between adjacent line points was considered suitable.

To find points on the line segments, two circles, with their centres at the approximate cross centre which was derived in the detection phase, are read in from the binary image. The four circle intersection points are found and serve as a first approximation to points on the lines. This was found to be satifactory for lines which are thin compared to the inner circle's radius. For thicker lines, line thickening at the intersection point occasionally caused an error since the circle only had three intersection points. For this reason, the inner circle was replaced with a square with its side equal to the diameter of the circle (Fig. 7.4).

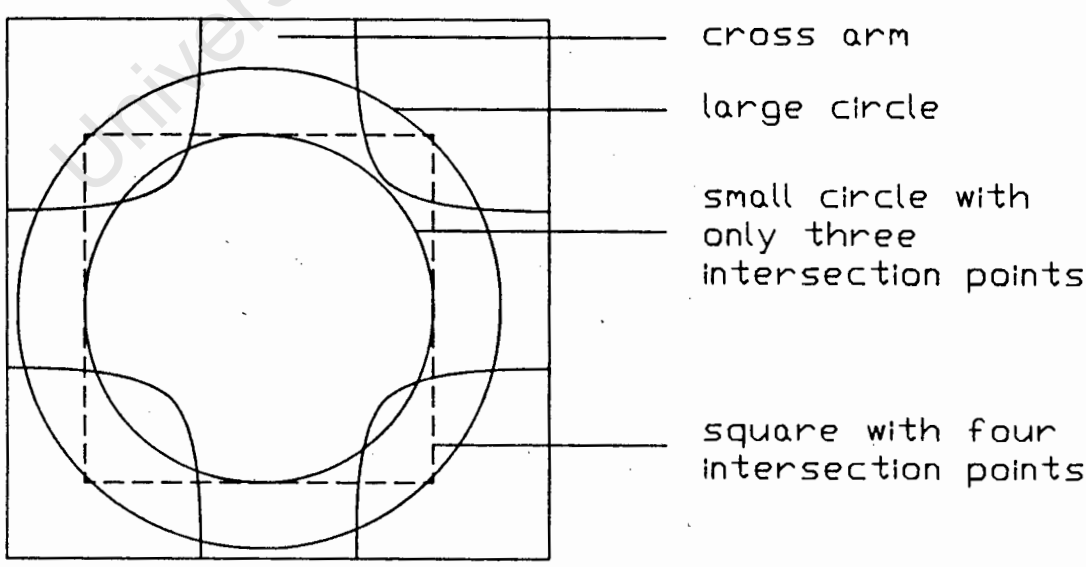

Fig. 7.4 Finding a first approximation to the points on the lines which form a cross

A better approximation to the line centre is found by calculating the weighted mean of an array vector of say 10 pixels in the grey image which is perpendicular to the line and symmetrical about the first approximation which was found in the binary image. For points on a line which is approximately parallel to the x-axis the precise y-coordinates are determined. Similarly, for points on a line approximately parallel to the y-axis the precise x-coordinates are determined. Thus far eight points on the cross arms have been located to sub-pixel accuracy (Fig. 7.5).

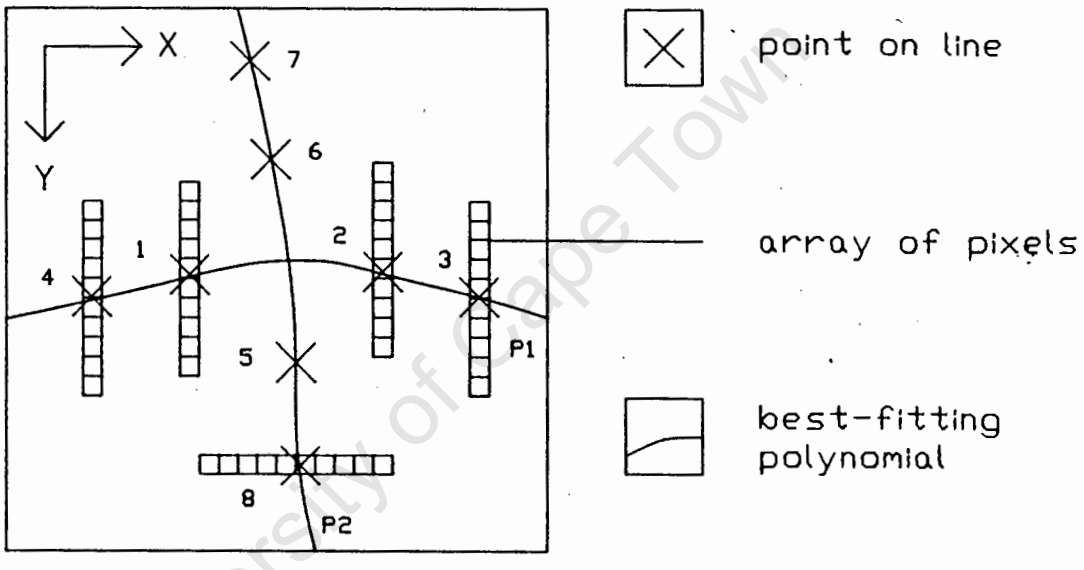

Fig. 7.5 Determining the position of the centre of the line to sub-pixel accuracy

An alternative method to finding the centre of a line to sub-pixel accuracy has been experimented with. However, it has not been used for reasons outlined in the next chapter.

Two third-order polynomials (P1 and P2) are then fitted to the points 1-4 and 5-8 respectively using the least squares technique. The approximately horizontal line segment is modelled as a function in x (P1), and the approximately vertical line segment is modelled as a function in y (P2) in order to deal with all

possible situations. The intersection point of the two polynomials is determined using Newton's method. The method of fitting polynomials to data points by the least squares approach was adopted from Davis (1988). The polynomials' intersection point represents the cross centre.

7.2 Cross Detection, Centering and Matching for PHOENICS

The algorithm described above which finds the position of crosses on a line, has been extended to find the x and y coordinates of grid intersections. The grid points are evaluated and numbered from top down, column by column, and from left to right from a given starting point. A computer program has been written in TRUE BASIC which analyses images generated with PHOENICS (Fig. 7.6). It has been linked with the MATROX image processing board to indicate the cross centres found on the images. The user can discard any unwanted crosses. The coordinates of the accepted targets are written to a file for input to the photogrammetric software.

In the following description of the computer program the numbers in brackets refer to the steps as shown in Fig. 7.6. A set of sample images on which the program has been run is shown in Fig. G.3 and G.4 in Appendix G.

At the start of the program the user is prompted for the image which is to be analysed (1). Although the IP card does not support the TRUE BASIC programming language, a way has been found of interfacing the two (Appendix D). The IP is initialised, the appropriate image displayed and a regular grid with scale markings is superimposed on the image (2) (see Fig. G.7 in Appendix G). This assists the user to choose the starting point which must be entered as x and y image coordinates (3).

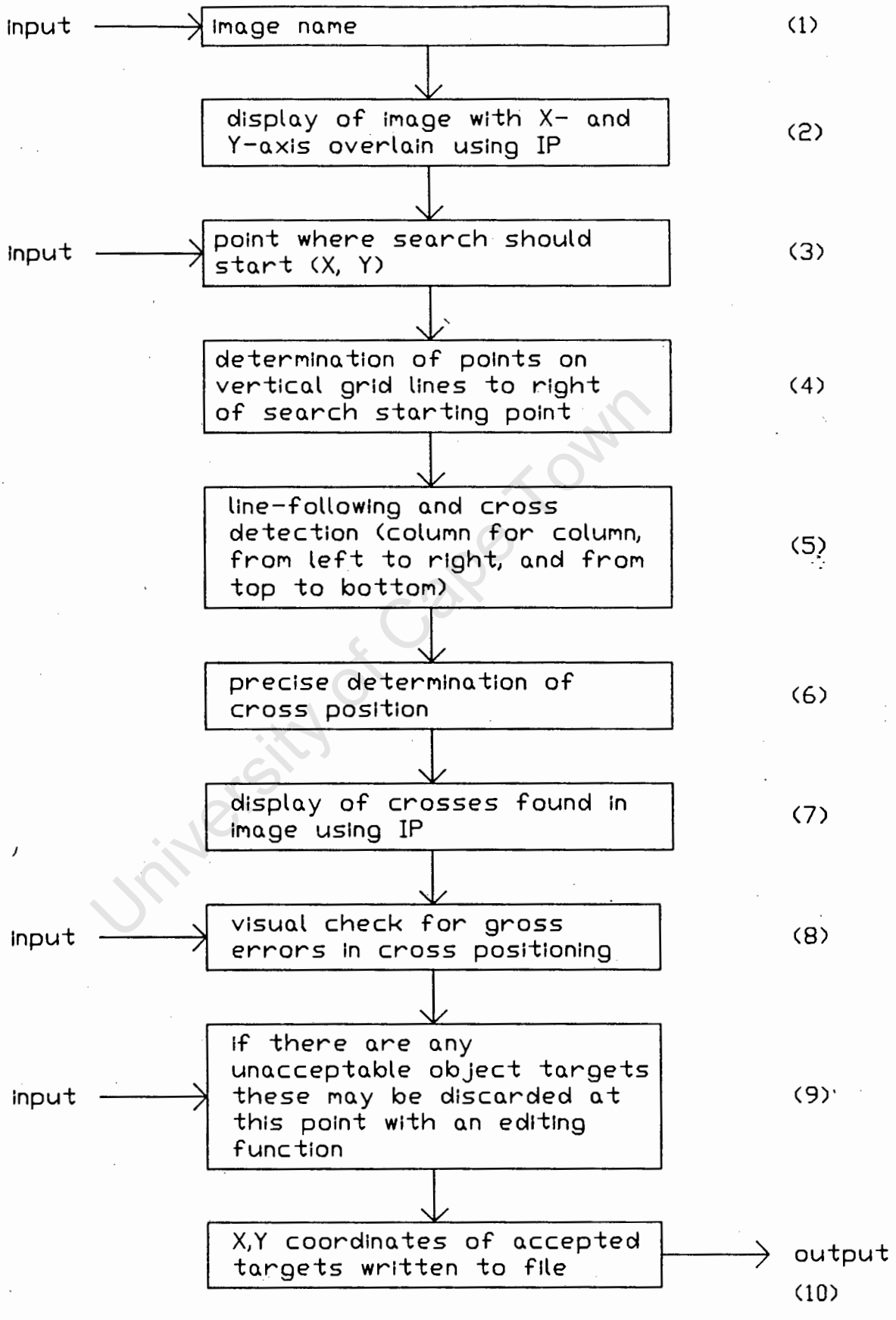

Fig. 7.6 Cross detection, centering, and matching with PHOENICS

The program searches for vertical lines from the given starting point to the end of that row - ie. the program expects to find the vertical lines of the grid on the row of the starting point (4). The grid will be evaluated below and to the right of the starting point (5). The approximate positions of crosses on each vertical line are found with the line following and cross detection algorithms which have been described above. The position of each cross to sub-pixel accuracy is then found.

Once the positions of all the grid points have been determined, the IP is used to display the results obtained (7). All the points which were found on the lines to determine the cross centre are indicated on the image and numbered circles show where crosses were found. As these points can only be displayed on the image to the nearest pixel, only gross errors will be apparent. The display also serves as a check that no crosses have been missed (8).

The user is prompted to enter any targets which are to be rejected (9). The accepted object crosses are displayed on the image via the IP, and written to a file for input to the photogrammetric software (10).

Although the cross detection and positioning phases could have been interlinked to produce a more efficient program, the two parts were kept separate so that alternate strategies for cross detection or positioning can be readily introduced to the program. Alternatively, either of the phases can be adopted in other programs.

The problem of matching corresponding object crosses in one or more images has been addressed as follows. At the start of the program, the image is displayed and a grid overlayed. The user must enter the x and y coordinates of a starting point which is visible on the object in all the images that are to be evaluated.

Now, if grid points are evaluated in two or more overlapping images starting from the same object point, then corresponding object crosses will have the same numbering in each of the images. For each of the overlapping images, the program will create a file which contains the cross number and its x and y coordinates.

two iterations for the original method, and after two and three iterations for variations 1 and 2 respectively. These three ways of finding a first approximation to the cross centre were compared for 70 crosses. The following observations were made:

1. For all three methods, the deviations in the x and y coordinates of the calculated cross centres from the true cross centre had the same sign (ie. + or -) for all 70 crosses.
2. The weighted mean technique applied in the binary image only, converged fastest and gave the best approximation to the cross centre.
3. Variations 1 and 2 gave identical results for 80% of the crosses. For the rest of the crosses the two variations differed by a maximum of 0.9 pixels in x and 0.7 pixels in y.
4. The cross centre calculated with variations 1 and 2 was always between 0.8 pixels in x and 0.3 pixels in y worse than that obtained in the binary image.
5. Despite the differences in results obtained from the three methods discussed in points 1-3 above, the first approximation is usually the same when rounded to the nearest pixel. The x and y coordinates rounded to the nearest pixel are used as input for precise point determination.

In conclusion, these observations illustrate that there is nothing to be gained from the two variations which were tested, because they are computationally more expensive and do not improve accuracy.

8.2 Precision of Determining the Cross Centre

As described in chapter 7 the first step in determining the precise position of a cross, is to determine two line points on

each cross arm. The distance along the cross arms where these line points are determined depends on the first approximation of the cross centre which is found during the detection phase. However, as the weighted mean technique is used in the binary image to determine this first approximation, this value can vary for different thresholding values or lighting conditions. In order to investigate how a different first approximation affects the final position of the cross, the starting point was moved through a 3x3 kernel with its central pixel at the cross centre. For each position, line points were found, polynomials fitted and their intersection point found. The mean value of the nine values was calculated and the deviations of each of the nine calculated centres from this mean value was calculated. Table 8.1 shows the maximum deviations in x and y for a nummber of crosses investigated.

Cross no.	max. deviation in x (pixels)	max. deviation in y (pixels)
1	0.08	0.02
2	0.03	0.02
3	0.38	0.02
4	0.38	0.01
5	0.30	0.30
6	0.27	0.06
7	0.28	0.06
8	0.02	0.23
9	0.38	0.28
10	0.03	0.02
11	0.10	0.06
12	0.10	0.02
13	0.10	0.02
14	0.02	0.01
15	0.18	0.03
16	0.19	0.04
17	0.18	0.02

Table 8.1 Maximum deviations in x and y of the calculated cross position from the mean cross centre

Two conclusions may be drawn from these results. Firstly, precision of the y coordinate is generally better than the

precision in the x coordinate, and by inspection, there is no relationship between the two. Secondly, the precision of locating a cross varies between 0.02 and 0.38 pixels. A precision of 0.05 pixels is considered to be good as it is equivalent to approximately 0.75 microns in the image plane for PHOENICS.

The root cause of the large deviations is inaccurate line determination. At first, it was thought that the weighted mean technique can be applied and would yield satisfactory results as the lines are well defined (ie. contrast) and are symmetrical in crossection in terms of grey shades. Although these assumptions are correct, the ratio of grey values on a line to grey values adjacent to a line is not high enough (typically only 1.5 - 2). As a result the weighted mean technique gives poor results if the first approximation to the line centre is not good (Appendix E). This can and does occur in practice.

In an attempt to determine more precisely the centre of the line, a normal distribution curve was fitted to the grey value profile across a line using the least squares technique. Refering to Fig. 8.1 it can be seen that the shape of the pixel intensity profile across a line is similar to a normal distribution curve. The axis of symmetry of the best-fit normal distribution curve was considered to be the line centre. This approach proved to be unsuitable as again markedly different results were obtained for different first approximations to the line centre.

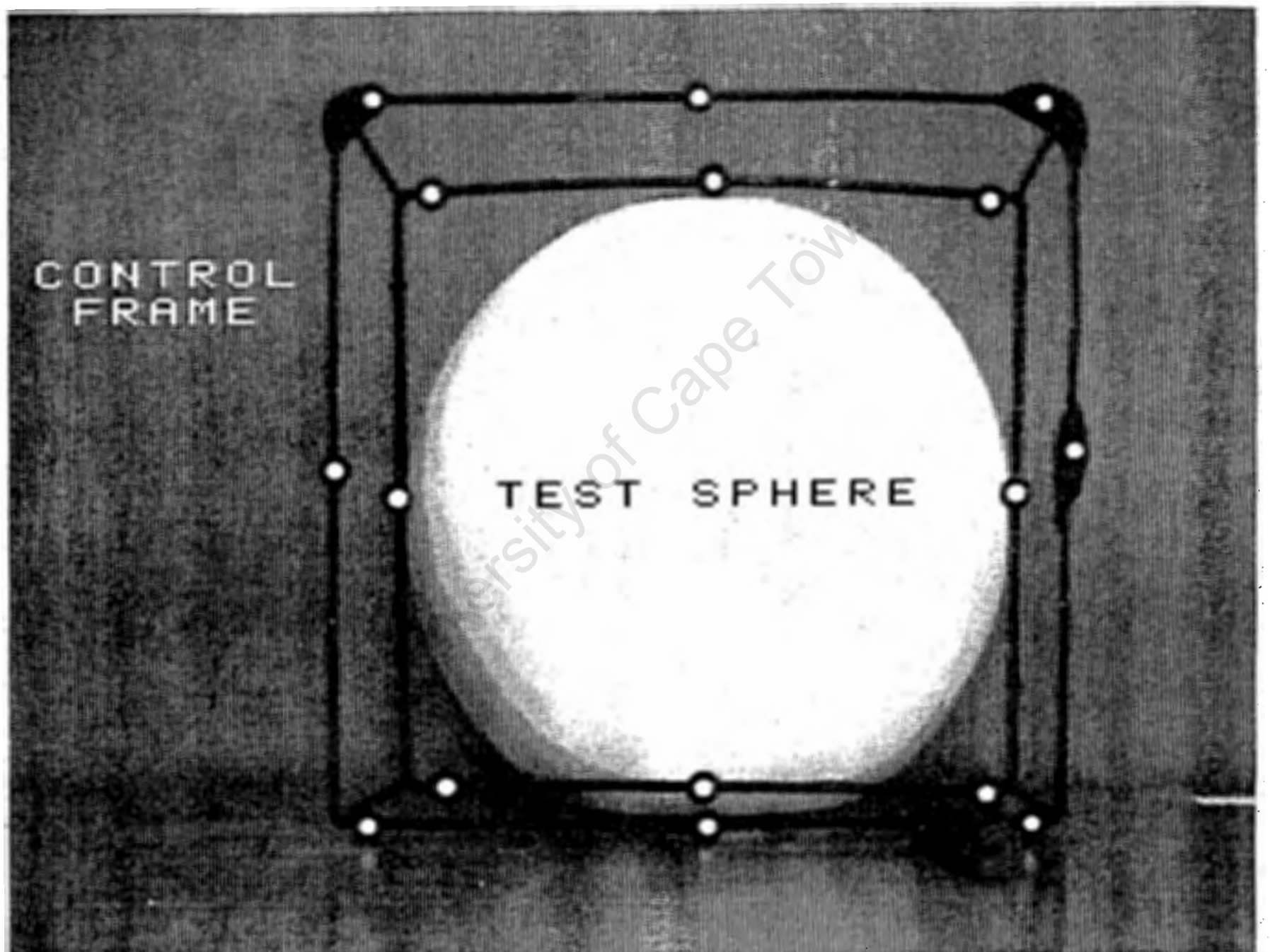

Fig. 8.2 Control frame and test surface

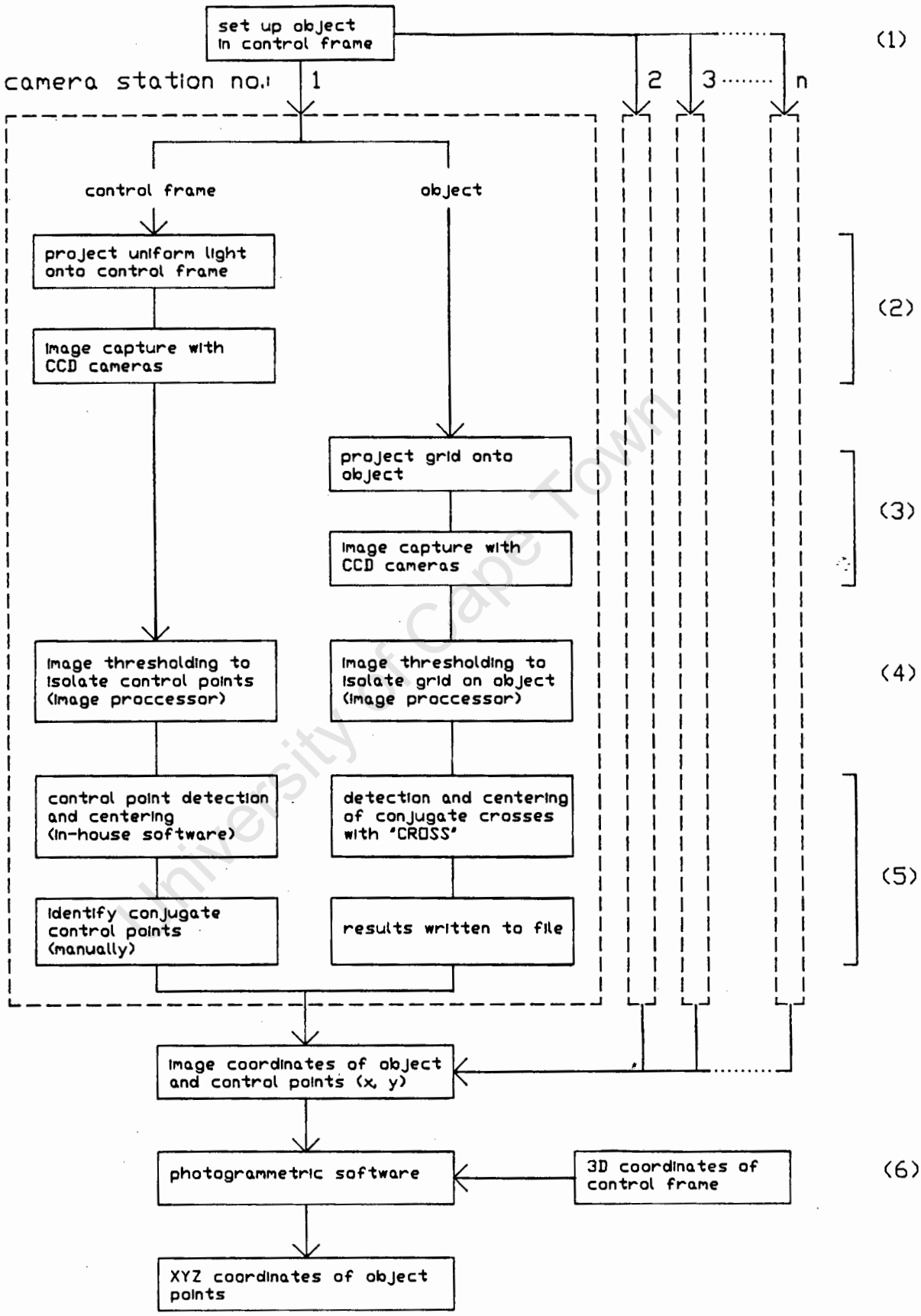

Fig. 8.3 Surface measurement with PHOENICS

5. The images showing the control points (circular targets) and those showing the object points (grid intersections) are evaluated with separate computer programs. A computer program written by Parkyn and Rüther is used to determine the image coordinates of the control points. Conjugate control points are then matched manually. The image coordinates of conjugate object points are determined with CROSS. CROSS is the computer program which implements the cross detection, centering and matching algorithm developed for this thesis.
6. Photogrammetric software written by Rüther is used to determine th XYZ coordinates of the object points.

8.3.3 Results of Measuring the Test Surface

81 points on the sphere in a 9x9 grid were measured as described in 8.3.2 (see Appendix G for some sample images and Appendix I for a sample output of the photogrammetric software).
Analysis of the XYZ coordinates of the object points was done as follows:

1. It was assumed that the actual surface was perfectly spherical with a radius of 125.95 mm.
2. The centre coordinates of the best-fit sphere to the data points was then determined using the least squares technique assuming a fixed radius of 125.95 mm. This was done with a computer program written by Rüther.
3. The normal distance from the surface to each data point was determined by comparing the distance between the centre of the sphere and the data points with the radius.

For the test sphere, the results obtained are summarised as follows:

Distance between camera and sphere	1.5 m
Number of data points	81
Mean normal distance of data point from best-fitting sphere of radius 125.95 mm	0.66 mm
Sum of normal distances of data points to best-fitting sphere	-0.01 mm
Standard deviation of measuring a point on the sphere (σ)	0.92 mm (*)

Table 8.2 Results of measuring the test sphere with PHOENICS

(*) $\sigma = \sqrt{(\Sigma \text{ normal distances btw. sphere and data points})^2/81}$

This represents the accuracy of measuring points with PHOENICS at a distance of 1.5 m.

CHAPTER NINE

9.0 DISCUSSION OF THE ERRORS AND LIMITATIONS OF PHOENICS

The results of the two test stages show that the developed cross detection and centering algorithm is effective. The accuracy with which points on a surface were measured was 0.92 mm at a distance of 1.5 m and corresponds to a relative accuracy of approximately 1:1600. This is acceptabe at the prototype stage of PHOENICS and is compareable to similar systems being developed elsewhere. In this chapter the accuracies and limitations of PHOENICS are discussed.

9.1 Accuracy Limitations in Measuring a Surface with PHOENICS

Apart from errors which are a direct result of the cross detection and centering algorithm, the measuring accuracy of PHOENICS is affected by the following.

1. Determination of the control field

   The XYZ coordinates of the control points which had a diameter of 5 mm were measured with a reflex metrograph with an uncertainty of 0.5 mm. If, for example, smaller targets are used, the target centres can be estimated more precisely and thus the coordinates of the points can be determined with greater accuracy. The limiting accuracy of the reflex metrograph is 0.1 mm.

2. Determination of image coordinates of the control points

   The algorithm which is presently being used to determine the centre of the circular control points can be described as follows: The extents of the target in the binary image are used to determine the size of a rectangular window around the target of which the weighted mean is calculated in the real image. This value is taken as the target centre. This means that that the size and/or the

5. Camera resolution and image size

Camera resolution directly affects the accuracy with which the x and y coordinates of targeted points can be determined in the image plane. Presently, cameras with a higher resolution than those used with PHOENICS are available but expensive. At the time of writing, a high resolution CCD camera (1000x1000 pixels) cost in excess of ten times more than those used with PHOENICS (500x582 pixels). However, rapid advancement in the manufacturing technology of CCDs is continually lowering the purchase price. Furthermore, dimensionally larger pixel arrays which have an even higher pixel density are being developed and promise to significantly increase the accuracies that can be achieved with CCD cameras.

6. Relative camera orientation and number of images

The test sphere was measured using two slightly convergent images. If images from more than two camera positions are used, the accuracy with which points are fixed in space improves considerably. The photogrammetric software of PHOENICS can evaluate the input of up to six images in a single solution. Rüther (1982) has shown that the best results are obtained when the axes normal to the image planes are at 90° to one another.

9.2 Limitations of Surface Measurement with PHOENICS

It has been stated earlier that the most important step in RTP is the acquisition of images which are suitable for a specific intended image processing operation. In particular, this refers to the thresholded images which must be created so that targeted points may be identified automatically. The creation of such images without any operator assistance is a difficulty that has as yet not been overcome with PHOENICS.

The experience that the writer has gained suggests that retroreflective targets used in conjunction with a slide projector (or any other suitable light source) is the simplest and most effective method of creating scenes with highly contrasting targeted points. This method was successfully used to generate suitable images for automatic thresholding. Since only one light source was used, the position and orientation of the cameras was restricted. It is ideal to have a light source at each camera station, or mounted to each camera.

Apart from this general problem, some of the present limitations which are specific to the algorithm that was developed are given below.

1. The object being measured may not change in depth by more than approximately 100 mm, as otherwise, the grid which is projected onto the object will not be in focus over the entire surface.

2. Adjacent crosses must be at least 20 pixels apart. The density of crosses which can be found successfully with the developed algorithm is directly proportional to the camera's resolution. For the cameras used with PHOENICS, the limiting distance between points on the object (ie. projected grid intersections) which can be measured is 10 mm at an object-to-camera distance of 1.5 m. This means that the ratio of grid spacing to the object-to-camera distance may not be smaller than 1:150. An alternative to higher resolution cameras is to decrease the diameter of the small and large search-circles. However, this is not recommended as it would reduce the reliability of the algorithm.

3. Program execution is slow. For the test surface, for which 81 crosses were detected and centered, the program ran for

20 minutes on the IBM PC. More expensive hardware such as a 80386 processor in conjunction with parallel processors will reduce execution time considerably.

CHAPTER TEN

10.0 CONCLUSIONS AND RECOMMENDATIONS

10.1 Conclusions

From the test results which were obtained and the discussion in the previous chapter, the following conclusuions can be drawn.

1. The primary objective of the thesis was to develop a non-contact measuring system for mapping sculptured surfaces so that these can be represented by a set of XYZ coordinates in the form required by the milling system developed by Back (1988). This was successfully completed. A grid is projected onto an object with a slide projector and the XYZ coordinates of the surface at the grid intersections are determined with PHOENICS.

2. An algorithm for the detection, centering and matching of conjugate grid intersection points has been developed and successfully tested.

3. The computer program which was written to implement the developed algorithm can be reliably used as an image matching tool with PHOENICS.

4. The non-contact surface measuring technique which was developed was used in conjunction with the milling system developed by Back (1988) to replicate a test object. This test proved that the combined system is suitable for the manufacture of "sculptured surfaces".

5. The accuracy requirements for the manufacture of medical prostheses can be achieved with the combined measuring and milling system. For example, at an object-to-camera distance of 0.5 m, points on a surface can be measured

with an accuracy of approximately 0.3 mm at an interval of 5 mm. Back (1988) reported an average undercutting error of 0.46 mm for the milling system. This combines to an uncertainty of 0.55 mm.

6. The relative accuracy (absolute accuracy/distance) of PHOENICS may be improved in a number of ways.
   - more accurate determination of the control point coordinates
   - more accurate algorithms for determination of control point image coordinates
   - elimination or compensation for linejitter and other electronic noise
   - correction of lens distortion in the photogrammetric software
   - use of higher resolution cameras
   - use of multiple images and optimal camera orientation

7. The use of retroreflective control point targets in conjunction with a light source is the most effective way of generating images suited to PHOENICS' algorithms for automatic target detection.

10.2 Recommendations

As a result of the findings and conclusions of this thesis, the following recommendations are made.

1. An investigation should be undertaken to determine whether a more accurate method for determining the centre of a line section will increase the accuracy of finding the position of a cross centre. Frobin and Hierholtzer (1983a) and Davis (1988) present some algorithms which should be investigated.

2. A complete error analysis of the PHOENICS measuring process must be done.

3. Smaller control point targets must be used so that the control field may be coordinated more accurately.

4. Investigation of target centering algorithms.

5. The CCD cameras of PHOENICS should be modified to accommodate a suitable light source to be used in conjunction with retroreflective targets.

6. Development and implementation of a control point matching algorithm.

10.3 Closing remarks

PHOENICS is an ongoing project and some of the above recommendations are already being investigated. Presently, work is being carried out in the following areas.

1. Improvement of the algorithm used for finding the centres of the circular control targets.

2. Improvement of the photogrammetric software.

3. Development of user-friendly, front-end software which will integrate all the steps of surface measurement of PHOENICS.

4. Introduction of parallel processors to PHOENICS in order to decrease execution time.

In the near future, PHOENICS will be a fully operational, PC-based, NRTP vision system with a wide range of applications.

11.0 REFERENCES

American Society of Photogrammetry 1980. Manual of Photogrammetry. Fourth Edition. Falls Church, Virginia: American Society of Photogrammetry, p. 1.

Ackermann, F. 1984. Digital Image Correlation: Performance and Potential Application in Photogrammetry. Potogram. Rec., Vol. 11, No. 64, pp. 429-439.

Adams, L. P. 1978. The Use of a Non-Metric Camera for Very Short Range Photogrammerty. Photogrm. Rec., Vol. 9, No. 51, pp. 405-414.

Adams, L. P. 1980. The Use of Short Range Photogrammetry in the study of the Shoebill Bill. Photogrammetric Record, Vol. 10, No. 55, pp. 73-84.

Adams, L. P. 1981. X-ray Photogrammetry for locating the precise, three-dimensional position of image points. Medical and Biological Engineering and Computing, Sept. 1981, No. 19 pp. 569-578.

Back, D. R. 1988. A Computer Aided Machining System for the Manufacture of Three-Dimensional Surfaces. Unpublished B.Sc. Thesis. University of Cape Town, Dept. of Mechanical Engineering. 105 pp.

Badekas, J. 1974. Photogrammetric Surveys of Monuments and Sites. Proceedings of the First Symposium on Photogrammetric Surveys of Monuments and Sites, Athens (edited by J. Badekas), 176 pp.

Beyer, H. A. 1988. Linejitter and Geometric Calibration of CCD Cameras. International Archives of Photo. and R.S., Vol. 27, No. B10, pp. V315-V324.

Berelowitz, M. 1986. The Use of CAD/CAM in the Managemet of Orthopedic Patients. Unpublished B.Sc. Thesis. University of Cape Town, Dept. of Mechanical Engineering.

Dähler, J., 1986. Ladungsgekoppelte Elemente (CCD). Bericht Nr. 107, Institut für Geodäsie und Photogrammetrie, ETH Zürich, 35 pp.

Davis, M. 1988. Target Centering and Image Matching in a NRTP system. Unpublished B.Sc.(Hons) Thesis. University of Cape Town, Dept. of Applied Mathematics. 52 pp.

Duncan, J. P. and S. G. Mair 1983. Sculptured Surfaces in Engineering and Medicine. Cambridge University Press, Cambridge.

El Hakim, S. F. 1985. A Photogrammetric Vision System for Robots. Photogrammetric Engineering and Remote Sensing, Vol. 51, No. 5, pp. 545-552.

El Hakim, S. F. 1986. A Real-Time System for Object Measurement with CCD Cameras. International Archives of P. and R.S., Vol. 26, No. 5, pp. 363-373.

Frobin, W. and E. Hierholzer 1981. Rasterstereography: A Photogrammetric Method for Measurement of Body Surfaces. Photogrammetric Engineering and Remote Sensing, Vol. 47, pp. 1717-1724.

Frobin, W. and E. Hierholzer 1982. Calibration and Model Reconstruction in Analytical Close-range Photogrammetry, Part II. Photogrammetric Engineering and Remote Sensing, Vol. 48, No. 2, pp. 215-220.

Frobin, W. and E. Hierholzer 1983a. Automatic Measurement of Body Surfaces Using Rasterstereography, Part I. Photogrammetric Engineering and Remote Sensing, Vol. 49, No. 3, pp. 377-384.

Frobin, W. and E. Hierholzer 1983b. Automatic Measurement of Body Surfaces Using Rasterstereography, Part II. Photogrammetric Engineering and Remote Sensing, Vol. 49, No. 10, pp. 1443-1452.

Frobin, W. and E. Hierholzer 1985. Simplified Rasterstereography Using a Metric Camera. Photogrammetric Engineering and Remote Sensing, Vol. 51, No. 10, pp. 1605-1608.

Gruen, A. 1985. Adaptive Least Squares Correlation - A Powerful Image Matching Technique. Presented Paper to the ACSM-ASP Convention, Washington, D. C., March 1985.

Gruen, A. 1986. The Digital Photogrammetric Station at the ETH Zürich. Paper Symposium ISPRS Commission 2, Baltimore, May 1986.

Gruen, A. 1987. Towards Real-Time Photogrammetry. Invited Paper, 41. Photogrammetric Week, Stuttgart, September 14-19, 33 p.

Gruen, A. W. and Beyer, H. A. 1987. Real-Time Photogrammetry at the Digital Photogrammetric Station (DIPS) of ETH Zürich. The Canadian Surveyor, Vol. 41, No. 2, pp. 181-199.

Haggren, H. 1986. Real-Time Photogrammetry as used for Machine Vision Applications. International Archives of Photogrammetry and Remote Sensing, Vol.26, No. 5, pp. 374-382.

Hirschberg, I. 1985. Advances in High-Resolution Imagers. Electronic Imaging, April 1985, pp. 56-62.

Keefe, M. and D. R. Riley 1986. Capturing Facial Surface Information. Photogrammetric Engineering and Remote Sensing, Vol. 52, No. 9, pp. 1539-1548.

Knödler, G. and Kupke, H. 1974. The use of Industrial Photogrammetry in the Production of Ship's Screws. Jena Review, No. 3, 1974.

Luhmann, T. 1986. Ein Verfahren zur rotationsinvarianten Punktbestimmung. Bildmessund und Luftbildwesen, 54 (1986), Heft 4.

Luhmann, T. and Webster-Ebbinghaus, W. 1986. Rolleimetrics RS - A new system for digital image processing. Paper Symposium ISPRS Commission 2, Baltimore 1986.

Real, R. R., 1986. Components for Video-Based Photogrammetry of Dynamic Processes. International Archives of Photogrammetry and Remote Sensing, Vol. 26, No. 5, pp.432-444.

Real, R. R. and Y. Fujimoto 1986. Digital Video Stereoscopy: Real-Time Instrumentation Issuses. Paper Symposium ISPRS Commission 2, Baltimore, May 1986.

Rüther, H. 1982. Relative Orientation with Limited Control. Unpublished Ph.D. Thesis. University of Cape Town, Dept. of Surveying.

Rüther, H. and Hall-Martin, A. 1979. Application of Stereo Photogrammetric Techniques for Measuring African Elephants. Koedoe, No. 22, pp. 187-198.

Rüther, H. and Parkyn, N. 1988. The Development of a PC-based Near-Real-Time Photogrammetry System - PHOENICS. International Archives of Photo. and R.S., Vol. 27, No. B8, pp. V105-V116.

Schild, W. 1988. Zeilen, Linien oder Megahertz?. Funkschau, September 1988, pp. 48-51.

Turner-Smith, A. R. and J. D. Harris 1986. Measurement and Analysis of Human Back Surface Shape. International Archives of Photo. and R.S., Vol. 26, No. 5, pp. 355-362.

Vaughn, C., G. Brooke, M. Price and J. Ireland 1986. The Micron Eye Toposcanner: A Versatile Anthropometric Instrument. Presented Paper, 2nd Annual Congress, Ergonomics Society of Southern Africa, Cape Town.

Wong, K. W. 1986. Stereo Solid State Cameras. International Archives of Photogrammetry and Remote Sensing, Vol. 26, No. 5, pp. 454-458.

Wong, K. W. and Wei-Hsin Ho 1986. Close-Range Mapping with Solid-State Cameras, Photogrammetric Engineering and Remote Sensing, Vol. 52, No. 1, pp. 67-74.

Wong, K. W. 1987. Real-Time Machine Vision Systems, The Canadian Surveyor, Vol. 41, No. 2, pp. 173-180.

12.0 BIBLIOGRAPHY

American Society of Photogrammetry 1980. Manual of Photogrammetry. Fourth Edition. Falls Church, Virginia: American Society of Photogrammetry, 1056 pp.

Wolf, P. R. 1983. Elements of Photogrammetry. Second Edition. Singapore: Mc Graw-Hill Book Co, 628 pp.

Moffit, F. H. and Mikhail, E. M. 1980. Photogrammetry. Third Edition. New York: Harper and Row, Inc., 648 pp.

APPENDIX A : Derivation of the Orientation Matrix

The most direct way of deriving a matrix which will transform cartesian coordintes from a reference system (XYZ system) into one which is rotated about each of the X, Y and Z axes (xyz system) is to sequentially perform these rotations.

Consider the XYZ system shown below:

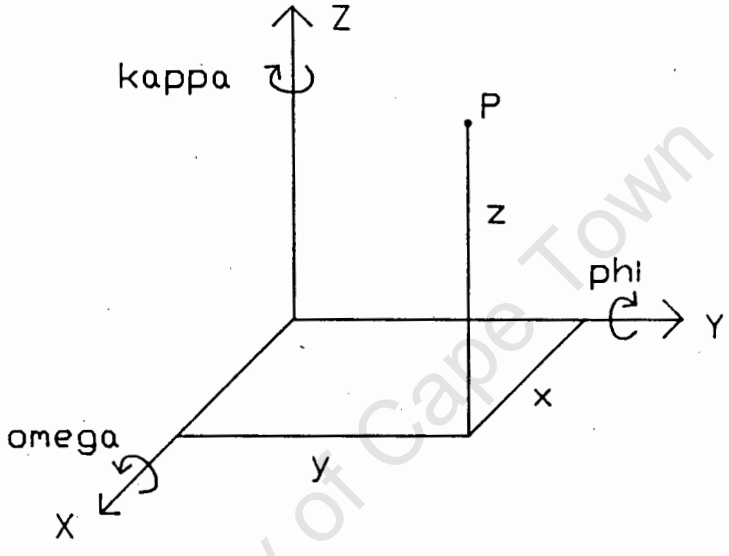

Fig. A.1 Three-dimensional right-handed coordinate system

The rotation matrices for rotations omega, phi and kappa are:

$$\underline{M}_w = \begin{bmatrix} 1 & 0 & 0 \\ 0 & \cos w & \sin w \\ 0 & -\sin w & \cos w \end{bmatrix}$$

$$\underline{M}_\varphi = \begin{bmatrix} \cos \varphi & 0 & -\sin \varphi \\ 0 & 1 & 0 \\ \sin \varphi & 0 & \cos \varphi \end{bmatrix}$$

$$\underline{M}_k = \begin{bmatrix} \cos k & \sin k & 0 \\ -\sin k & \cos k & 0 \\ 0 & 0 & 1 \end{bmatrix}$$

The orientation matrix $\underline{M}$ is then obtained by simply performing the matrix multiplication $\underline{M}_w * \underline{M}_{\bar{\varphi}} * \underline{M}_k$ to yield:

$$\underline{M} = \begin{bmatrix} m_{11} & m_{12} & m_{13} \\ m_{21} & m_{22} & m_{23} \\ m_{31} & m_{32} & m_{33} \end{bmatrix}$$

where:
$m_{11} = \cos\bar{\varphi} * \cos k$
$m_{12} = \sin w * \sin \bar{\varphi} * \cos k + \cos w * \sin k$
$m_{13} = -\cos w * \sin \bar{\varphi} * \cos k + \sin w * \sin k$
$m_{21} = -\cos \bar{\varphi} * \sin k$
$m_{22} = -\sin w * \sin \bar{\varphi} * \sin k + \cos w * \cos k$
$m_{23} = \cos w * \sin \bar{\varphi} * \sin k + \sin w * \cos k$
$m_{31} = \sin \bar{\varphi}$
$m_{32} = -\sin w * \cos \bar{\varphi}$
$m_{33} = \cos w * \cos \bar{\varphi}$

APPENDIX B : Derivation of the Collinearity Equations

Collinearity is the condition which states that the exposure station, an object point and its image point must all lie on a straight line (see Fig. B.1). Here the image coordinates are xyz and the object coordinates are XYZ.

The principal point has coordinates x_o, y_o in the image space and hence, the coordinates of any point 'a' in the image space are $(x - x_o)$, $(y - y_o)$ relative to the principal point. x and y are measured from an arbitrary origin on the image.

The exposure station has coordinates X_o, Y_o, Z_o in the object space, and hence, the coordinates of a point 'A' corresponding to the image point 'a' will have coordinates $(X_A - X_o)$, $(Y_A - Y_o)$, $(Z_A - Z_o)$ relative to the exposure station.

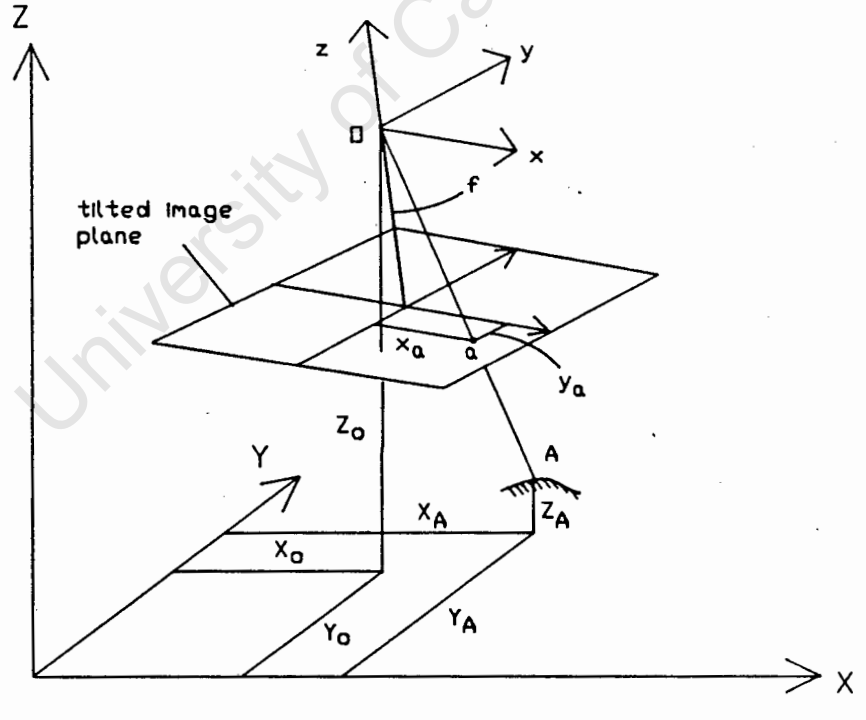

Fig. B.1 Diagram of the collinearity condition

In order to develop the condition equations, the image plane must first be rotated so that its coordinate system is parallel

to that of the object space. This is done with the rotation matrix M (derived in Appendix A) which has elements that are functions of omega, phi and kappa (rotations about the x, y and z axes). The new coordinate system (x'y'z') is shown in Fig. B.2.

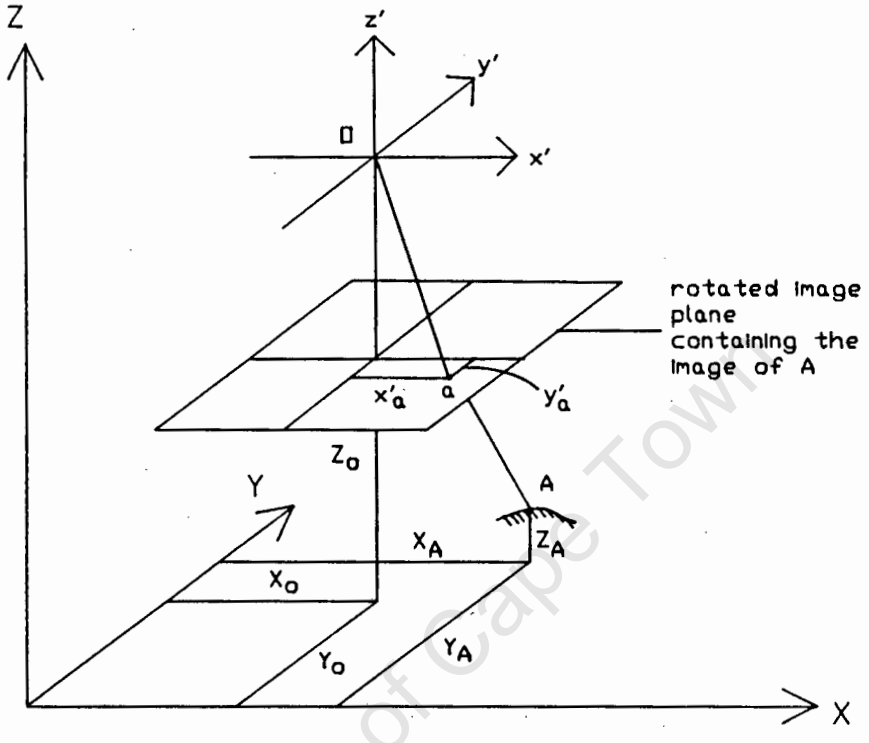

Fig. B.2 Image coordinate system rotated so that it is parallel to the object space

Thus

$$\begin{bmatrix} x_a - x_o \\ y_a - y_o \\ z_a - z_o \end{bmatrix} = M^T * \begin{bmatrix} x_a' - x_o' \\ y_a' - y_o' \\ z_a' - z_o' \end{bmatrix} \qquad (B-1)$$

Using Fig. B.2 the collinearity condition equations can be derived from similar triangles subtended from the exposure station (O) into the image and object space.

Thus

$$\frac{x_a' - x_o'}{X_A - X_o} = \frac{y_a' - y_o'}{Y_A - Y_o} = \frac{z_a' - z_o'}{Z_A - Z_o}$$

Or

$$\begin{aligned} x_a' &= ((X_A - X_o) / (Z_A - Z_o)) * (z_a' - z_o') \\ y_a' &= ((Y_A - Y_o) / (Z_A - Z_o)) * (z_a' - z_o') \\ z_a' &= ((Z_A - Z_o) / (Z_A - Z_o)) * (z_a' - z_o') \end{aligned} \qquad \text{(B-2)}$$

Expanding equation (B-1), substituting equations (B-2) and dropping the 'a'/'A' subscript (since A is an arbitrary point), get:

$$x - x_o = (m_{11}*\frac{X - X_o}{Z - Z_o} + m_{12}*\frac{Y - Y_o}{Z - Z_o} + m_{13}*\frac{Z - Z_o}{Z - Z_o})*(z'-z_o') \qquad \text{(B-3)}$$

$$y - y_o = (m_{21}*\frac{X - X_o}{Z - Z_o} + m_{22}*\frac{Y - Y_o}{Z - Z_o} + m_{23}*\frac{Z - Z_o}{Z - Z_o})*(z'-z_o') \qquad \text{(B-4)}$$

$$z - z_o = (m_{31}*\frac{X - X_o}{Z - Z_o} + m_{32}*\frac{Y - Y_o}{Z - Z_p} + m_{33}*\frac{Z - Z_o}{Z - Z_o})*(z'-z_o') \qquad \text{(B-5)}$$

Dividing equation (B-3) and (B-4) by (B-5) and noting that all image points will have z' = -f (the focal length) yields:

$$\begin{aligned} x &= (-f - z_o) * \frac{m_{11}(X - X_o) + m_{12}(Y - Y_o) + m_{13}(Z - Z_o)}{m_{31}(X - X_o) + m_{32}(Y - Y_o) + m_{33}(Z - Z_o)} + X_o \\ y &= (-f - z_o) * \frac{m_{21}(X - X_o) + m_{22}(Y - Y_o) + m_{23}(Z - Z_o)}{m_{31}(X - X_o) + m_{32}(Y - Y_o) + m_{33}(Z - Z_o)} + Y_o \end{aligned} \qquad \text{(B-6)}$$

Now, multiplying out the parentheses, transposing x_o, y_o to the right hand sides of the equations, and defining new constants, equation (B-6) can be rewritten as:

$$x = \frac{b_{11}*X + b_{12}*Y + b_{13}*Z + b_{14}}{b_{31}*X + b_{32}*Y + b_{33}*Z + 1}$$

$$y = \frac{b_{21}*X + b_{22}*Y + b_{23}*Z + b_{24}}{b_{31}*X + b_{32}*Y + b_{33}*Z + 1} \qquad \text{(B-7)}$$

APPENDIX C : Epipolar Geometry

If the interior and exterior orientation of a pair of stereo images are known, then for any point in the first image a relationship between the x and y image coordinates of the corresponding point in the second image can be determined using photogrammetric algorithms. This relationship describes what is called an epipolar line and has the form $y = ax + b$.

Epipolar lines are lines of intersection between the image planes and a plane passing through an object point and the perspective centres of the two images (Fig. C-1).

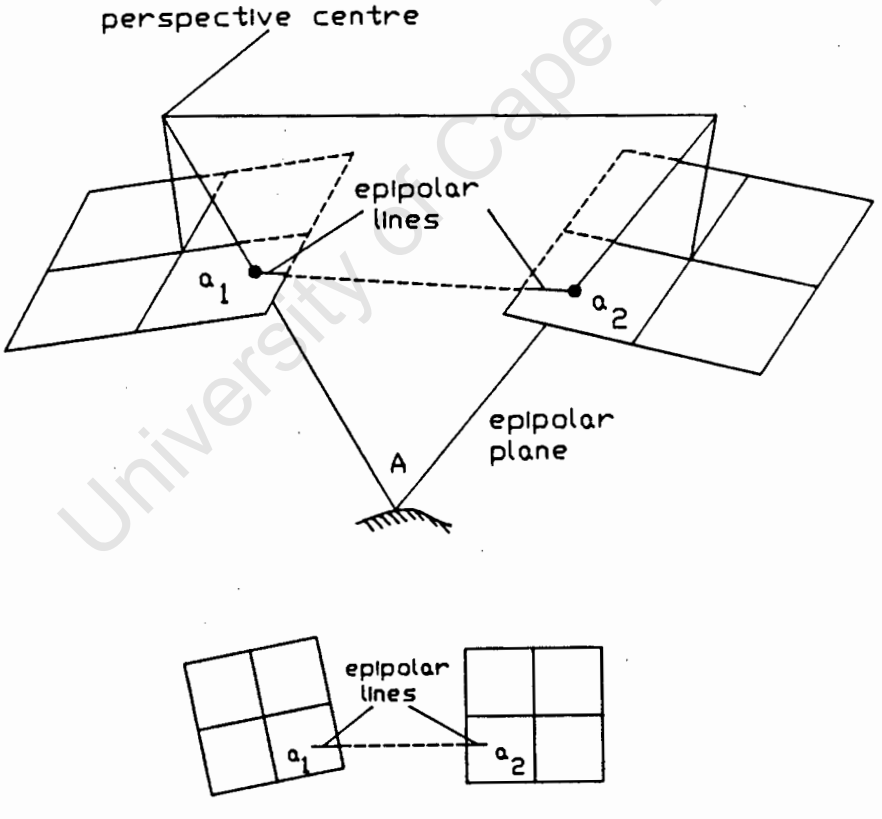

Fig. C-1 Epipolar plane and epipolar lines

Any point on the object contained in the epipolar plane, will lie on the epipolar lines in the images. Thus, for any object point in image 1 (point A), its corresponding point in image 2 must lie on the respective epipolar line (BC).

APPENDIX D : A Method of Interfacing the PIP Image Proccessing Board with a Computer Language other than those it supports

The PIP IP supports the MS-'C' and the MS-FORTRAN computer languages. This means that the built-in functions of the IP can be directly executed in a program written in either of these two languages. With any other computer language, this is not possible.

In this thesis the software was written in TRUE BASIC. This meant for example that the position of a cross that was detected and its centre found, could not be displayed on the image. The image could not be called up, nor could any of the IP graphics routines be executed from a TRUE BASIC program. Thus there was no way of easily checking the results obtained.

In order to check the results, it was neccessary to:

1. note the coordintes of the point
2. exit from TRUE BASIC
3. use the interpreter program of the IP (*) to call up the particular image
4. use the graphics facilities of the IP to indicate the point on the imge (two commands per point)

(*) The interpreter program of the IP (PIPINT.EXE) is a program which allows the user to enter any of the IP functions from the keyboard.

A way of using the IP from within a TRUE BASIC program was found by the author.

When the interpreter program is executed, it automatically searches for the file INIT.PIP which contains the appropriate interpreter commands to initialise the board to a desired state. Any interpreter command in this file is automatically executed. The INIT.PIP file is a text file which the user can modify to

suit his or her needs. All the interpreter commands must be in lower case letters. The INIT.PIP file can also be modified from within a TRUE BASIC program by specifying its organization as "TEXT" in the "OPEN" statement. In TRUE BASIC the "OPEN" statement associates a channel with a file saved on disk.

Once the INIT.PIP file has been edited, all that remains to be done is to run the interpreter program. There are two ways of doing this:

1. A batch file is used in which first the TRUE BASIC program is executed and then the interpreter program is run.

   Example of commands in a batch file:

HELLO MYPROG.TRU	(loads TRUE BASIC, executes "MYPROG.TRU" and returns to DOS)
PIPINT.EXE	(runs the interpreter program automatically executing the commands in INIT.PIP)

   Note: Drive and path specifications have been omitted here, but are neccessary.

2. The TRUE BASIC EXEC_RETURN subroutine is used in a TRUE BASIC program. The EXEC_RETURN subroutine is contained in the EXEC.TRC library file of the TRUE BASIC RUNTIME PACKAGE. At the start of the program the statement "LIRARY EXEC.TRC" must be included. In order to execute the interpreter program, the subroutine EXEC_RETURN must be called with argument "PIPINT.EXE" ie. as a program statement: CALL EXEC_RETURN("PIPINT.EXE").

In the latter case it is recommended that the INIT.PIP file contains as its last statement the "quit" command which will terminate the interpreter program as the writers of TRUE BASIC

do not encourage the use of the EXEC_RETURN subroutine to run "execute-and-stay-resident programs".

APPENDIX E : Evaluation of Using the Weighted Mean Technique for Determining the Position of a Line-Section with Sub-Pixel Accuracy

Typical pixel intensity profiles of two line sections are shown in Fig. E.1. The position of the line section was taken to be at the peak of the best-fit curve to the data points. The curve was generated with a CAD program which uses B-splines for curve fitting. The pixel intensity values are given in Table E.1 below.

	Pixel intensity	
Pixel position	Line 1	Line 2
1	105	106
2	106	111
3	120	112
4	128	114
5	146	127
6	170	150
7	198	186
8	198	194
9	195	192
10	174	173
11	138	137
12	124	125
13	118	117
14	109	111
15	107	111
Centre of line	7.75	8.35

Table E.1 Pixel intensity values of two typical line sections

The weighted mean of an initial mask of 8 pixels was calculated. This value was then used as the centre of the next mask. The process was iterated until the position of the weighted mean converged. This was done for a number of different positions of the initial mask for both line sections. The results obtained are tabulated in table E.2.

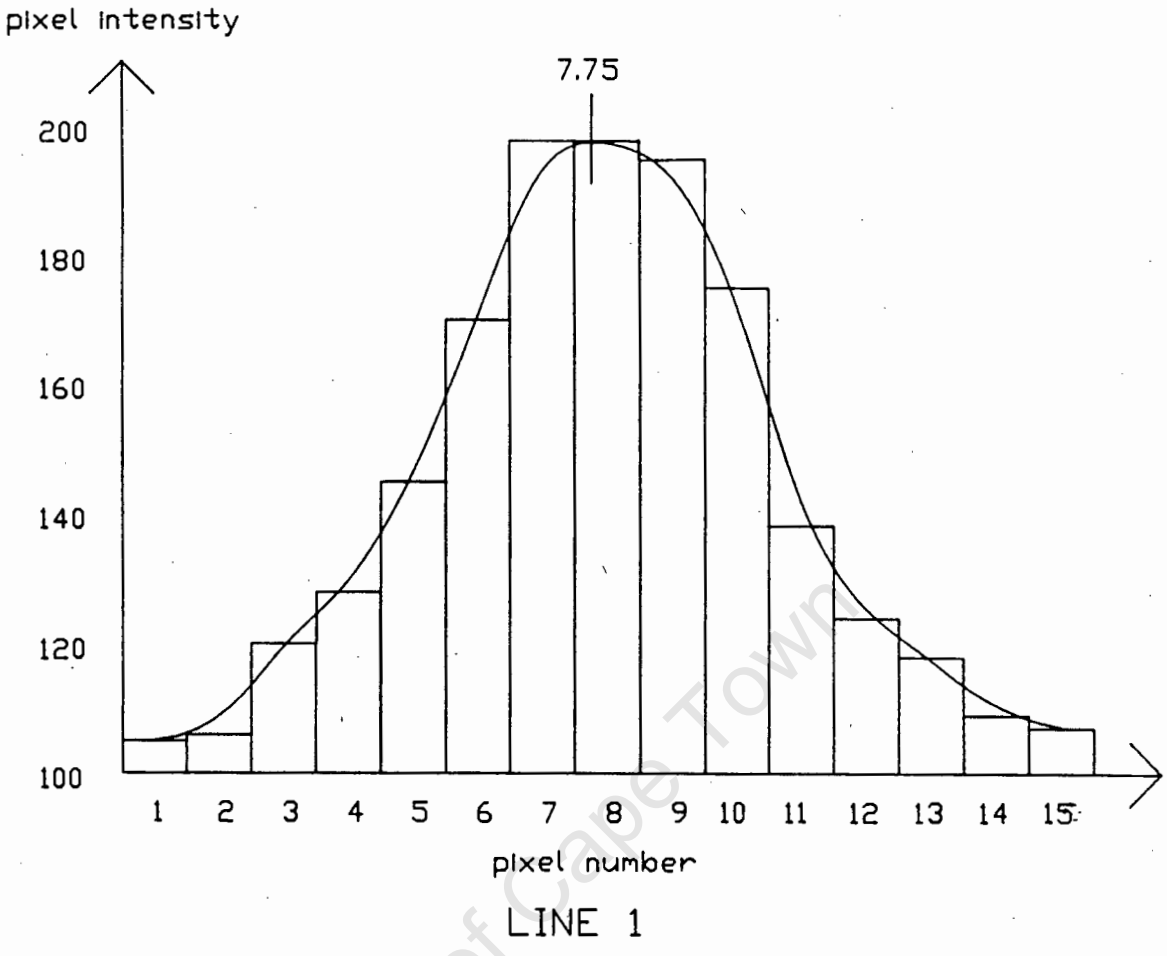

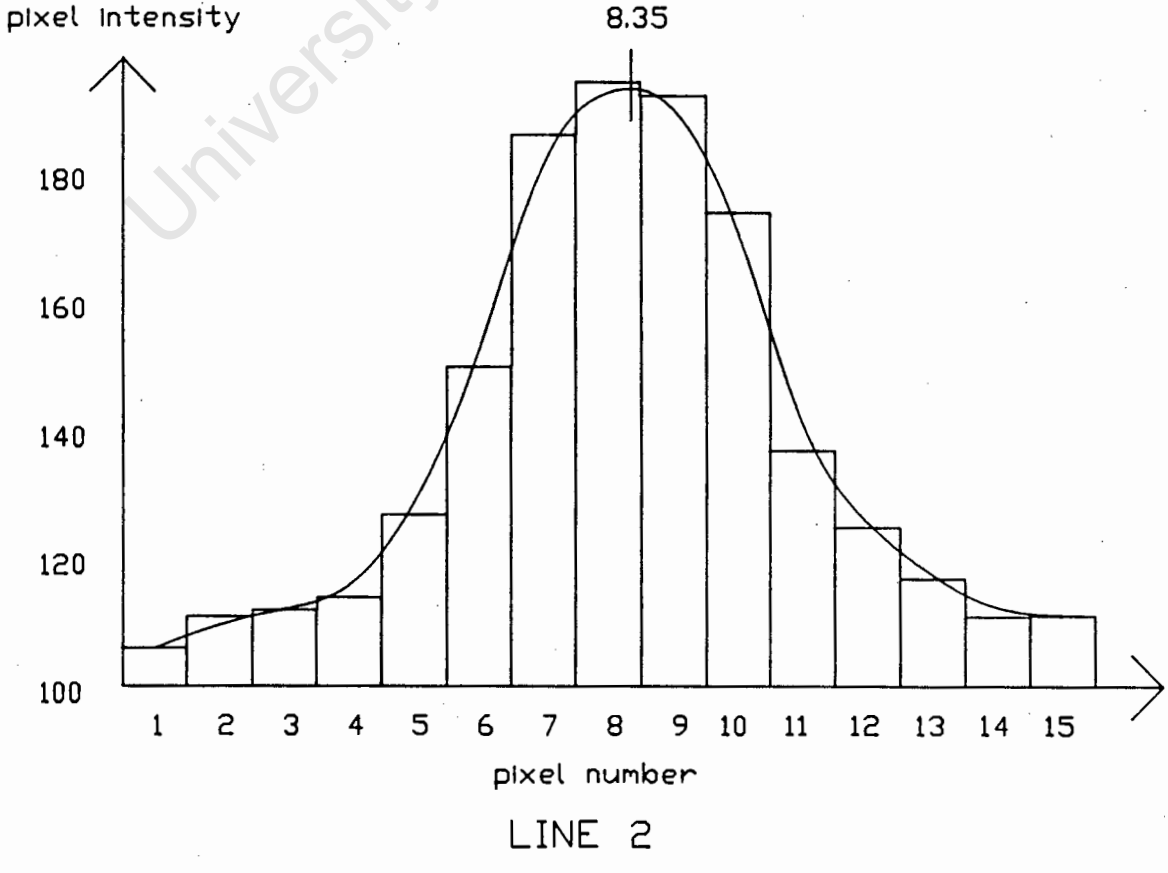

Fig. E.1 Pixel intensity profiles of two typical line sections

Centre of initial mask	Position of line centre (pixels)				Deviation from approx. centre (pixels)	
	Line 1		Line 2		Line 1	Line 2
	1st iteration	2nd iteration	1st iteration	2nd iteration		
6	6.48	-	6.52	-	-1.27	-1.83
7	7.30	-	7.33	-	-0.45	-1.02
8	7.98	-	8.09	-	0.23	-0.26
9	8.73	-	8.83	-	0.98	0.48
10	9.52	-	9.60	-	1.77	1.25
11	10.39	9.52	10.45	9.6	1.77	1.25

Table E.2 Results of applying the weighted mean technique for finding the position of a line section

From the results it became clear that this method is not suitable for determining the position of a line section as it does not converge. In addition, it only gives an acceptable result if the first approximation to the line section is good. As the thresholded image is used to determine the first approximation, it is quite possible that it will be one, or even two, pixels from the "true" value.

APPENDIX F : List of Computer Programs for use with PHOENICS

This Appendix contains a list of the computer programs which have been written by the author and a brief explanation of their use. These programs may be useful to future researchers. The user is expected to have a working knowledge of DOS, TRUE BASIC, and the PIP image processor. The neccessary background of PHOENICS has been given in the main text.

F.1 TRUE BASIC Programs

These programs can be run using the TRUE BASIC compiler.

Program name	Coments
CROSS.TRU	determines the position of grid intersections in an image to sub-pixel accuracy. The following files must be on disk: CIRPOS_S.TRU CIRPOS_L.TRU SQUPOS_S.TRU SQUPOS_L.TRU CIRXY_S.TRU CIRXY_L.TRU IPLIB.TRC EXEC.TRC (part of the TB RUNTIME package)
IPLIB.TRU	a library file containing image processing routines - it cannot be run on its own.
IPLIB.TRC	compiled version of IPLIB.TRU
VIEW.TRU	the pixel intensity values of a portion of an image may be: a. displayed on the computer screen b. printed on the printer c. written to a text file for later manipulation (eg. using LOTUS, VP-PLANNER)

INV_ALL.TRU	inverts (in terms of colour) a grey image and writes the result to a file
INV_BW.TRU	inverts (in terms of colour) a binary image and writes the result to a file
THRESH.TRU	thresholds an image and writes the result to a file
CONCH.TRU	computes the distance between two numbered points. The coordintes of the points must be in a TRUE BASIC record file (recsize = 8) in the following format: point number, X, Y, Z.
TR	converts a text file which contains numbered x,y (image) coordinates to a record file (recsize = 8) in the following format: point number, x, y
RT	converts a record file (recsize = 8) in the format point number, x coordinate, y coordinate, to a text file
TR6	general text-to-record file conversion
TR	converts a text file which contains numbered x,y (image) coordinates to a record file (recsize = 8) in the following format: point number, x, y
RT	converts a record file (recsize = 8) in the format point number, x coordinate, y coordinate, to a text file
REDIT	allows the user to alter the point numbering of image coordinates (x, y)in a record file (recsize = 8)
REDIT1	allows the user to alter the point numbering of space coordinates (X, Y, Z) in a record file (recsize = 8)

F.2 PIP Image Processor Macros

Certain desired functions which may be performed using the PIP image processor require a sequence of commands to be entered at

the keyboard. Such a sequence of commands may be written to a file (macro) and stored. A macro can be recalled later and executed.

A list of the macros which have been written is given below.

Program name	Coments
CAM.	camera initialised on current board
CAM.R	cameras initialised on both boards
CWR.R	the contents of "quad 0" of boards "0" and "1" are written to the files "cim1" and "cim2" respectively - grey images of control points
CWRT.R	the contents of "quad 0" of boards "0" and "1" are written to the files "cimt1" and "cimt2" respectively - binary images of control points
ITHI(.R)	image is thresholded and inverted (in terms of colour) at image capture (input), the user is prompted for the thresholding value
ITHO(.R)	image is thresholded and inverted (in terms of colour) at the display (output), the user is prompted for the thresholding value
NEGI(.R)	the image is inverted (in terms of colour) at image capture (input)
NEGO(.R)	the image is inverted (in terms of colour) at the display (output)
NORMI(.R)	the image is normalised at image capture (input) ie. any previous commands/macros which alter the input are neutralised
NORMO(.R)	the image is normalised at image display (output) ie. any previous commands/macros which alter the output are neutralised
OWR.R	the contents of "quad 0" of boards "0" and "1" are written to the files "oim1" and "oim2" respectively - grey images of object points

OWRT.R	the contents of "quad 0" of boards "0" and "1" are written to the files "oimt1" and "oimt2" respectively - binary images of object points
SCALES	a grid and xy scales are drawn onto the image which is currently being displayed
THI(.R)	image is thresholded at image capture (input), the user is prompted for the thresholding value
THO(.R)	image is thresholded at the display (output), the user is prompted for the thresholding value

Note: - the ".R" indicates that both boards are addressed in the macro

- the image name convention which has been adopted for PHOENICS is the following:

  [c/o][project name][image number]

  [c/o] denotes whether the image contains control points or object points

APPENDIX G : A Set of Typical Images which were used for Surface Measurement with PHOENICS

For each camera station there are four images: A grey and a thresholded image of the control field to determine the control point coordinates, and a grey and a thresholded image of the object to determine the object point coordinates. At present it is neccessary to have separate images of the control frame and the object, since it is difficult to obtain an image from which control and object points can be determined. Furthermore, the algorithms for point determination and matching of the two different types of targets (circular and cross shaped) have been developed independently.

The images shown in this Appendix were taken from two different camera positions and have been labeled "left" and "right". Fig. G.7 shows the grid and scales which are overlayed to assist the user when prompted to enter a starting point for the image search at the start of the CROSS program.

G.1 Gray image (left) for determining the central point

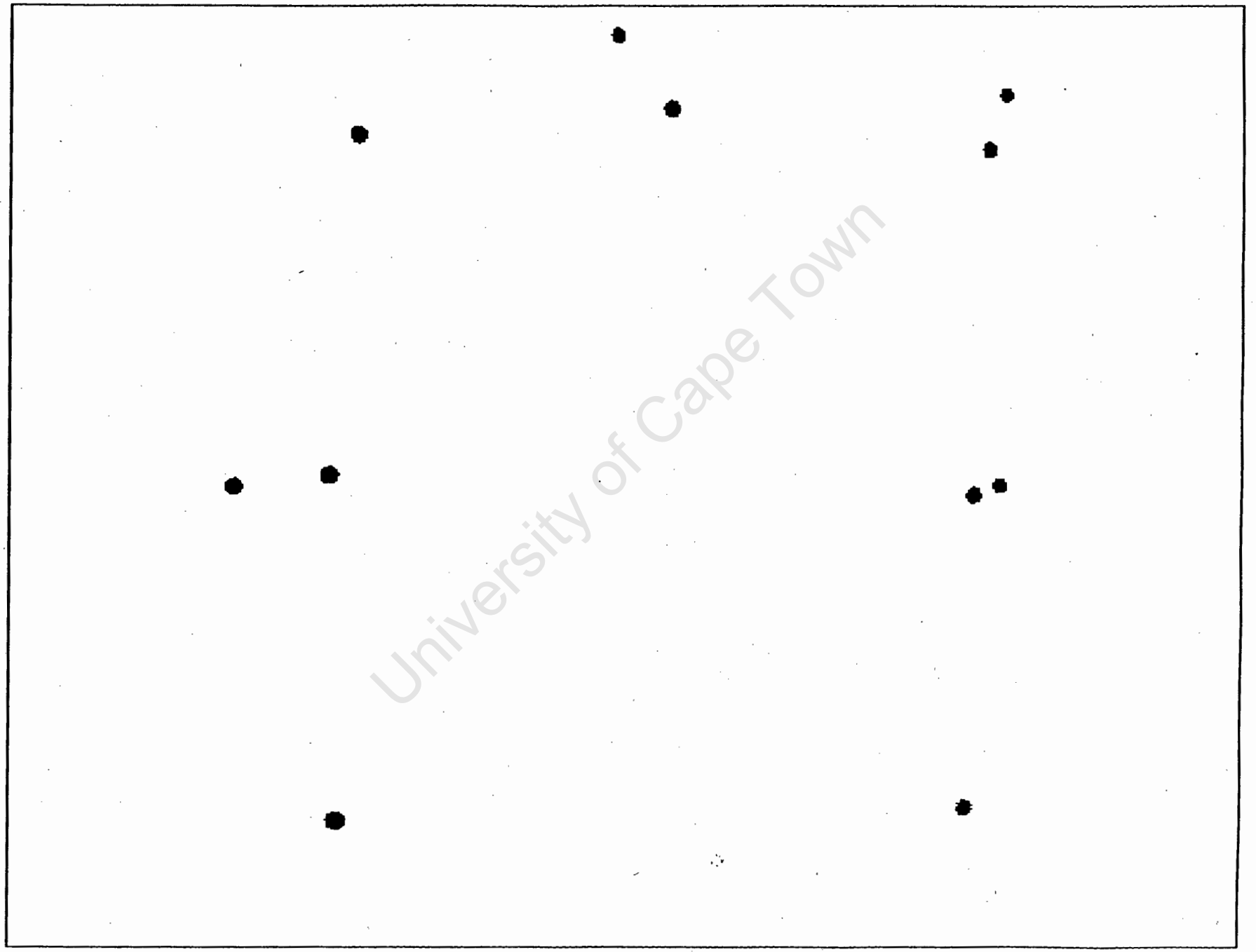

G.2 Thresholded image (left) for determining the contol points

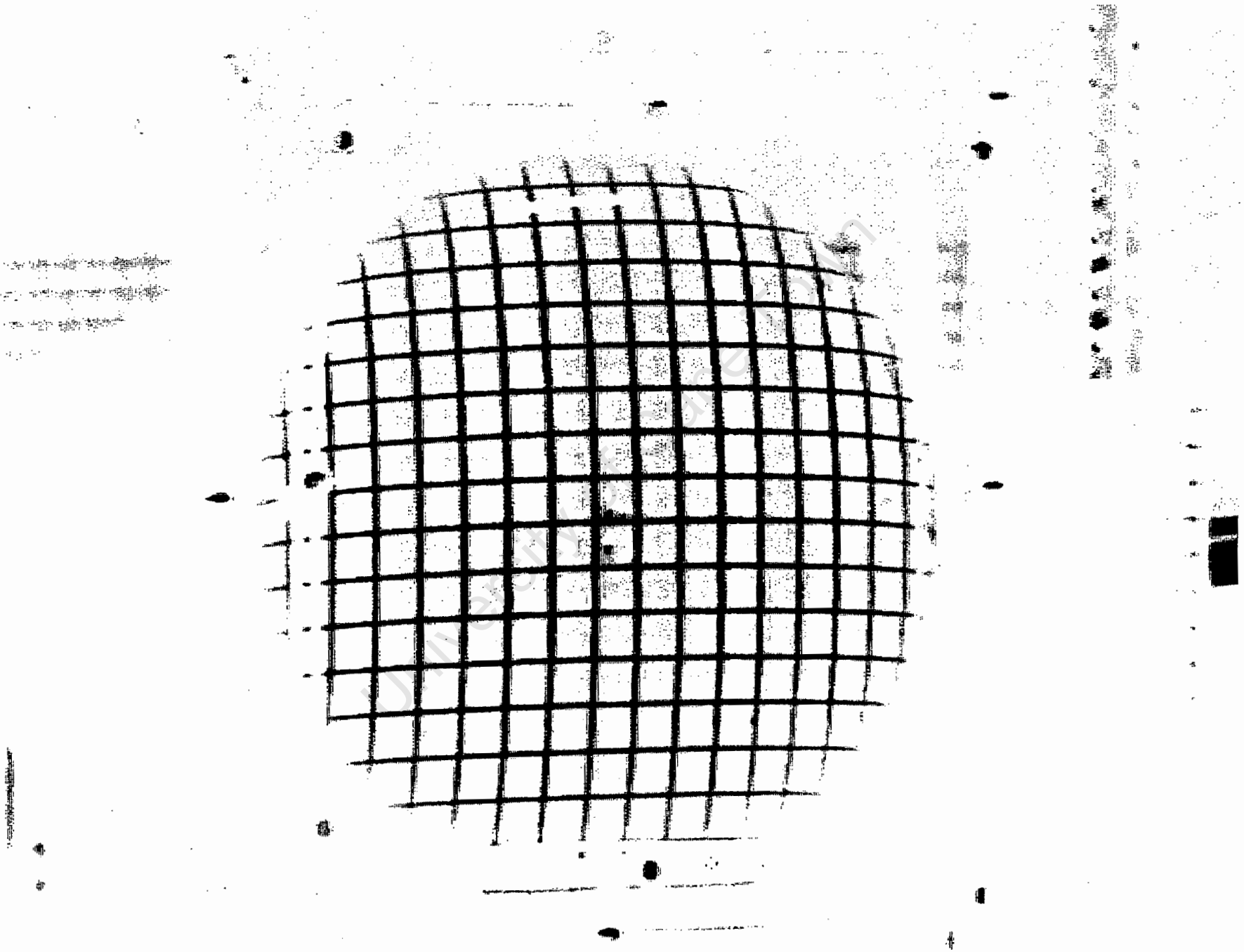

G.3 Grey image (left) for determining the object points

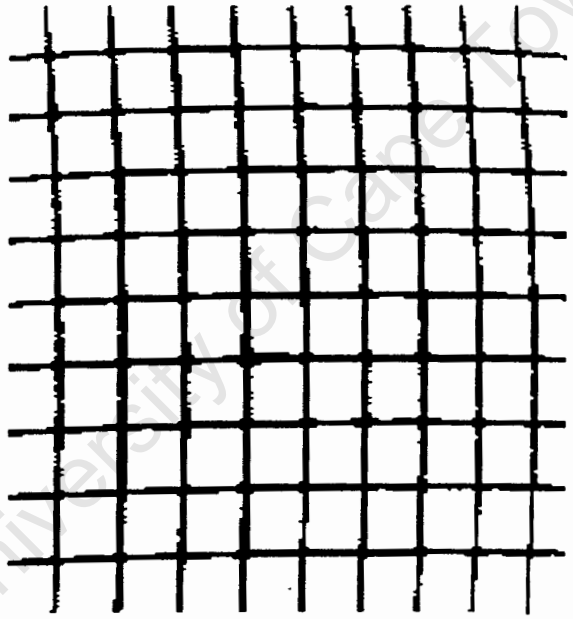

G.4 Thresholded image (left) for determining the object points

G.5 Grey image (right) for determining the control points

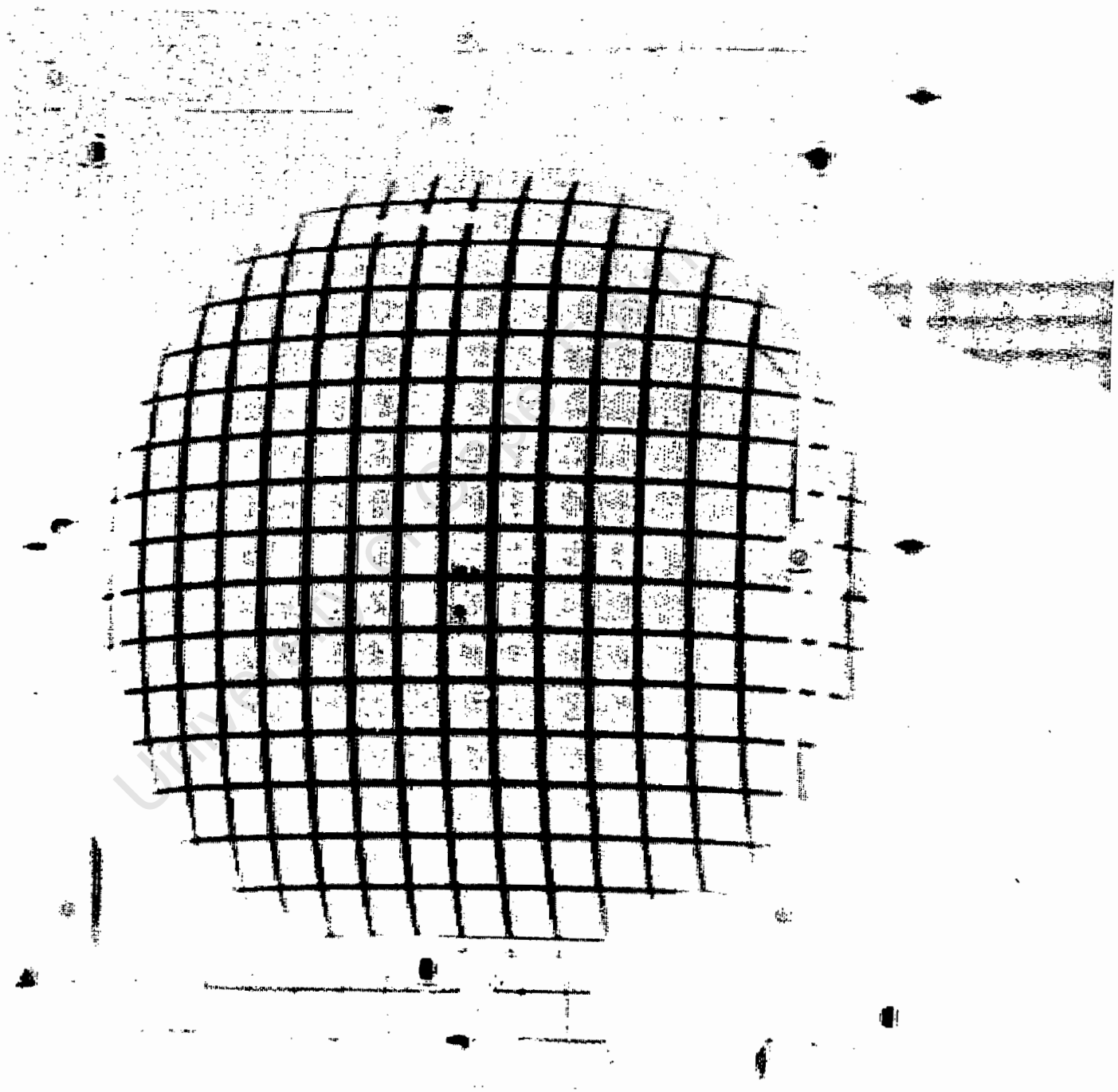

G.6 Grey image (right) for determining the object points

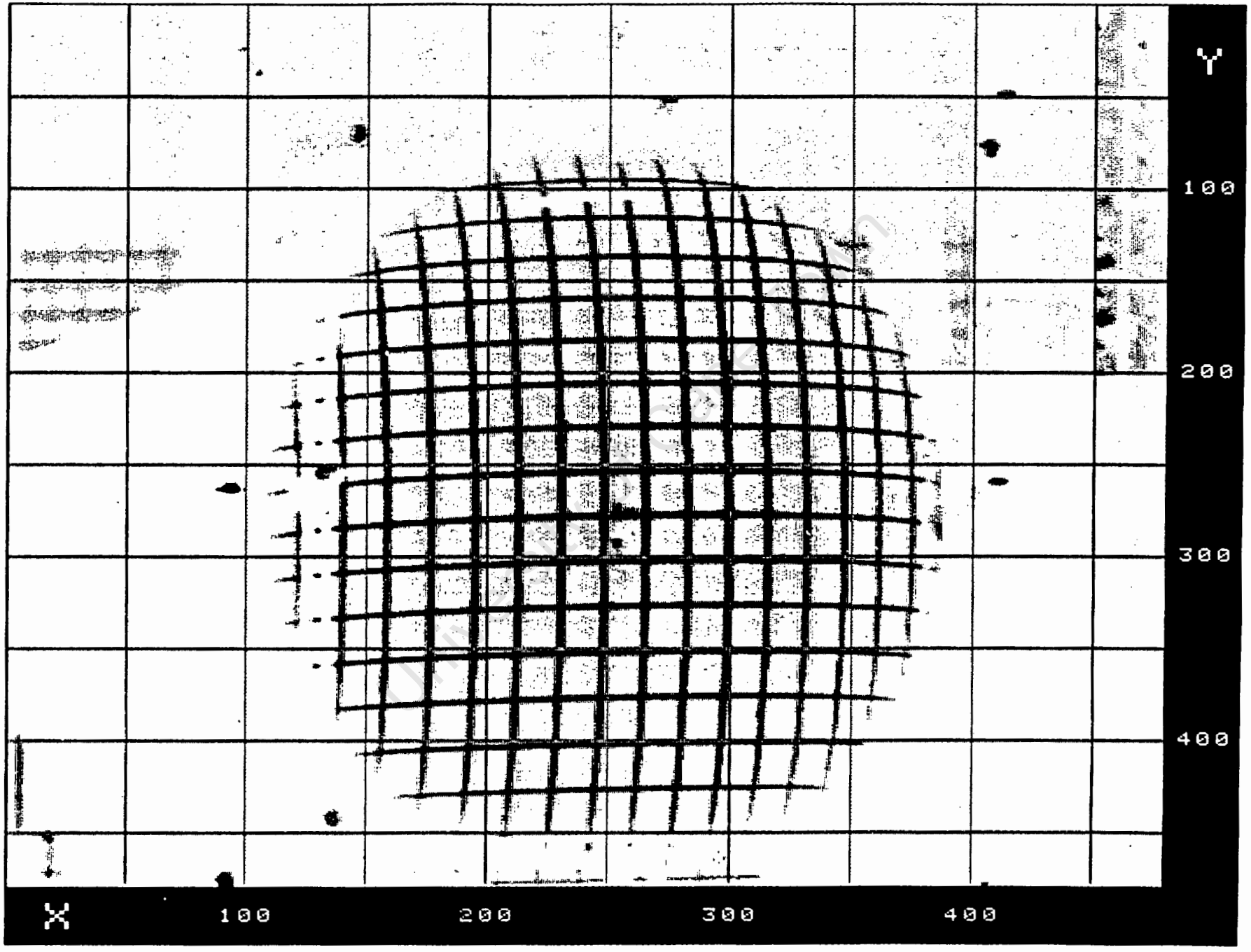

G.7 Image for determining the object points with a graduated grid overlayed

APPENDIX H : Coordinates of the Control Frame

Control point number	Coordinates of control points (mm) X	Y	Z
1	286.52	19.16	116.56
2	298.50	147.47	115.57
3	286.05	287.68	118.09
4	259.30	49.38	17.31
5	270.56	152.66	17.86
6	261.22	260.03	19.25
7	151.01	17.09	118.15
8	156.73	43.56	19.35
9	154.04	257.94	21.55
10	156.13	290.16	121.25
11	52.24	48.35	20.03
12	38.91	155.41	20.99
13	56.56	258.94	22.79
14	23.06	18.07	118.13
15	7.80	155.58	116.97
16	19.95	289.90	119.57

Table H.1 Coordinates of control frame

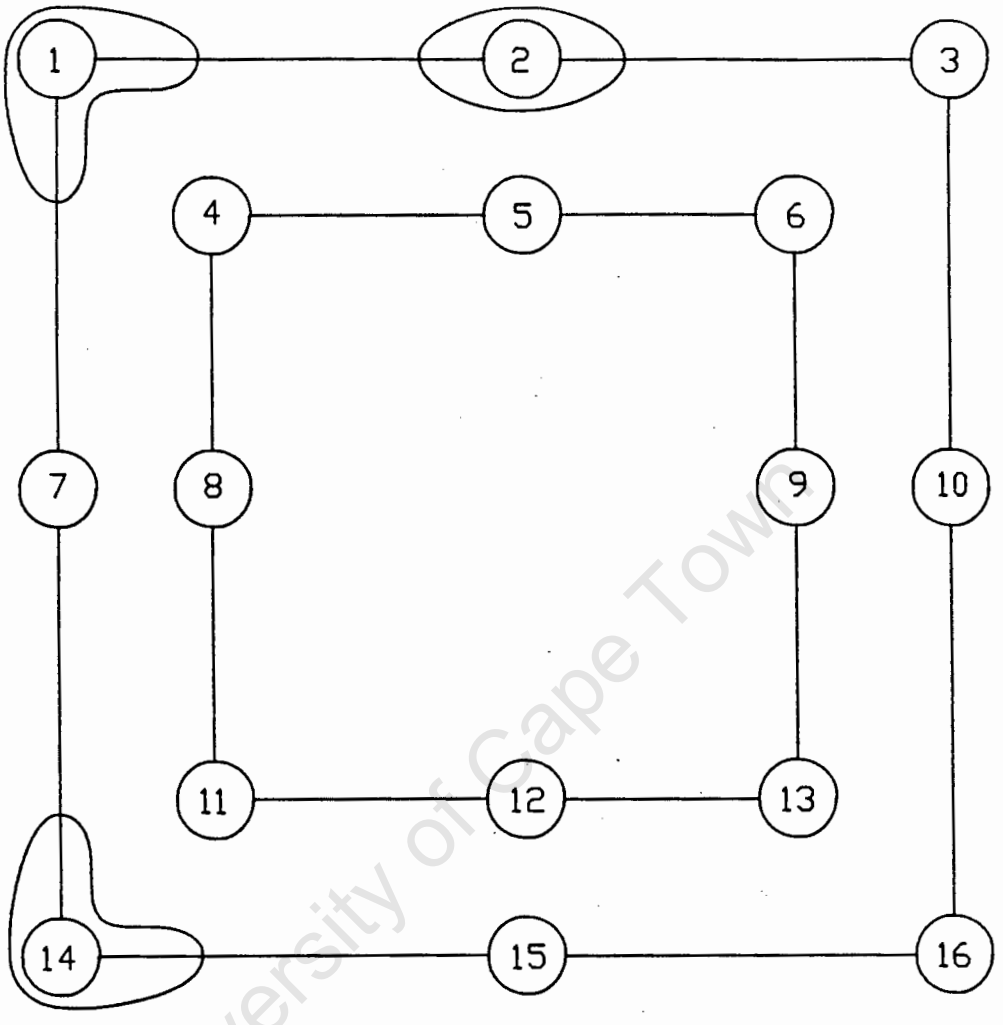

Fig. H.1 Numbering of control frame

APPENDIX I : Sample Output of Photogrammetric Software for the Test Sphere

- The algorithm of the 11-PARAMETER-TRANSFORMATION which is used in the photogrammetric software is outlined in section 2.5 of the main text.

Space Coordinates of Control Points

	X	Y	Z
1	286.517	19.157	116.555
2	298.498	147.472	115.568
3	286.050	287.682	118.092
4	259.300	49.383	17.315
5	270.555	152.655	17.860
6	261.218	260.028	19.247
7	151.013	17.087	118.153
8	156.728	43.560	19.350
9	154.040	257.938	21.550
10	156.130	290.157	121.248
11	52.242	48.352	20.033
12	38.910	155.413	20.990
13	56.562	258.938	22.788
14	23.057	18.068	118.133
15	7.802	155.578	116.968
16	19.948	289.905	119.572

Image Coordinates of Control Points

Image 1	X	Y
1	99.020	32.790
2	251.460	16.060
3	412.440	48.180
4	144.760	70.180
5	273.950	55.580
6	405.480	78.110
7	93.280	260.620
8	134.030	254.910
9	400.060	265.600
10	410.450	260.630
11	136.050	442.550
12	270.470	466.750
13	396.740	435.160
14	92.130	475.640
15	253.280	502.010
16	406.870	481.710

Image 2	X	Y
1	127.830	33.550
2	275.550	9.400
3	440.640	32.950
4	143.350	68.140
5	269.610	47.870
6	403.920	63.850
7	126.420	254.360
8	135.350	248.010
9	400.830	253.890
10	441.440	248.560
11	140.640	429.520
12	271.470	454.890
13	399.750	425.020
14	127.270	461.970
15	283.330	490.150
16	439.850	472.470

11 - P A R A M T E R - T R A N S F O R M A T I O N

Separate PDx and PDy evaluation with uniform scale

RESULT FOR IMAGE 1 AFTER 2 ITERATIONS

B11	B12	B13	B14
0.000438	0.019176	-0.002698	-2.715124
0.000000	0.000062	0.000052	0.009946
B21	**B22**	**B23**	**B24**
0.019339	-0.000335	0.000337	-3.010217
0.000061	0.000024	0.000053	0.010355
B31	**B32**	**B33**	
-0.000023	0.000121	0.000711	
0.000011	0.000012	0.000021	

Standard Deviation of Weight Unit = .010 mm

Principal Distance X = 26.818
Y = 26.789 Mean = 26.803 Ratio = 1.00107

Principal Point Position : X = 0.741 mm Y = -0.487 mm

Perspective Centre Position :

X = 178.833 mm Y = -58.040 mm Z = -1389.834 mm

CONTROL POINT IMAGE COORDINATES AND CORRECTIONS FOR IMAGE 1

No	X mm	vx mm	Y mm	vy mm
1	-2.355	-0.006	2.366	0.026
2	-0.068	-0.003	2.543	-0.011
3	2.347	0.001	2.203	-0.014
4	-1.669	-0.006	1.970	0.000
5	0.269	0.012	2.124	0.000
6	2.242	-0.004	1.886	-0.002
7	-2.441	0.006	-0.049	-0.001
8	-1.830	-0.002	0.012	0.002
9	2.161	-0.001	-0.102	-0.007
10	2.317	0.013	-0.049	0.004
11	-1.799	-0.005	-1.977	0.008
12	0.217	-0.014	-2.234	-0.005
13	2.111	-0.001	-1.899	-0.004
14	-2.458	0.008	-2.328	0.003
15	-0.041	0.003	-2.608	0.002
16	2.263	-0.001	-2.393	-0.001

RESULT FOR IMAGE 2 AFTER 2 ITERATIONS

B11	B12	B13	B14
0.000108	0.018431	0.002105	-2.675262
0.000000	0.000056	0.000049	0.009450

B21	B22	B23	B24
0.018550	-0.000086	0.000337	-2.823751
0.000054	0.000022	0.000048	0.009229

B31	B32	B33
-0.000039	-0.000071	0.000692
0.000010	0.000011	0.000019

Standard Deviation of Weight Unit = .009 mm

Principal Distance X = 26.605
Y = 26.591 Mean = 26.598 Ratio = 1.00054

Principal Point Position : X = 0.299 mm Y = -1.011 mm

Perspective Centre Position :

X = 179.109 mm Y = 304.308 mm Z = -1402.687 mm

CONTROL POINT IMAGE COORDINATES AND CORRECTIONS FOR IMAGE 2

No	X mm	vx mm	Y mm	vy mm
1	-1.923	-0.008	2.358	0.024
2	0.293	0.002	2.614	-0.014
3	2.770	-0.007	2.364	-0.010
4	-1.690	-0.003	1.991	-0.002
5	0.204	-0.001	2.206	-0.000
6	2.219	0.014	2.037	0.000
7	-1.944	-0.002	0.017	-0.001
8	-1.810	-0.004	0.085	-0.005
9	2.172	0.011	0.022	0.004
10	2.782	0.006	0.079	0.003
11	-1.730	-0.005	-1.839	0.006
12	0.232	-0.009	-2.108	-0.003
13	2.156	-0.005	-1.792	-0.004
14	-1.931	0.006	-2.183	0.001
15	0.410	0.005	-2.482	0.003
16	2.758	-0.001	-2.295	-0.002

Calculated Space Coordinates using 11-Parameter Solution

	Calculated Values of Control			Discrepancies (calculated - real)			Images used
	X	Y	Z	dX	dY	dZ	
1	285.856	18.964	115.425	-0.661	-0.193	-1.130	2
2	299.872	147.067	115.208	1.374	-0.405	-0.360	2
3	285.266	287.797	118.186	-0.784	0.115	0.094	2
4	259.338	50.055	17.797	0.038	0.672	0.482	2
5	270.558	152.425	18.625	0.003	-0.230	0.765	2
6	261.184	259.941	19.808	-0.034	-0.087	0.561	2
7	151.122	17.067	120.156	0.109	-0.020	2.003	2
8	156.698	43.735	17.674	-0.030	0.175	-1.676	2
9	154.256	258.550	21.221	0.216	0.612	-0.329	2
10	155.800	289.961	120.564	-0.330	-0.196	-0.684	2
11	51.934	47.703	21.021	-0.308	-0.649	0.988	2
12	38.759	155.227	20.193	-0.151	-0.186	-0.797	2
13	56.961	258.647	22.729	0.399	-0.291	-0.059	2
14	23.196	18.489	117.766	0.139	0.421	-0.367	2
15	7.716	155.534	117.032	-0.086	-0.044	0.064	2
16	20.044	290.190	120.028	0.096	0.285	0.456	2

Image Coordinates of Object Points

Image 1	X	Y
1	192.053	162.512
2	193.024	184.880
3	194.080	208.464
4	194.256	232.006
5	195.503	256.174
6	195.396	280.352
7	194.904	305.133
8	195.000	329.564
9	194.506	354.616
10	209.856	161.013
11	210.872	183.854
12	212.093	207.353
.	.	.
.	.	.
.	.	.
81	330.477	351.847

Image 2	X	Y
1	210.911	156.161
2	209.844	178.224
3	208.962	201.135
4	208.126	224.123
5	208.104	247.833
6	208.383	271.635
7	208.792	295.835
8	209.724	319.822
9	210.593	344.235
10	226.534	154.144
11	225.320	176.670
12	224.744	199.752
.	.	.
.	.	.
.	.	.
81	346.234	341.256

OBJECT POINT IMAGE COORDINATES AND CORRECTIONS

Point	Image	X mm	vx mm	Y mm	vy mm
1	1	-0.959	-0.000	0.991	-0.002
	2	-0.676	-0.000	1.058	0.002
2	1	-0.945	-0.000	0.754	-0.001
	2	-0.692	0.000	0.824	0.001
3	1	-0.929	-0.000	0.504	-0.002
	2	-0.706	0.000	0.582	0.002
4	1	-0.926	-0.000	0.254	-0.002
	2	-0.718	0.000	0.338	0.002
5	1	-0.907	-0.000	-0.002	-0.002
	2	-0.718	0.000	0.087	0.002
6	1	-0.909	-0.000	-0.258	-0.001
	2	-0.714	0.000	-0.166	0.001
7	1	-0.916	-0.000	-0.521	-0.002
	2	-0.708	0.000	-0.422	0.002
8	1	-0.915	-0.000	-0.780	-0.001
	2	-0.694	0.000	-0.677	0.002
9	1	-0.922	-0.000	-1.045	-0.002
	2	-0.681	0.000	-0.935	0.002
10	1	-0.692	-0.000	1.007	-0.002
	2	-0.442	-0.000	1.080	0.002
11	1	-0.677	-0.000	0.765	-0.001
	2	-0.460	0.000	0.841	0.001
12	1	-0.659	-0.000	0.516	-0.001
	2	-0.469	0.000	0.596	0.001
.	.	.	.	.	.
.	.	.	.	.	.
.	.	.	.	.	.
81	1	1.117	-0.000	-1.016	-0.001
	2	1.354	0.000	-0.904	0.001

Calculated Space Coordinates of Object Points

	X	Y	Z	Images used
1	210.631	95.598	87.239	2 : 1 2
2	197.423	95.858	79.330	2 : 1 2
3	183.736	96.231	71.795	2 : 1 2
4	170.140	96.205	67.402	2 : 1 2
5	156.244	96.979	62.231	2 : 1 2
6	142.258	97.228	62.556	2 : 1 2
7	127.898	97.349	64.573	2 : 1 2
8	113.664	97.934	66.447	2 : 1 2
9	98.975	98.226	70.050	2 : 1 2
10	211.715	109.699	81.192	2 : 1 2
11	198.267	109.857	72.675	2 : 1 2
12	184.614	110.358	65.706	2 : 1 2
.	.	.	.	.
.	.	.	.	.
.	.	.	.	.
81	101.643	212.023	72.168	2 : 1 2